

Aus dem Zentralinstitut für Seelische Gesundheit
(Direktor: Prof. Dr. med Andreas Meyer-Lindenberg)

Multimodal neural network connectivity and genetic risk factors for
Psychopathology

Inauguraldissertation
zur Erlangung des Doctor scientiarum humanarum (Dr. sc. hum.)
der
Medizinischen Fakultät Mannheim
der Ruprecht-Karls-Universität
zu
Heidelberg

vorgelegt von
Anais Buhl

aus
Hagen
2024

Dekan: Prof. Dr. med. Sergij Goerd
Referentin: Prof. Dr. med Dr. phil Heike Tost

TABLE OF CONTENTS

Seite

| | |
|--|----|
| ABREVIATIONS..... | 1 |
| | |
| 1 INTRODUCTION | 2 |
| 1.1 Neuroimaging genetics..... | 2 |
| 1.2 VNTRs and monoaminergic signaling | 3 |
| 1.2.1 VNTR polymorphisms..... | 3 |
| 1.2.2 5-HTTLPR | 5 |
| 1.2.3 MAOA..... | 7 |
| 1.3 Relevance of serotonergic candidate genes in psychiatry | 9 |
| 1.4 Network phenotypes..... | 12 |
| 1.5 Emotion regulation..... | 13 |
| 1.6 Goals and hypotheses..... | 15 |
| | |
| 2 MATERIALS AND METHODS | 17 |
| 2.1 Empirical study 1 | 17 |
| 2.1.1 Participants..... | 17 |
| 2.1.2 Genotyping | 18 |
| 2.1.3 MRI Modalities and Task Paradigm | 18 |
| 2.1.4 Data Acquisition..... | 19 |
| 2.1.5 Data Quality Control | 19 |
| 2.1.6 Amygdala Activation Analysis..... | 19 |
| 2.1.7 Brain Functional Network Analysis | 20 |
| 2.1.8 Follow-up analyses of the Identified Functional Network..... | 20 |
| 2.1.9 Test–retest reliability..... | 21 |
| 2.1.10 Relationship to emotion regulation | 21 |
| 2.1.11 Specificity of the identified genetic association..... | 21 |
| 2.1.12 Voxel-based morphometry (VBM) | 22 |
| 2.1.13 Tract-based spatial statistics (TBSS) | 22 |
| 2.2 Empirical study 2 | 23 |

| | | |
|----------|--|-----------|
| 2.2.1 | Participants | 23 |
| 2.2.2 | MAOA genotyping..... | 24 |
| 2.2.3 | MRI data acquisition | 25 |
| 2.2.4 | MRI paradigms | 26 |
| 2.2.5 | Functional MRI data processing and connectome construction..... | 27 |
| 2.2.6 | Structural MRI data processing and connectome construction | 28 |
| 2.2.7 | Data analysis and statistical inference..... | 28 |
| 2.2.8 | Supplemental exploratory analyses | 28 |
| 2.2.9 | Relationship to emotion regulation | 29 |
| 3 | RESULTS..... | 30 |
| 3.1 | Empirical study 1 | 30 |
| 3.1.1 | Amygdala Activation Analysis | 30 |
| 3.1.2 | Network-Based Functional Connectivity Analysis | 30 |
| 3.1.3 | Test–Retest Reliability of the Phenotype | 30 |
| 3.1.4 | Relationship to Emotion Regulation..... | 30 |
| 3.1.5 | Specificity of the identified genetic association | 30 |
| 3.1.6 | Gray Matter Structural Analysis | 31 |
| 3.1.7 | White Matter Structural Analysis..... | 31 |
| 3.2 | Empirical study 2 | 33 |
| 3.2.1 | Functional network analyses | 33 |
| 3.2.2 | Structural network analysis..... | 33 |
| 3.2.3 | Supplemental exploratory analyses | 34 |
| 3.2.4 | Relationship to emotion regulation | 35 |
| 4 | DISCUSSION | 36 |
| 4.1 | 5-HTTLPR discussion..... | 36 |
| 4.2 | MAOA discussion | 38 |
| 4.3 | General discussion | 41 |
| 4.4 | Limitations | 42 |
| 4.5 | Future directions..... | 44 |
| 5 | SUMMARY | 47 |

| | |
|-------------------------------|----|
| 6 ZUSAMMENFASSUNG..... | 48 |
| 7 REFERENCES..... | 49 |
| 6. SUPPLEMENTAL MATERIAL..... | 61 |
| 8 CURRICULUM VITAE | 74 |
| 9 ACKNOWLEDGEMENTS..... | 77 |

ABBREVIATIONS

| | |
|----------|---|
| 5-HTTLPR | Serotonin transporter linked polymorphic region |
| AAL | Automated anatomical labeling |
| ADHD | Attention Deficit Hyperactivity Disorder |
| DTI | Diffusion tensor imaging |
| DWI | Diffusion weighted imaging |
| CD | Conduct Disorder |
| FSL | FMRIB Software Library |
| GWAS | Genome wide association study |
| MAOA | Monoamine oxidase A |
| MRI | Magnetic resonance imaging |
| NBS | Network based statistics |
| OCD | Obsessive Compulsive Disorder |
| OPC | Oppositional Defiant Disorder |
| PPI | Psychophysiological interactions |
| SNP | Single nucleotide polymorphism |
| SPM | Statistical Parametric Mapping |
| SPSS | Statistical Package for the Social Sciences |
| PET | Positron emission tomography |
| TBSS | Tract based spatial statistics |
| VBM | Voxel based morphometry |
| VNTR | Variable number of tandem repeats |

1 INTRODUCTION

1.1 Neuroimaging genetics

Most neuropsychiatric disorders have strong genetic components in their etiology. Psychiatric disorders tend to run in families, concordance rates in twins are relatively high and high to moderate heritability estimates confirm a genetic component (Cardno & Gottesman, 2000; Corfield et al., 2017; Edvardsen et al., 2008; Faraone & Larsson, 2019; Grove et al., 2019; Lam et al., 2019; McGuffin et al., 2003; Sandin et al., 2017). However, the genetic architecture of these disorders is complex and not completely understood, thus making the identification of specific genetic risk factors challenging. One broadly used approach for the identification of genetic risk variants that are statistically associated with psychiatric disease risk are genome wide association studies (GWAS). This approach investigates large sets of genetic markers with high variance between individuals and compares the frequency of these large sets of genetic variants between individuals with a diagnosed disorder or trait of interest and unaffected individuals.

GWAS successfully identified genetic risk factors for a broad range of psychiatric disorders (Demontis et al., 2019; Grove et al., 2019; Jansen et al., 2020; Ripke et al., 2014; Stahl et al., 2019; Wray et al., 2018) confirming that the common disease-common variant model is applicable to neuropsychiatric disorders. This model states that common disorders are caused by a high number of common genetic variants. More specifically, large numbers of genetic variants with small individual penetrance add up to push genetic load of disease associated genetic variants in an individual towards a threshold for disease. Additional complex interactions of genetic risk with the environment contribute to the etiology of neuropsychiatric disorders as well (Reich & Lander, 2001). Neuropsychiatry lags behind other disciplines in the identification of risk genes and underlying biological mechanisms. Understanding of the pathophysiological pathways leading from genetic variance to neuronal alterations to behaviour and ultimately to psychiatric disorders is still incomplete. One problem that held back psychiatric research and thus contributed to this incomplete understanding is the lack of easily measured, standardized, quantitative phenotypes.

Several neuroanatomic abnormalities haven been linked to a broad range of neuropsychiatric disorders as well as genetic risk (A. Meyer-Lindenberg & D. R. Weinberger, 2006; Thompson et al., 2020). Moreover, neuroimaging phenotypes might be easier to quantify than psychiatric symptoms and could therefore be valuable quantitative biomarkers for psychiatric risk. They are however not part of a diagnostic process yet. Neuroimaging endophenotypes are quantitative indicators of brain structure or function that reflect genetic susceptibility for a disorder (Glahn et al., 2007). The concept behind this approach assumes that there is a complex pathway leading from genes to proteins to cells, the brain at the macroscopic level, to behavior and ultimately, psychiatric symptoms. On this pathway, neuroimaging phenotypes are several steps closer to genes than psychiatric diagnoses. Therefore, neuroimaging phenotypes might be more relevant to understand pathophysiology of disorders compared to directly linking genes to diagnosis. In addition, genetic risk factors may have a higher penetrance at the level of the brain than at the level of psychiatric diagnosis because of the neural level being more closely aligned to biology. Furthermore, genetic architecture of neuroimaging phenotypes might be less complex than that of diagnostic categories (Glahn et al., 2007; A. Meyer-Lindenberg & D. Weinberger, 2006).

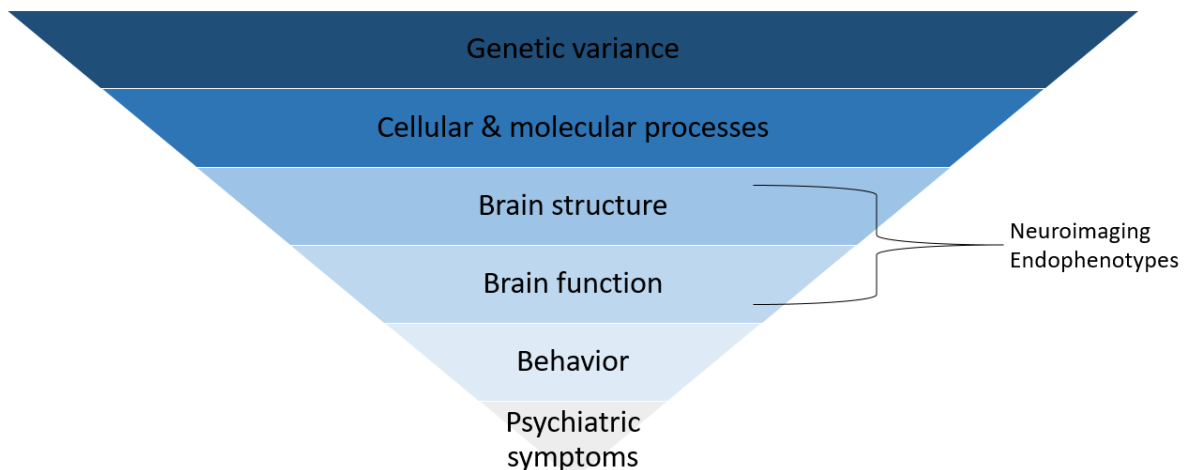


Figure 1: Schematic illustration of the pathway from genetic variance to psychiatric symptoms. Neuroimaging phenotypes are closer to genetic variance than psychiatric symptoms (own illustration).

To be considered an endophenotype for a disorder, a marker has to meet the following criteria (Beauchaine, 2009; Gershon & Goldin, 1986; Gottesman & Gould, 2003):

- 1) be highly heritable
- 2) be associated with the phenotype of interest (e.g. formal diagnosis) and segregation with clinical diagnosis in the population
- 3) be detectable independent of clinical state, e.g. presence prior to manifestation of illness and persistence even during periods of remission
- 4) cosegregate with the illness in families
- 5) be more common in the unaffected family members compared to the general population
- 6) can be reliably measured, with some degree of specificity to the disorder of interest

Several neuroimaging brain markers such as grey matter volume (Turner et al., 2012), neural function (Erk et al., 2014), structural (Bohlken et al., 2016) and functional connectivity (Cao et al., 2016) fulfill these criteria and have been considered as potential endophenotypes for psychiatric disease. Nevertheless, the genetic architecture of neuroimaging phenotypes remains complex. For instance, the surface area and average thickness of the human cerebral cortex are associated with a large number of genetic loci which do not reach genome-wide significance (Grasby et al., 2020). Therefore, there is a need for novel phenotypes, with higher sensitivity and higher specificity to alterations in the brain that are connected to psychiatric entities.

1.2 VNTRs and monoaminergic signaling

1.2.1 VNTR polymorphisms

Many neuropsychiatric disorders are highly heritable and most do not follow classical Mendelian inheritance patterns (Sullivan et al., 2012). These multifactorial disorders with a complex genetic architecture include several common diseases like diabetes (Ali, 2013) and asthma (Ferreira et al., 2014). Most neuropsychiatric disorders also fall

into that category. These disorders are hypothesized to arise due to the complex interactions of several genetic variants with small individual effect sizes. None of these genetic risk factors is sufficient or necessary to cause the disorder in the absence of other risk factors. Genetic risk factors interact with additional environmental risk factors in the causation of complex disorders (Sullivan et al., 2012). The genetic and environmental risk factors that lead to complex disorders are heterogeneous among affected individuals. Many complex diagnostic entities can be usefully subdivided into subgroups based on variables such as age of onset, disease progression or biomarkers (e.g. blood leptin levels as an indicator of metabolic health).

Several GWAS (Genome wide association studies) have been performed to better understand the genetic architecture of complex, multigenetic disorders. GWAS have successfully identified genetic risk factors for several complex disorders, for instance schizophrenia (Ripke et al., 2014). However, even for highly heritable traits, the genetic variants identified by GWAS only explain a small proportion of the estimated heritability. This phenomenon has been referred to as missing heritability (Maher, 2008; Owen & Williams, 2021). Several explanations have been proposed. One hypothesis is that in addition to the single nucleotide polymorphisms (SNP), which are well studied and easy to genotype with high throughput, other types of genetic variants contribute to the heritability of complex disorders. The majority of published GWAS investigated only SNPs. However, a significant proportion of heritability might be explained by under-researched genetic variants (Maher, 2008; Manolio et al., 2009; Marian, 2012).

Variable number of tandem repeats (VNTRs) are one type of genetic polymorphism that is not included in GWAS but might still be interesting and relevant in the genetic architecture of complex, polygenic disorders (Hannan, 2010). VNTRs are variations in the length of repeated sequences in the genome, which are organized in tandem repeats. They can be classified as a type of mini-satellite ranging in length from ten to one hundred base pairs (Brookes, 2013). Although VNTRs are commonly used in genetic finger-printing for individual identification and paternity testing (Pena & Chakraborty, 1994), VNTRs are more difficult to genotype than SNPs as there is no high throughput technology allowing easy, fast and cost-efficient genotyping of VNTRs. Another problem is the lack of a standardized nomenclature for VNTRs similar to reference SNP (rs) numbers that identify SNPs uniquely (Brookes, 2013). Due to these challenges, screening large numbers of VNTRs is still difficult. However, VNTRs might be promising candidates to further our understanding of the genetic architecture underlying complex disorders. Several additional lines of evidence confirm this suggestion. VNTRs have higher potential for mutations leading to a lot of variation that could be potentially relevant and show higher penetrance than biallelic markers (Fondon et al., 2008).



Figure 2: Schematic illustration of alternative alleles of a VNTR on a single strand. Allele A has 4 repeats, allele B has 5 repeats (own illustration).

Genes with a high number of VNTRs were shown to be expressed disproportionately in the brain (Linthorst et al., 2020) and to be involved in the risk architecture of several non-psychiatric complex disorders (Wang et al., 2012), therefore making VNTRs promising candidate for better understanding the genetic risk for neuropsychiatric disorders. Several VNTRs have been shown to be involved in regulating gene expression. This type of VNTR is mostly located in the promoter regions of adjacent genes and has been shown to have functional effects by altering transcriptional efficiency, thus fine tuning gene expression levels (Brookes, 2013). Two well studied functional promoter VNTRs that have been linked to neuropsychiatric disorders and associated neuropsychological traits are the monoamine oxidase A (MAOA)-uVNTR polymorphism (Sabol et al., 1998) and the 5-HTTLPR (serotonin-transporter-linked polymorphic region) (K. P. Lesch et al., 1996) polymorphism.

Allelic variation in both of these promoter polymorphisms has been linked to risk for various neuropsychiatric disorders including depression (Brummett et al., 2007), anxiety (K. P. Lesch et al., 1996) and traits like impulsivity and aggression (Manuck et al., 2000). However, even for these clearly functional VNTRs, outcomes depend on the presence of additional risk factors. The most relevant risk factors interacting with these two VNTRs are early life adversity and stress (Caspi et al., 2003; Kim-Cohen et al., 2006). Earlier neuroimaging studies in healthy individuals showed that variation in these promoter VNTRs affected brain structure and function most prominently in the limbic system (Hariri et al., 2005).

1.2.2 5-HTTLPR

Serotonin is a key neurotransmitter regulating several physiological functions and psychological processes including mood, aggression, memory, arousal and sleep. The serotonin transporter protein facilitates the uptake of serotonin by the synapse and thereby terminates the action of serotonin in the synaptic cleft. The serotonin transporter is a primary target of widely used pharmacological treatments for several psychiatric disorders including major depression and anxiety.

A common VNTR in the promoter region of the serotonin transporter gene has been shown to influence transcriptional efficiency of the serotonin transporter gene. This length polymorphism consists of a 44-basepair insertion or deletion resulting in a short and a long allele which can be subdivided further (Canli & Lesch, 2007; Hariri & Holmes, 2006; Nakamura et al., 2000). The long variants have been linked to increased transcription of the serotonin transporter in human cell lines (K.-P. Lesch et al., 1996).

This polymorphism is triallelic: Additional SNPs have been shown to influence serotonin transporter transcription levels in humans. More specifically, the G allele of rs25531 polymorphism results in reduced transcriptional activity that is similar to the short VNTR even in the presence of the long allele whereas the A allele results in higher levels of SERT and corresponding mRNA (Hu et al., 2005).

Allelic variation in the serotonin transporter has been linked to susceptibility for different psychiatric disorders and related psychological traits (Canli & Lesch, 2007; Hariri et al., 2005; Hariri & Holmes, 2006). Psychiatric disorders that have been associated with this polymorphism include but are not limited to major depression (Caspi et al., 2003), anxiety disorders (K.-P. Lesch et al., 1996), eating disorders (Calati et al., 2011), ADHD (Eun et al., 2016) and autism (Camille W. Brune et al., 2006). However, these associations with psychiatric disorders have been inconclusive and hard to replicate.

Findings regarding a strong main effect of serotonin transporter on psychiatric risk were mixed and effect sizes might have been overestimated by previous under-powered studies. Nonetheless, serotonin transporter genotype has been consistently shown to moderate the relationship between affective disorders and stress. More specifically, early life adversity negatively affected carriers of the transcriptionally less efficient variant who developed increased affective disorders and suicidality whereas no such relationship was found in carriers of the more transcriptionally efficient variant. This observation agrees well with the diathesis stress model. The diathesis stress model states some multifactorial disorders or traits are caused by an interaction of an inherent biological vulnerability with environmental stressors. In the absence of adverse environmental conditions, individuals with this increased vulnerability are indistinguishable from non-risk-carriers. Only if adverse environmental factors like stress are present, increased vulnerability raises the probability for poor outcomes, e.g. developing a neuropsychiatric disorder whereas less vulnerable individuals are less severely affected (Colodro-Conde et al., 2018).

Several imaging genetics studies investigated the neural processes underlying this interaction between 5-HTTLPR genotype, stress and affective disorders (Hariri et al., 2005; Hariri & Holmes, 2006; Heinz et al., 2005). Although a link between amygdala structure and function with 5-HTTLPR genotype was identified in several fMRI studies, findings have been mixed and initial findings could not always be replicated in larger samples (Bastiaansen et al., 2014; Murphy et al., 2013; Viviani et al., 2010).

In addition, several studies have confirmed an association between serotonin transporter genotype and susceptibility to affective disorders and alterations in neural regions involved in emotion processing, mixed findings, relatively small initial sample sizes and a complex relationship between genotype and phenotype (e.g. moderation by environment) have made this area of research challenging.

These conflicting results may be explained by at least two factors. First, given the small effect size of common genetic variants, earlier studies with small sample sizes may be more vulnerable to noise and false-positive findings (Bastiaansen et al., 2014; Murphy et al., 2013). Second, as reported previously (Johnstone et al., 2005; Plichta et al., 2012), amygdala activation during emotion processing per se is a rather unreliable phenotype. Prior work of our group has shown a superior reliability and sensitivity of connectomic, network-based neuroimaging measures in the study of functional neuroimaging phenotypes (Cao et al., 2016; Cao, Plichta, Schäfer, et al., 2014). This findings suggest the potential utility of network-based methods for the study of potential associations 5-HTTLPR genetic variation with neuroimaging phenotypes.

There is converging evidence from several independent lines of research suggesting that the 5-HTTLPR may impact the connectivity of multiple regions in the emotional processing network in humans. Nevertheless, many prior studies focused exclusively on the amygdala. Apart from the amygdala, efficient emotion processing in humans relies on the coordination of multiple other regions including the fusiform gyrus, hippocampus, striatum, thalamus, anterior cingulate cortex, insula, and orbitofrontal cortex (Etkin et al., 2015; Phillips et al., 2003). These regions form an integrated functional brain network that is essential for emotion identification and regulation (Etkin et al., 2015; Phillips et al., 2003). Earlier studies reported that the connectivity of this emotional brain network is heritable (Budisavljevic et al., 2016) and have connected alterations in this network with the genetic risk for mental disorders including schizophrenia (Cao et al., 2016; Cao, Plichta, Schäfer, et al., 2014) and bipolar disorder (Dima et al., 2016). Further evidence from animal research confirms this suggested association between genetic variance in the 5-HTT gene and alterations in neural networks involved in emotion processing with changes in 5-HTT knock-out mice extending beyond the amygdala (Fabre et al., 2000; Mathews et al., 2004; Rioux et al., 1999). PET studies in human also demonstrated that the S allele of the 5-HTTLPR is associated with altered 5-HTT concentrations and serotonin receptor binding potentials in several brain regions involved in emotion processing including the striatum (Praschak-Rieder et al., 2007), hippocampus, anterior cingulate gyrus, orbitofrontal cortex, and lateral temporal lobe (David et al., 2005).

Because of this converging evidence suggesting the involvement of a complex network in the association between 5-HTT, the brain and psychiatric risk, further imaging genetics research using novel analysis methods in large cohorts applying connectomic methods might be promising.

1.2.3 MAOA

The monoamine oxidases catalyze the oxidation of monoamines and serve to inactivate neurotransmitters including serotonin, dopamine and norepinephrine (Shih et al., 1999). In humans, two types of monoamine oxidase are expressed. Monoamine oxidase A (MAO-A) and monoamine oxidase B (MAO-B). MAOA is present in the outer membrane of mitochondria in most cell types. In the human brain, MAOA is expressed in neurons and astroglia (Westlund et al., 1988). MAOA is encoded by the *MAOA* gene, which is located on the X-chromosome (Shih et al., 1999). MAOA has been first linked to aggression in a Dutch family with a loss of function mutation of this gene. Male members of that family presented with a distinctive phenotype including aggression, impulsive behavior but also general developmental delays (Brunner et al., 1993). A more common VNTR located upstream to the first exon of the *MAOA* gene has been shown to have functional effects on MAOA expression levels. This MAOA uVNTR consists of a 30-basepair motif that can be repeated 2, 3, 3.5, 4, and 5 times. The 2, 3, and 5 repeats are defined as low expression variants (MAOA-L), while the 3.5 and 4 repeat variants are associated with high MAOA expression. In human cell lines, high expression variants of *MAOA* were associated with a 2-10-fold increase in transcription efficiency (Guo et al., 2008; Sabol et al., 1998).

Allelic variance in this *MAOA* u-VNTR has been associated with a board range of psychiatric disorders as well impulsive and aggression traits. More specifically, the low expressing allelic variants of *MAOA* have been associated with several aggression related outcomes (Buckholtz & Meyer-Lindenberg, 2008; Meyer-Lindenberg et al., 2006). However, this relation with aggression seems to be less specific than previously

assumed. Instead, *MAOA* has been associated with multiple neuropsychiatric disorders including bipolar disorder (Lim et al., 1995), ADHD (Manor et al., 2002), panic disorder (Reif et al., 2014), autism, depression (Brummett et al., 2007) and alcohol dependence (Contini et al., 2006). An important commonality of these disorders might be emotion regulation. A further commonality might be a relation with stress, particularly during sensitive periods in neurodevelopment in early childhood. Interaction between *MAOA* genotype and early life adversity are stronger and more consistent than main effects of genotype (Kim-Cohen et al., 2006).

The neurobiological mechanisms by which *MAOA*-L impacts aggression are not completely understood. Although *MAOA* genotype might moderate responses to stress to influence certain behavioral and psychological traits, neuroimaging might be a more sensitive marker to subtle differences between individuals carrying the *MAOA*-high and low expression variants and therefore might be able to identify main effects of *MAOA* genotype. Several MRI studies in healthy participants confirmed an effect of *MAOA* genotype that was consistent with the suspected link between *MAOA* genotype and emotion regulation, such as structural and functional alterations in the limbic system with carriers of the *MAOA*-L variant showing reduced grey matter volume (Cerasa et al., 2008; Meyer-Lindenberg et al., 2006) and increased amygdala reactivity (Lee & Ham, 2008; Meyer-Lindenberg et al., 2006). So the most consistent evidence is converging on cortico-limbic regions. However, sample sizes in these initial neuroimaging genetics studies were often relatively small and the resulting effects were hard to replicate. Furthermore, PET studies directly investigating activity of *MAOA* did not find consistent genotype effects (Fowler et al., 2007). Together, these data suggest that the low-expression allele of *MAOA* contributes to global alterations in cortico-limbic circuits critically involved in adequate regulation of negative emotions and inhibitory control. The most likely mechanism behind this association is excessive serotonergic signaling during vulnerable periods of early brain development (Cases et al., 1995) in carriers of low expressing variants of *MAOA*. Additional environmental risk factors including early life adversity and drug intake might exacerbate its impact on monoaminergic neurotransmission (Heinz et al., 2011; Meyer-Lindenberg et al., 2006) most likely by epigenetic mechanisms. Although there are several prior studies investigating potential associations of *MAOA* genotype and variation in brain structure and function, most imaging genetics studies on *MAOA* focused on specific brain functional domains, a limited set of predefined neural regions or a single neuroimaging data modality, making a more comprehensive understanding of the neural connectomic effects difficult (Klein et al., 2017).

Several converging lines of evidence suggest more widespread, global effects of *MAOA* on neural structural and functional network architecture. First, positron emission tomography (PET) and postmortem studies revealed a broad topological distribution of *MAOA* binding potentials and mRNA expression levels across the human brain (Komorowski et al., 2017; Tong et al., 2013). Second, the encoded enzyme is a central modulator of stem cell neural differentiation and neural circuit segregation during early brain development (Ou et al., 2006; Wang et al., 2011). The results of this human imaging research are supported by similar findings in animal models. In *MAOA*-deficient mice, the ensuing disturbances in brain maturation are well-established and include distributed neural regions and a range of behavioral alterations (Bortolato et al., 2013; Cheng et al., 2010; Upton et al., 1999). These data suggest that a functional change in the *MAOA* gene can lead to distributed network effects, which extend across brain functional domains and neuroimaging data modalities.

Taken together, these prior findings suggest that additional research in larger cohorts applying novel network phenotypes might be useful to further clarify the role of *MAOA* genotype in brain structure and function.

1.3 Relevance of serotonergic candidate genes in psychiatry

Neuropsychiatric disorders are moderately to highly heritable (Burmeister et al., 2008). However, identifying genetic variants involved in the etiology of these disorders has been challenging.

There are several approaches that aimed at identifying genetic risk factors for multifactorial disorders with complex genetic architecture. Historically, many studies focused on so called candidate genes. Candidate genes are genes which are suspected to be involved in the etiology of a disorder based on prior knowledge (Tabor et al., 2002). One source of this prior knowledge is pharmacological evidence. For example, agents affecting the serotonergic systems have been widely used in the treatment of depression and anxiety disorders. This inspired many studies to investigate genes with a known function related to serotonin receptors, serotonin transporters or breakdown of serotonin, including 5-HTTLPR and *MAOA*.

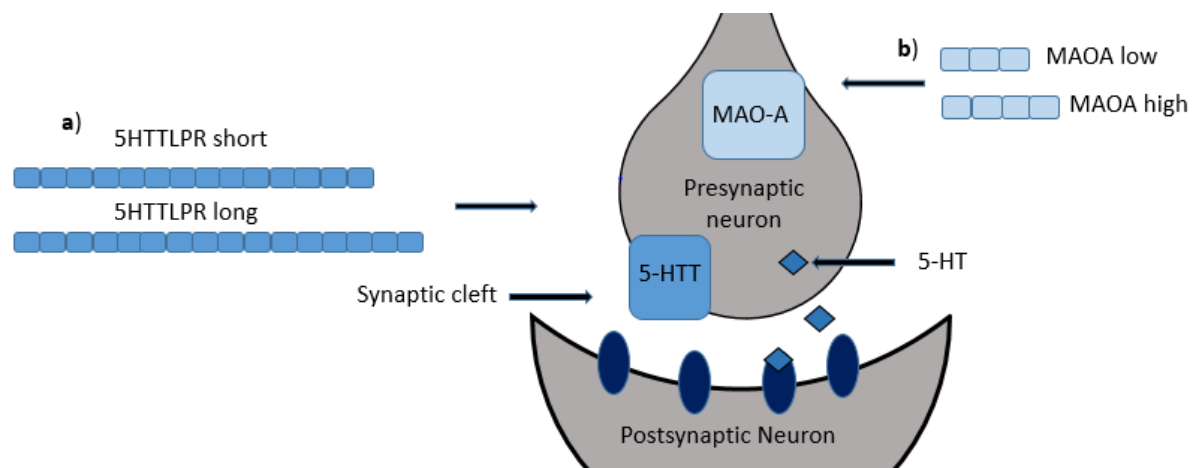


Figure 3: The duration of action of serotonin in the synaptic cleft is limited by reuptake of serotonin in the presynaptic neuron and degradation of serotonin by enzymes. Genetic variation in the promoter regions of the MAOA-gene (b) and the 5-HTT gene (a) contributes to individual differences in the efficiency of these processes (own illustration).

Several studies linked these candidate genes to risk for neuropsychiatric disorders and related negative outcomes. However, these early findings were difficult to replicate questioning the idea that serotonergic variants have a large effect on psychiatric risk (Bosker et al., 2011). Some researchers suggested that these mixed findings might be, at least to some extent explained by the presence of interactions between genotype and environmental risk factors. Interactions between environmental risk factors including stress and early life adversity have been confirmed for both *MAOA* (Kim-Cohen et al., 2006) and 5-HTTLPR (Caspi et al., 2003). Genetic variance in these polymorphisms modulated the effect of stress on disease risk. In the presence of additional

environmental risk factors, genetic variance in serotonergic polymorphisms was associated with risk for several adverse outcomes, e.g. developing a psychiatric disorder or increased aggression (Caspi et al., 2003; Kim-Cohen et al., 2006).

Additional studies challenged the notion of a risk variant and a protective variant by showing that carriers of the risk variant did benefit more from favorable environmental conditions. For example, children carrying the risk variant of *MAOA* who were exposed to psychosocial risk environments showed increased criminality whereas in a supportive environment, risk for criminality was reduced (Oreland et al., 2007). Therefore, genetic variants traditionally thought of as risk variants might be more accurately described as plasticity variants. In contrast to risk variants which make carriers more susceptible to negative environmental influences, plasticity variants increase sensitivity to environmental influences for better or worse (Belsky et al., 2009). This might make it challenging to find simple associations of genetic variants with psychopathology and related negative outcomes, especially in large cohorts with only minimal phenotyping. An alternative approach to traditional candidate genes are genome-wide association studies. With the advent of high-throughput genotyping of large cohorts, a genome-wide, unbiased search for genetic risk variants became a feasible option (Manolio, 2010).

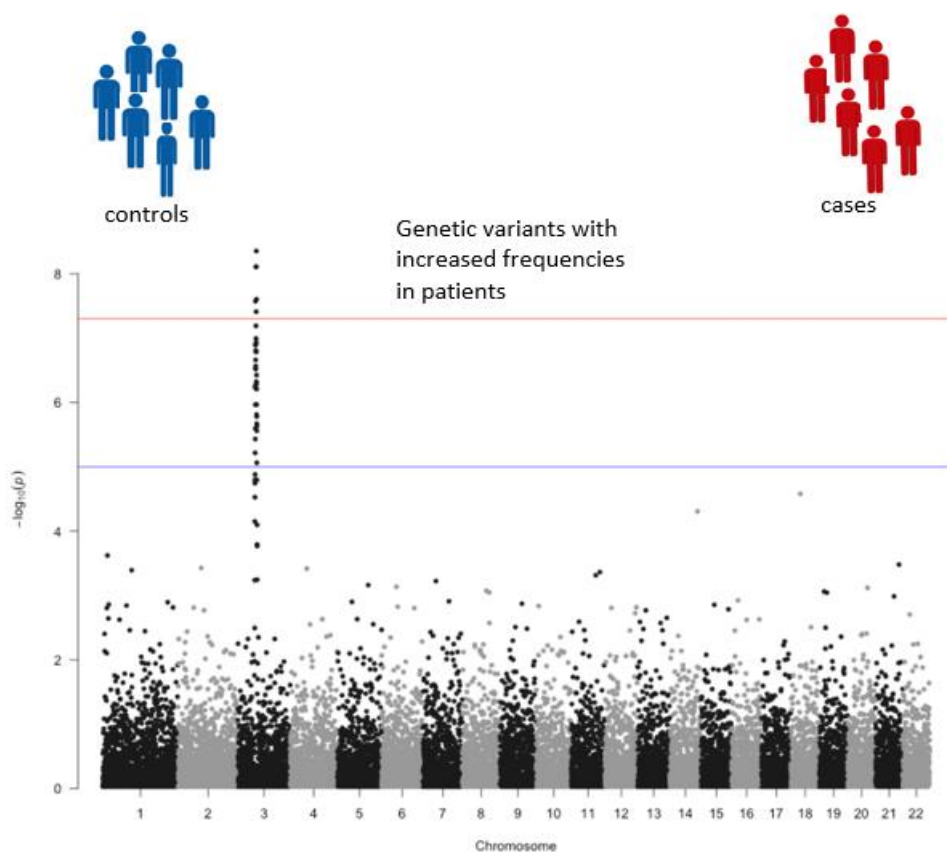


Figure 4: Large groups of healthy controls (blue line) and patients (red line) are genotyped using high-throughput technologies. Subsequent statistical analyses identify genetic variants that are significantly more common in affected individuals compared to healthy controls. A genetic variant that is significantly associated with the disorder of interest is identified on chromosome 3 (own illustration).

These GWAS mainly focused on SNPs, but some studies did include selected candidate genes in addition to a GWAS panel. However, candidate genes rarely show statistically significant associations with disease status in large samples. Most evidence

for a role of candidate genes in the etiology of neuropsychiatric disorders was derived from studies with relatively small sample sizes and failed to replicate in adequately powered samples. The same holds true for candidate gene by environment interactions. Several well powered study did not find any evidence of an interaction between risk genotypes and environmental risk factors (Border et al., 2019; Fergusson et al., 2011). This lack of replication has led some experts in the field to question the validity of the candidate gene approach altogether (Arango, 2017). However, concluding that candidate genes do not play a role in neuropsychiatric disorders at all might be premature. Even in the absence of convincing main effects of most candidate genes on disease risk, studying the relation of these candidate genes to brain structure and function as well as behavioral traits might be informative. Traditional diagnostic categories used in the classification of neuropsychiatric disorders do not map well onto biological pathways connecting genes to the brain to behavior and ultimately to psychiatric illness (Insel et al., 2010).

Patients with the same diagnosis under the current classification system are heterogeneous on several levels. For instance, two patients diagnosed with major depression do not necessarily have even one common symptom. Furthermore, it has been shown that different depression symptoms are not interchangeable indicators of disease (Fried & Nesse, 2015). Therefore, grouping study participants in binary categories of affected and unaffected individuals without accounting for presence and severity of specific symptoms might not be a suitable approach for neuroimaging genetics research aimed at the identification of biological pathways from genetic risk factors to manifestations of disease. In addition, symptom domains are rarely specific for one psychiatric disorder but usually shared among several disorders. For instance, difficulties with emotion processing have been observed across diagnostic categories. Altered emotion regulation has been observed in depression, several anxiety disorders but are also common in externalizing disorders like ODD or CD and antisocial personal disorder in adults (Fernandez et al., 2016).

At the neural level, a considerable overlap in neuroimaging phenotypes has been shown suggesting that neural alterations might be more closely related to specific domains of functioning than to traditional diagnostic categories. For instance, altered activity in brain regions linked to inhibitory control and salience processing are shared between mood disorders and anxiety disorders (Janiri et al., 2020). Similarly, alterations in white matter integrity affecting interhemispheric structural connectivity are shared between autism spectrum disorders, ADHD and OCD (Ameis et al., 2016).

A similar pattern of overlap between psychiatric disorders emerged for their genetic underpinnings. Several large studies show a strong overlap of genetic risk between different neuropsychiatric disorders. For instance, schizophrenia, bipolar disorder, major depression, ADHD and autism spectrum disorders share a large proportion of genetic risk attributed to common variants (Lee et al., 2013). In contrast, neurological disorders do not share genetic risk with psychiatric disorders suggesting that these shared genetic risk factors are common between psychiatric disorders but do not generalize to other disorders of the brain (Anttila et al., 2018). This confirms again that traditional diagnostic boundaries might not map directly to distinct biological pathways. Taken together, this evidence suggests that even in the absence of strong genotype effects on specific disease risks, candidate genes could potentially be linked to specific neuroimaging endophenotypes and psychological traits which in turn might be relevant for understanding biological mechanisms behind variance in the brain structure,

function and behavior. Therefore, our understanding of the pathway from genes to the brain to psychological traits might benefit from investigating risk variants with well-established biological functions.

1.4 Network phenotypes

Brain function and thereby complex cognition depends on the orchestration and interaction of widely distributed brain regions (Bassett & Sporns, 2017; Medaglia et al., 2015). Neuropsychiatric disorders have been hypothesized to arise from alterations in the communication of complex neural circuits rather than localized, focal aberrations in specific brain regions (Canu et al., 2015; Hulshoff Pol & Bullmore, 2013).

Methodological advances in diverse fields ranging from the social sciences to genetics led to methods for describing complex phenomena which might be useful for understanding the human brain and the complex interactions between highly distributed neural circuits. The most commonly applied method among these approaches is graph theory. Graph theory represents complex interconnected systems in the form of discrete, non-overlapping entities called nodes and their pairwise connections called edges, which can be summarized as graphs. The patterns by which edges connect nodes make up the networks topology. Local and global aspects of network topology can be analyzed using a broad array of measures. This abstract form and simple representation result in broad applicability to different spatial and temporal patterns and scales of brain physiology (Bassett & Sporns, 2017; Braun et al., 2018).

Network approaches can be applied to neuroscientific questions at different scales. In humans, the most commonly studied scale is the macroscale, which is investigated using neuroimaging techniques like magnetic resonance imaging. At this scale, the smallest elements are individual voxels. For network analyses, these voxels are often grouped together based on regions of interest or parcels according to their features which then represent the nodes of the brain network (Bassett & Sporns, 2017). In brain network approaches, nodes are distinct neural elements, for example brain regions from a predefined atlas. Brain connectivity maps show how brain regions interact. These interactions can be anatomical or functional and are referred to as structural or functional connectivity respectively. Structural connectivity refers to the physical connections between brain regions. Structural networks are usually sparse and relatively stable over time. Most neuroimaging techniques investigate axon bundles, which can be measured by diffusion weighted MRI sequences. The most common technique used is DWI followed by reconstruction of fiber tracts for connectomic research (Yeh et al., 2021). Functional connectivity measures correlated, coordinated activity of brain regions. It can be defined by any measure of statistical similarity between pairs of brain regions. The most commonly applied method is using (bivariate) Pearson correlations between pairs of brain regions or nodes. These temporal patterns can be extracted from task-based or resting state data (Friston, 2011).

The shift in perspective to distributed brain function within complex interconnected networks resulted in a lot of evidence confirming the relevance of brain network architecture for cognition and complex behavioral phenotypes including neuropsychiatric disorders (Hulshoff Pol & Bullmore, 2013). Furthermore, several network phenotypes have been shown to fulfill the criteria for endophenotypes or are heritable (Cao et al., 2016; Thompson et al., 2013). These links to both variance in clinically relevant behav-

journal traits and neuropsychiatric disorders in combination with at least moderate heritability suggests that network phenotypes might be promising for the field of neuroimaging genetics. This is especially relevant because the genetic architecture of several traditional, well established neuroimaging phenotypes has been shown to be nearly as complex as diagnostic categories (Elliott et al., 2018). Therefore, traditional neuroimaging measures might not always be optimal endophenotypes for neuroimaging analyses as one of the main goals of the endophenotype approach is reducing complexity of the investigated phenotypes to facilitate the identification of associations between genetics and the brain. Therefore, new analysis methods with improved sensitivity for the usually subtle effects of genetic risk factors on the brain and a less complex genetic architecture are urgently needed to further the field of neuroimaging genetics.

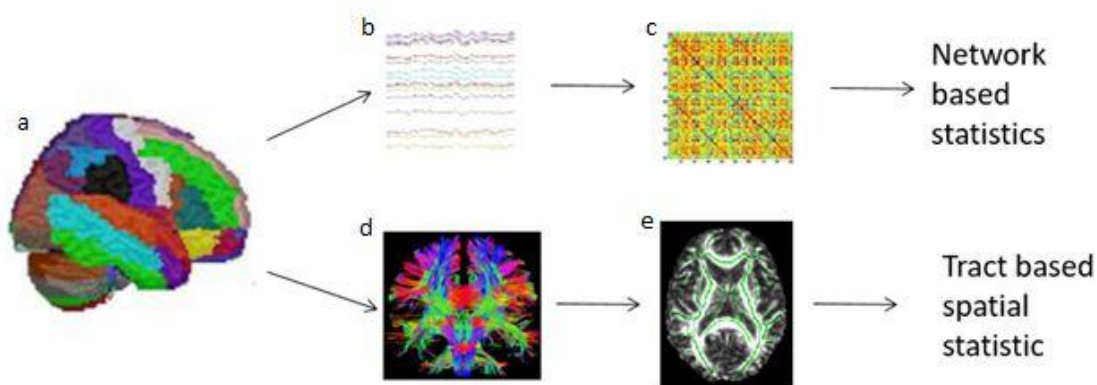


Figure 5: Schematic of a pipeline for the connectomic network analyses applied in empirical study 1 as an example for a connectomic approach. The upper panel (b-c) represents the functional connectivity analyses applied in the current work. The lower panel (d-e) represents the structural connectivity analyses of empirical study 1. For both types of connectivity analyses, the brain was parcellated according to the same atlas (a). For the functional connectivity analyses, timelines from a functional MRI were extracted (b). A connectivity matrix with Pearson correlations between each pair of brain regions was derived (c). For the structural connectivity analyses, diffusion weighted MRI images were used to estimate the diffusion tensor for further processing. (d) For statistical analyses of structural connectivity we applied tract based spatial statistics, a technique for a whole brain voxel wise analysis of diffusion weighted data (own illustration).

1.5 Emotion regulation

Genetic variation in the serotonergic system has been linked to the risk for several neuropsychiatric disorders including depression (Brummett et al., 2007), bipolar disorder (Lim et al., 1995) and ADHD (Manor et al., 2002). A similar association with serotonergic polymorphisms has been described for dimensional measures of normal var-

iance in personality traits linked to emotional reactivity and regulation. Examples include a broad range of personality traits like neuroticism (Gonda et al., 2009), trait anxiety (K.-P. Lesch et al., 1996) and impulsive aggression (Buckholtz & Meyer-Lindenberg, 2008). Further evidence confirms that genetic risk for complex psychiatric disorders overlaps with genetic influences on personality traits linked to negative emotionality. For instance, neuroticism and major depression appear to share some of their respective genetic backgrounds (Luciano et al., 2018).

Altered emotion regulation has been shown to be present in several psychiatric disorders (Fernandez et al., 2016) and is associated with treatment response (Slee et al., 2008) and present even after remission (Visted et al., 2018). This suggests that at the level of behavioural traits, emotion regulation might be underlying the link between risk for neuropsychiatric disorders and genetic variance in serotonergic genes.

Human neuroimaging research shows that the risk variants of some serotonergic polymorphisms are associated with altered brain function during functional fMRI tasks that activate the emotion processing system. The brain regions that were shown to be most consistently affected were predominantly in the limbic system and prefrontal regions (Hariri et al., 2005; Heinz et al., 2005; Lee & Ham, 2008; Meyer-Lindenberg et al., 2006; Passamonti et al., 2008). Similar alterations in brain structure have been shown in carriers of serotonergic risk variants. For instance, the short allele of the 5-HTTLPR length polymorphism is associated with reduced grey matter volume in the amygdala and the perigenual cingulate (Pezawas et al., 2005). Emotion processing in human relies on the efficient coordination of activity in a network of multiple brain regions including the amygdala, fusiform gyrus, hippocampus, striatum, thalamus, anterior cingulate cortex, insula, and orbitofrontal cortex (Etkin et al., 2015; Phillips et al., 2003). Prior research shows that this network is heritable (Budisavljevic et al., 2016) and implicated in genetic risk for neuropsychiatric disorders in humans (Cao et al., 2016; Dima et al., 2016) suggesting a potential link of serotonergic risk genes with connectivity in emotion processing networks. This is further supported by earlier research showing that the S allele of the 5-HTTLPR length-polymorphism is associated with altered 5-HTT concentrations and serotonin receptor binding potentials in multiple regions in the emotion processing network (David et al., 2005; Praschak-Rieder et al., 2007).

Serotonin transporter knock-out mice shows very similar alterations in brain regions within the emotion processing network (Fabre et al., 2000; Mathews et al., 2004; Rioux et al., 1999). Furthermore, knock-out animal models with modifications in the serotonergic system show a complex phenotype including alterations in emotion processing. Extensive phenotyping using batteries of tests showed increased anxiety and depression like behaviour in rodents lacking the serotonin transporter (Holmes et al., 2003) and MAO-A deficient mice display increased aggression and impulsivity (Godar et al., 2011; Scott et al., 2008).

Taken together, these findings suggest that genetic variance in polymorphisms linked to altered monoaminergic neurotransmission may impact the connectivity of multiple regions in the emotional processing network in humans and in turn, alter emotion processing abilities even in the general population.

1.6 Goals and hypotheses

Genetic variance in the serotonergic system has been repeatedly associated with structural and functional alterations in the limbic system in human neuroimaging studies. However, the mechanism underlying this link between genetic variance and the brain in humans is not well understood. Initial studies had several limitations, e.g. relative small sample sizes, focus on predefined regions of interest in the brain, and use of neuroimaging phenotypes with limited reliability. These shortcomings resulted in mixed evidence concerning the effect of serotonergic risk variants on neural structure and function. Initial neuroimaging findings relating genetic risk to neural alterations were hard to replicate and could not be consistently confirmed by meta-analytic evidence. A comprehensive understanding of the effect of serotonergic variants at the whole-brain level is still elusive.

The current project investigates connectomic network phenotypes in a large sample of thoroughly phenotyped healthy controls who underwent multimodal MRI, i.e. structural and functional using an extensive battery of neuroimaging tasks. For statistical comparison of genotype groups I applied an unbiased, whole-brain approach to detect potential effects of serotonergic risk variants on neural connectivity patterns.

More specifically, the following hypotheses were derived:

- 1) Network phenotypes are more sensitive to the subtle effects of typical genetic risk variants than traditional neuroimaging approaches. Therefore, network phenotypes might be beneficial for the study of genetic risk for psychiatric disorders on the brain.
- 2) Serotonergic risk variants affect connectivity patterns in fronto-temporal circuits confirming earlier work. Additionally, applying a whole-brain, connectomic approach will detect more widespread effects showing that the influence of serotonergic risk genes is not limited to specific brain regions.
- 3) Genetic variance in the serotonergic system impacts structural and functional connectivity patterns even without an active task. However, a task that challenges a significant cognitive domain, e.g. emotion processing might increase sensitivity.
- 4) Networks showing altered connectivity patterns in carriers of serotonergic risk variants are also associated with differences in emotion regulation.

To assess these hypotheses, we conducted two empirical studies investigating the relationship of genetic variation in the 5-HTTLPR and the *MAOA* polymorphism with brain connectivity at the neural network level and assessing clinical relevance of the potential network phenotypes by testing for potential associations with emotion processing.

The first empirical study aimed to identify potential connectomic phenotypes related to genetic variation in the 5-HTTLPR polymorphism in healthy participants. The study used functional magnetic resonance imaging (fMRI) and applied a well-established emotional face-matching task (Hariri et al., 2002). Specifically, this study aimed to (a) follow-up on earlier mixed results on the effects of this genotype on amygdala activation in a larger, well powered sample, (b) search for novel functional phenotypes linked to 5-HTTLPR genotype at the neural network level, and (c) investigate the utility and reliability of the identified network-based phenotype by multiple follow-up analyses. More specifically, this included probing the identified networks test–retest reliability, assessing the clinical relevance of the identified network phenotype by testing for associations with emotion regulation and assessing the specificity of potential findings by

testing for the presence of a structural basis or structural confounds in grey and white matter.

The aim of the second empirical study was to extend earlier research on *MAOA* by studying the human brain connectome using multimodal neuroimaging and a regionally unconstrained whole-brain network-based analysis approach that had to our knowledge, not been applied to the study of the *MAOA* polymorphism before. Again, the study analyzed healthy individuals to prevent confounding by the presence of psychiatric disorders. More specifically, the goal of the study was to examine whether functional connectomic alterations during negative emotion processing (a) are limited to the cortico-limbic circuits connected with variation in *MAOA* genotype by prior studies, (b) are specific to the emotion processing domain, and (c) go along with similar structural alterations in neural network architecture. In supplementary analyses, we additionally assessed the spatial distribution of *MAOA* sensitive links across several neuroimaging tasks probing different cognitive domains and neuroimaging modalities. We further tested the identified sub-networks for potential associations with emotion regulation ability and recent stressful life events to assess clinical relevance of the potential neuroimaging genetic findings. Based on the existing connectivity literature (Buckholtz et al., 2008; Denson et al., 2014), we expected to detect a regionally distributed pattern of “hyperconnected” link clusters in the *MAOA*-L carriers. We expected this hyperconnectivity pattern to extend across multiple brain functional domains and to include comparable structural connectomic alterations.

Please note that several parts of this thesis have already been published by the doctoral candidate as a first author. Therefore, certain sections, tables, or figures of this thesis will be identical to the following publications:

Cao H*, **Harneit A***, Walter H, Erk S, Braun U, Moessnang C, Geiger LS, Zang Z, Mohnke S, Heinz A, Romanczuk-Seiferth N, Mühleisen T, Mattheisen M, Witt SH, Cichon S, Nöthen MM, Rietschel M, Meyer-Lindenberg A, Tost H. The 5-HTTLPR Polymorphism Affects Network-Based Functional Connectivity in the Visual-Limbic System in Healthy Adults. *Neuropsychopharmacology*. 2018 43(2):406-414. Epub 2017 Jun 7. *Shared first authors.

Harneit A, Braun U, Geiger-Primo L, Zang Z, Hakobjan M, van Donkelaar MM, Schweiger J, Schwarz K, Gan G, Erk S, Heinz A, Romanczuk-Seiferth N, Witt S, Rietschel M, Walter H, Franke B, Meyer-Lindenberg A, Tost H. *MAOA*-VNTR genotype affects structural and functional connectivity in distributed brain networks. *Hum Brain Mapp*. 2019 40(18):5202-5212. Epub 2019 Aug 23.

2 MATERIALS AND METHODS

2.1 Empirical study 1

2.1.1 Participants

Two hundred and twenty-three healthy individuals with available data on 5-HTTLPR genotype as well as functional and structural imaging participated in empirical study 1 (mean age 33.35 ± 9.92 years, 107 males). The participants were recruited from the communities in Mannheim, Bonn and Berlin. All individuals were of European ancestry and had no first-degree relative with a mental illness. The exclusion criteria included a lifetime history of significant general medical, psychiatric or neurological illness, prior drug or alcohol abuse, and head trauma. The participants were assessed with neuro-psychological measures on emotion regulation and intelligence, including the Emotion Regulation Questionnaire (ERQ) (Abler & Kessler, 2009; Gross & John, 2003) and the Matrix Reasoning subscale of Wechsler Adult Intelligence Scale (WAIS-MR) (Wechsler, 1997). Stressful life events for the last two years were quantified using the Social Readjustment Rating Scale (SRRS) (Holmes & Rahe, 1967).

| Table 1: Sample Characteristics Stratified by 5-HTTLPR Genotype | | | | |
|---|---------------------|---------------------|---------------------|---------|
| | ll (n=55) | ls (n=108) | ss (n=60) | p-value |
| Demographic data | | | | |
| Age (year) | 34.47 ± 10.01 | 33.19 ± 9.72 | 34.30 ± 10.04 | 0.83 |
| Sex (M/F) | 27/28 | 55/53 | 25/35 | 0.51 |
| Site (Berlin/Bonn/Mannheim) | 20/27/8 | 55/41/12 | 20/26/14 | 0.08 |
| Education (year) | 15.33 ± 2.87 | 15.57 ± 2.44 | 15.65 ± 2.51 | 0.79 |
| Handedness (right/left/both) | 48/6/1 | 98/6/4 | 53/7/0 | 0.33 |
| Neuropsychological data | | | | |
| ERQ-suppression | 13.35 ± 4.72 | 13.06 ± 5.15 | 13.98 ± 4.30 | 0.53 |
| ERQ-reappraisal | 25.86 ± 7.03 | 27.25 ± 6.81 | 28.00 ± 6.70 | 0.27 |
| WAIS-MR | 20.51 ± 4.52 | 20.97 ± 3.44 | 20.98 ± 3.67 | 0.74 |
| SRRS | 327.36 ± 236.24 | 274.82 ± 180.85 | 277.93 ± 191.06 | 0.27 |
| fMRI task performances | | | | |
| Correct ratio face (%) | 98.79 ± 0.02 | 99.00 ± 0.02 | 98.89 ± 0.03 | 0.87 |
| Correct ratio form (%) | 97.27 ± 0.04 | 97.42 ± 0.04 | 98.06 ± 0.02 | 0.38 |
| fMRI data quality | | | | |
| Signal to noise ratio | 95.16 ± 16.04 | 93.22 ± 18.36 | 94.39 ± 20.69 | 0.81 |
| Sum motion translation (mm) | 0.42 ± 0.41 | 0.43 ± 0.37 | 0.36 ± 0.29 | 0.43 |
| Sum motion rotation (degree) | 0.63 ± 0.40 | 0.66 ± 0.55 | 0.59 ± 0.51 | 0.72 |
| Mean frame-wise displacement (mm) | 0.09 ± 0.04 | 0.09 ± 0.03 | 0.09 ± 0.04 | 0.76 |

Abbreviations: ERQ: Emotion Regulation Questionnaire; SRRS: Social Readjustment Rating Scale; WAIS-MR: Matrix Reasoning Subscale of Wechsler Adult Intelligence Scale, ll: long/long 5-HTTLPR Genotype, ls: long/short 5-HTTLPR Genotype, ss: short/short 5-HTTLPR Genotype

Note that ERQ subscale scores were calculated as the sum of contributing item scores, and SRRS were derived from the assessment of life events in the last 2 years.

Categorical variables are reported as numbers of cases, continuous variables are reported as mean and SD.

2.1.2 Genotyping

For each individual, DNA was extracted from EDTA anti-coagulated venous blood samples using standard techniques. Polymerase chain reaction was conducted following previously described methods with oligonucleotide primers flanking the polymorphic region (forward: 5'-TCCTCCGCTTTGGCGCCTCTTCC-3' and reverse: 5'-TGGGGGTTGCAGGGGAGATCCTG-3') (Wendland et al., 2006). The 5-HTTLPR was assessed with agarose gel electrophoresis. For the long allele a band of 512 basepairs and for the short allele a band of 469 basepairs were visible. In addition, we genotyped rs25531 A/G single nucleotide polymorphism (SNP) given the evidence that the G allele renders the L allele functionally similar to the S allele (i.e. LG is equivalent to S) (Hu et al., 2005). The SNP was genotyped using restriction enzyme digest of the PCR amplicon using HpaII and subsequent agarose gel electrophoresis. The observed genotype distribution did not deviate from Hardy-Weinberg equilibrium ($P = 0.94$).

Genotypes for all additional SNPs, including BDNF rs6265, were available from genotyping using Illumina Human 610-Quad and Illumina Human 660W-Quad Bead Arrays (Illumina, Inc. San Diego, CA, USA). Subsequently, subjects were classified into three groups based on the combination of the L/S and rs25531 A/G polymorphisms: ll group (including LA/LA, 55 subjects), ls group (including LA/LG and LA/S, 108 subjects), and ss group (including LG/LG, LG/S and S/S, 60 subjects). The three genotype groups did not show significant differences in demographic, psychological and fMRI performance data (all P -values > 0.08 , Table 1).

2.1.3 MRI Modalities and Task Paradigm

Multimodal magnetic resonance imaging (MRI) data were collected from all participants. During the fMRI scan, participants completed a well-established emotional face-matching task as previously described (Hariri et al., 2002). In brief, the face-matching task is an implicit emotional processing paradigm consisting of two conditions: an emotional face condition (matching faces) and a control condition (matching forms). In the emotional face condition, subjects were presented with trios of faces depicting fearful or angry expressions and were instructed to match the two facial displays belonging to the same individual. In the control condition, participants were presented with trios of geometric shapes (circles, vertical and horizontal ellipses) and were asked to match the two identical shapes. In addition, high-resolution T1-weighted images for each individual and diffusion weighted images (DWI) for part of the subjects (141 out of 223) were acquired. These data allow exploration of potential brain network changes at both the functional and structural level.

2.1.4 Data Acquisition

MRI data were acquired with three identical Siemens 3-Tesla scanner systems (Siemens Trio, Erlangen, Germany) located in Berlin, Bonn and Mannheim. The fMRI and T1-weighted images were acquired with the same protocol across sites whereas DWI data were acquired with slightly different protocols. For fMRI data, gradient-recalled echo-planar imaging (GRE-EPI) sequences were used with the following parameters: TR 2000ms, TE 30ms, 28 oblique slices per volume, 4mm slice thickness, 1mm slice distance, 80° flip angle, 192mm FOV, and 64 × 64 matrix. High-resolution T1 image data were acquired by using 3D magnetization-prepared rapid gradient-echo (MP-RAGE) sequences with the following parameters: TR 1570ms, TE 2.75ms, TI 800ms, 176 sagittal slices, 1 mm voxel size, 256mm FOV, and 15° flip angle. DWI data were acquired by using spin echo EPI sequences with the following parameters: 1) Mannheim: TR 14000ms, TE 86ms, 2mm slice thickness, 60 non-collinear directions, b-value 1000 s/mm², 1 b0 image, FOV 256 mm; 2) Bonn: TR 12000ms, TE 100ms, 1.7mm slice thickness, 60 non-collinear directions, b-value 1000 s/mm², 11 b0 images, FOV 220mm; 3) Berlin: TR 8200ms, TE 92ms, 2.3mm slice thickness, 64 non-collinear directions, b-value 1200 s/mm², 7 b0 images, FOV 220mm; 4) additional Mannheim cohort: TR 1400ms, TE 93ms, 1.7mm slice thickness, 60 non-collinear directions, b-value 1500 s/mm², 3 b0 images, FOV 220mm.

2.1.5 Data Quality Control

For assessment of fMRI data quality, we quantified several head motion parameters as previously described (Cao et al., 2016; Plichta et al., 2012; Yan et al., 2013), including the sum of volume-to-volume translational excursions across the time series, the sum of volume-to-volume rotational excursions across the time series, and the mean voxel-based frame-wise displacement. Volume-to-volume excursions were calculated as the difference of the root mean squared translation ($\text{rms}(x^2+y^2+z^2)$) or root mean squared rotation ($\text{rms}(\alpha^2+\beta^2+\gamma^2)$) between two successive volumes. Moreover, the signal-to-noise ratios (SNR) for each participant were computed using the New York University dataQuality toolbox (<http://cbi.nyu.edu/software/dataQuality.php>). As shown in Table 1, the three genotype groups were well balanced for all image quality measures ($P > 0.43$).

2.1.6 Amygdala Activation Analysis

The first analysis of study 1 attempted to replicate the association between 5-HTTLPR and amygdala activation findings reported in previous studies (Hariri et al., 2005; Hariri et al., 2002). Here, we closely followed the methods detailed in these studies and used standard procedures in Statistical Parametric Mapping (SPM8, <http://www.fil.ion.ucl.ac.uk/spm/software/spm8/>). In brief, functional images were realigned to the first image of the scan, slice time corrected, normalized to the Montreal Neurological Institute brain template with resampling to 3 × 3 × 3 mm³ voxels, and spatially smoothed with a 9 mm full-width at half-maximum Gaussian kernel. The pre-processed images were then subjected to first-level general linear model estimation, where data were high-pass filtered (cutoff 128 s) and individual maps of the ‘face-matching>form-matching’ contrast were computed. The contrast images were used for a second-level random effects analysis. Here, two different models were employed: a linear regression model with genotypes ll, ls, and ss encoded as 0, 1 and 2,

and an analysis of covariance (ANCOVA) model where subjects with risk allele *s* were compared with those with *ll* (*ll* vs *s*, ie, the same model as used in Hariri et al (Hariri et al., 2002). In both models, age, sex, and site were included as nuisance covariates. As in prior work, results were reported after family-wise error (FWE) correction across the mask of bilateral amygdala from the Automated Anatomical Labeling atlas (Tzourio-Mazoyer et al., 2002).

2.1.7 Brain Functional Network Analysis

The functional network analysis followed previously published procedures of our group (Cao et al., 2016; Cao, Plichta, Schäfer, et al., 2014). Here, mean time series for each of the 270 nodes detailed in Power et al (Power et al., 2011) were extracted from the preprocessed images. Notably, the original Power atlas only contained 264 nodes without bilateral hippocampus, bilateral amygdala, and bilateral ventral striatum. To achieve whole-brain coverage, we included these nodes based on previously published coordinates from meta-analyses (Liu et al., 2011; Sabatinelli et al., 2011; Spreng et al., 2009), thereby increasing the total number of nodes to 270 (one node per region and hemisphere). The time series were then corrected for mean effects of task conditions, white matter and cerebrospinal fluid signals, and six head motion parameters, and were high-pass filtered (cutoff 128 s). Afterwards, we computed pairwise Pearson correlation coefficients between the processed time series of each node, resulting in a 270×270 two-dimensional connectivity matrix for each subject.

Following the procedures described in earlier work from our group (Cao et al., 2016), we used network-based statistic (NBS) to identify clusters of functional links that were linearly correlated with the number of risk allele *s*. NBS is a statistical method that can be applied to identify connections in a whole brain network that are related to a variable of interest like genotype group. This method tests all connections of the graph making up the brain network for potential associations with measures of interest and effectively controls cluster-level FWE for link-wise comparisons, which provides a larger power than mass-univariate tests on independent links. To achieve this increased power, NBS utilizes the high level of interconnectedness between the connections involved in the effect or contrast of interest (Zalesky et al., 2010).

Here, an initial linear model for the three genotypes *ll*, *ls*, and *ss* (encoded as 0, 1, and 2) was applied to each of the $N(N-1)/2=36315$ ($N=270$) links in the connectivity matrices, with age, sex, and site as covariates of no interest. This produced a P-value matrix representing the probability of accepting the null hypothesis for each link. All links with $P\text{-values} \leq 0.0001$ were then thresholded into a set of suprathreshold links, and connected subnetwork clusters were subsequently identified from the set. The significance of the identified clusters was tested by 5000 permutations, where each subject was randomly reassigned into a genotype group during each permutation and the maximal extent of the identified cluster was recalculated. The corrected P-value for the identified cluster was determined by the proportion of the derived cluster sizes in the permutation distribution that were larger than the observed group difference.

2.1.8 Follow-up analyses of the Identified Functional Network

Following the strategy used in prior work of our group (Cao et al., 2016) we performed several supplementary analyses to probe the validity of the identified subnetwork by examining its test-retest reliability, neuropsychological associations, and potential

structural confounds. Here, we reduced data dimensionality by averaging the connectivity of subnetwork links and gray matter volumes of subnetwork nodes for each subject. This aimed to increase sensitivity and to stay consistent with the NBS method *per se*, which treats the whole cluster as an entity for which the null hypothesis can only be rejected at the cluster level (Zalesky et al., 2010).

2.1.9 Test–retest reliability

Test–retest reliability is an important quality measure for a potential imaging phenotype. Here, we reanalyzed the test–retest data from a prior study published by our group (Cao, Plichta, Schäfer, et al., 2014) where 26 healthy subjects were scanned twice with the same emotional face-matching task within 2 consecutive weeks (mean time interval: 14.6 ± 2.1 days, mean age: 24.4 ± 2.8 years, 11 males, see (Cao, Plichta, Schäfer, et al., 2014) for sample details). Data processing and analysis followed the same procedures described above, and the mean connectivity estimates of the subnetwork were extracted for each subject and session. Intra-class correlation coefficients (ICCs) were used to quantify reliability, including ICC(2,1) and ICC(3,1), which reflect absolute agreement and relative consistency of the measurements between sessions, respectively. Based on established criteria (Cicchetti & Sparrow, 1981), $ICC > 0.40$ indicates fair reliability, and $ICC > 0.59$ indicates good reliability.

2.1.10 Relationship to emotion regulation

As 5-HTTLPR is a key regulator of the serotonin system and has been related to (mal)adaptive responses to emotional experiences (Caspi et al., 2003), we further examined whether individuals with higher or lower subnetwork connectivity differed in their preferred tendency to regulate emotions. Here, we analyzed the subscale scores of the ERQ, a 10-item scale measuring the respondents' tendency to regulate their emotions by either cognitive reappraisal or expressive suppression (Gross & John, 2003). For the analysis, we median-split participants into low and high connectivity groups and used ANCOVA models for the statistical comparison of ERQ subscale scores between groups, controlling for age, sex and site. Significance was set at $P < 0.05$ after multiple corrections for both the suppression and the reappraisal subscale.

2.1.11 Specificity of the identified genetic association

To assess the specificity of the identified subnetwork showing a negative association with the number of risk alleles for 5-HTTLPR, the network-based statistic (NBS) analysis described in paragraph 2.1.7 was repeated for an additional unrelated genetic polymorphism, the rs6265 in the brain derived neurotrophic factor (BDNF) gene. The rs6265 Val66Met is a non-synonymous coding variant which causes a valine to methionine substitution in the BDNF gene. This gene encodes for brain derived neurotrophic factor, a key regulator of neural plasticity and development (Minichiello, 2009). The BDNF rs6265 polymorphism has been associated with altered activity-dependent BDNF secretion (Egan et al., 2003) brain structure and function (Egan et al., 2003; Ho et al., 2006; Montag et al., 2009), deficits in cognition (Egan et al., 2003; Pezawas et al., 2004; Tost et al., 2013) and susceptibility for a host of psychiatric disorders, includ-

ing depression (Verhagen et al., 2010), bipolar disorder (Sklar et al., 2002) and schizophrenia (Neves-Pereira et al., 2005). The NBS analysis for the BDNF rs6265 polymorphism was performed using exactly the same parameters as specified in the manuscript. Apart from the original stringent threshold used in our main analysis ($P < 0.0001$), we also examined the association using two more liberal thresholds ($P < 0.001$ and < 0.005). Out of the 223 subjects included in the main analysis, BDNF rs6265 genotypes were available for 210 individuals (130 G/G, 69 A/G, 11 A/A). Due to the low frequency of the A allele, genotypes A/A and A/G were combined into a single A-carrier group for statistics. A multiple regression model with BDNF rs6265 genotype (A-carriers, GG) as variate of interest, and age, sex and site as nuisance covariates was applied.

In addition to the BDNF gene analysis, we performed another supplemental analysis to further confirm the specificity of our main finding. In this analysis, we tested 10,000 randomly selected SNPs for potential associations with mean functional connectivity of the identified subnetwork. Whole-genome genotype data were available for 210 of the individuals included in the main analysis. Mean connectivity estimates for the subnetwork were extracted for these participants. The set of available SNPs was pruned using a linkage disequilibrium (LD) cutoff of $R^2 = 0.8$. Further quality control was performed to exclude SNPs with missing genotype information for any of the 210 participants and with low minor allele frequencies (i.e. less than 20 individuals for any genotype subgroups). From a set of 124,663 SNPs meeting the specified criteria, 10,000 SNPs were randomly selected. Each of these randomly selected SNPs was tested for potential association with the mean subnetwork connectivity using an ANCOVA model with genotype as variate of interest and sex, age and site as variates of no interest. Bonferroni correction for multiple testing was applied ($P < 5e-6$).

2.1.12 Voxel-based morphometry (VBM)

As 5-HTTLPR genotype has been associated with altered volume of several brain regions in earlier studies (Frodl et al., 2008; Pezawas et al., 2005), we further tested whether the identified functional alterations were related to gray matter differences. Here, we analyzed high-resolution T1 structural data for each subject with VBM. The data preprocessing procedures followed those of a previously published study from our group (Cao et al., 2016) and the defaults implemented in the VBM8 toolbox (<http://dbm.neuro.uni-jena.de/vbm8/>). In brief, the images were tissue segmented, spatially normalized to the MNI space with a diffeomorphic image registration algorithm (DARTEL), corrected for image intensity non-uniformity and global brain gray matter volume, and smoothed with a 10 mm FWHM Gaussian kernel. The mean gray matter volumes across all subnetwork nodes for each subject were entered as dependent variable into an ANCOVA model with genotype (ll, ls, ss) as variable of interest and age, sex, and site as nuisance covariates. In addition, partial correlation was used to examine the association between mean gray matter volume and mean subnetwork connectivity while controlling for age, sex, and site.

2.1.13 Tract-based spatial statistics (TBSS)

Earlier studies suggest an association between 5-HTTLPR genotype and microstructural integrity of brain white matter tracts (Benedetti et al., 2015; Pacheco et al., 2009). To test potential white matter correlates, we performed an analysis for participants with available DWI data (141 subjects, 39 ll, 62 ls, 40 ss) using TBSS implemented in the

FMRIB Diffusion Toolbox (<http://www.fmrib.ox.ac.uk/fsl/>). For DTI preprocessing the following preprocessing steps were performed: correction of the diffusion images for head motion and eddy currents by affine registration to a reference (b0) image, extraction of non-brain tissues (Smith, 2002), and linear diffusion tensor fitting. The resulting maps contained voxel-wise parameter estimates for fractional anisotropy (FA), radial diffusivity (RD) and axial diffusivity (AD) in individual spaces. After data preprocessing, statistical analysis was performed using TBSS (Smith et al., 2006). First, all FA images were non-linearly registered into a common reference space (FMRIB58_FA template) using the FMRIB's Non-linear Registration Tool (FNIRT) (Rueckert et al., 1999). Subsequently, the resulting transformation matrices were applied to axial and radial diffusivity maps. The mean FA image was calculated to create the mean FA 'skeleton', an alignment-invariant representation of the center of all tracts common to the group. A threshold of $FA > 0.2$ was chosen to minimize the effects of incidental tracts and partial voluming. Each subject's aligned FA data were then projected onto this skeleton via perpendicular search for the highest FA value. The estimated non-linear warps and projection vectors were subsequently used to register each individual's diffusion data onto the skeleton. The processed images were then fed into a linear regression model with genotypes ll, ls, and ss (encoded as 0, 1 and 2) as variable of interest and age, sex and site as nuisance variables. Statistical inference was performed using FSL Randomize with 5000 permutations and the significance threshold was set to $P < 0.05$ after FWE correction. To restrict the initial analysis to white matter structures anatomically consistent with the identified subnetwork, we constricted our search range by creating a merged mask of the major visual-limbic fiber tracts (i.e., bilateral cingulate fasciculus, inferior longitudinal fasciculus and uncinate fasciculus) as defined by the Johns Hopkins University (JHU) white matter atlas (Susumu Mori, 2005). In addition, to explore potential genotype effects outside this mask, a secondary analysis of whole fractional anisotropy (FA) skeleton was also performed. In addition, given that only 141 individuals had available DWI data, we further added the DWI data of additional 89 healthy subjects from a different cohort into the analysis to achieve a comparable sample size between the functional and structural studies. The added subjects were recruited from communities in and around Mannheim (mean age 26.52 ± 9.28 years, 35 males). The same DTI analysis was then performed in the combined sample (in total 230 subjects, 65 ll, 106 ls, 59 ss).

2.2 Empirical study 2

2.2.1 Participants

We included data from 219 to 284 healthy adult participants per neuroimaging modality. Individuals were of European ancestry and were recruited from the general population at three German sites (Mannheim, Berlin, Bonn). General exclusion criteria were a lifetime history of significant general medical, psychiatric, or neurological illness, the presence of a first-degree relative with a history of psychiatric illness, prior drug or alcohol abuse, and head trauma. All subjects provided written informed consent for protocols approved by the institutional ethical review boards of the Universities of Heidelberg, Bonn, and Berlin. Demographic and clinical information was available for all individuals. Data on the preferred tendency to regulate emotions (as measured by the Emotion Regulation Questionnaire, ERQ) were available in a subset of 259 individuals (Gross & John, 2003). Data on the extent of stressful life events in the preceding 2 years (as measured by the social readjustment rating scale, SRRS) were available in a subset of 260 individuals (Holmes & Rahe, 1967).

2.2.2 MAOA genotyping

| Table 2: MAOA genotype distribution | | | | | | | | | | | | |
|-------------------------------------|----------------------|-----------|-----------|----------------------|---------------|-----------|-------------------|-------------|-------------|-----------|-----------|-----------|
| | L hemi-/ homozygotes | | | H hemi-/ homozygotes | | | L/H heterozygotes | | | | | |
| Female s | 2r/2 r | 3r/3 r | 5r/5 r | 3.5r/4 r | 3.5r/3.5 r | 4r/4 r | 2r/3.5 r | 3r/3.5 r | 5r/3.5 r | 2r/4 r | 3r/4 r | 5r/4 r |
| | 1 | 27 | 1 | 5 | 0 | 129 | 0 | 2 | 0 | 0 | 104 | 4 |
| Males | 2r | 3r | 5r | 3.5r | 4r | - | | | | | | |
| | 1 | 85 | 4 | 3 | 138 | | | | | | | |

We genotyped a total of 504 individuals using standard methods to extract genomic DNA from lymphoblastoid cell lines. The MAOA 30 bp repeat polymorphism was genotyped using 30 ng genomic DNA as template. PCR was performed with 1x AmpliTaq Gold® 360 Master Mix (Life Technologies) and 0.33 mM fluorescently labeled forward primer (FAM, VIC, PET or NED - 5'- ACAGCCTGACCGTGGAGAAG-3') and reverse primer (5'- GAACGGACGCTCCATTCGGA -3') in a total volume of 7,5 µl. Amplification was performed using the following protocol: 95°C for 10 min followed by 35 cycles of denaturation for 30 s at 95°C, 30 s annealing at 60°C, and primer extension at 72°C for 1 min, followed by a final extension at 72°C for 10 min. The product of the amplification was diluted 1:20 in H₂O.

Determination of the length of the alleles was performed by direct fragment length analysis on an automated capillary sequencer (ABI3730, Applied Biosystems, Nieuwerkerk a/d IJssel, The Netherlands) using standard conditions (1 µl of the diluted PCR product together with 9.7 µl formamide and 0.3 µl GeneScan-600 Liz Size Standaard™ (Applied Biosystems, Nieuwerkerk aan de IJssel, the Netherlands)). Results were analyzed with Genemapper version 4.0 (Applied Biosystems). Generally, the MAOA genotyping assay has been validated earlier, and 5% blanks as well as duplicates between plates were taken along as quality controls during genotyping.

Genotyping was performed in a JCI-accredited laboratory at the Department of Human Genetics of the Radboud University Medical Center in Nijmegen. We categorized 2, 3 and 5 copies of the repeat sequence as MAOA-L and 3.5. or 4 copies as MAOA-H (Guo et al., 2008). The exact allele frequencies are given in table 2. As detailed in the main manuscript, we excluded all MAOA female heterozygotes from subsequent analysis.

Since the MAOA gene is located on the X chromosome, males are hemizygous carriers of either one L or H allele. Women carry two alleles and can thus be heterozygous, although one of the two alleles is (fully or incompletely) silenced by random X chromosome inactivation (Berletch et al., 2011). We addressed this ambiguity by excluding all MAOA heterozygous females from subsequent analysis. Sex distribution differed significantly between MAOA genotype groups in our study cohort ($p < .001$). We addressed this issue by adding sex as a covariate in all statistical analyses. There were no additional significant differences in demographic, psychological, and fMRI performance data between genotype groups (all p -values > 0.27 Table 3).

Table 3: Sample characteristics stratified by MAOA genotype

| | H allele carriers | L allele carriers | p-value |
|---|--------------------------|--------------------------|----------------|
| <i>Demographics</i> | | | |
| Age (year) | 33.69 ± 10.00 | 33.18 ± 9.53 | 0.69 |
| Sex (males/females) | 107 / 89 | 65 / 15 | <0.001 |
| Site (Berlin/Bonn/Mannheim) | 50 / 81 / 65 | 24 / 33 / 23 | 0.68 |
| Education (years), mean ± SD | 15.35 ± 2.48 | 15.69 ± 2.71 | 0.32 |
| Handedness (right/left/both) | 174 / 17 / 4 | 73 / 6 / 1 | 0.85 |
| <i>Questionnaires</i> | | | |
| ERQ-suppression | 14.13 ± 4.99 | 13.30 ± 4.78 | 0.91 |
| ERQ-reappraisal | 27.12 ± 6.57 | 27.49 ± 6.87 | 0.62 |
| SRRS | 273.05 ± 190.77 | 321.11 ± 203.93 | 0.76 |
| <i>fMRI task performance</i> | | | |
| Faces condition (% correct) | 98.74 ± 2.84 | 97.97 ± 4.89 | 0.32 |
| Forms condition (% correct) | 97.28 ± 4.07 | 96.64 ± 5.02 | 0.55 |
| 2-back condition (% correct) | 75.91 ± 21.47 | 73.75 ± 21.19 | 0.40 |
| 0-back condition (% correct) | 98.41 ± 5.93 | 98.40 ± 5.39 | 0.94 |
| <i>MRI data quality</i> | | | |
| Faces task: Mean frame-wise displacement (mm) | 0.16 ± 0.08 | 0.17 ± 0.08 | 0.99 |
| n-back task: Mean frame-wise displacement (mm) | 0.14 ± 0.006 | 0.13 ± 0.06 | 0.27 |
| Resting task: Mean frame-wise displacement (mm) | 0.17 ± 0.06 | 0.16 ± 0.05 | 0.48 |
| DTI: Mean frame-wise displacement (mm) | 0.86 ± 0.33 | 0.81 ± 0.32 | 0.32 |

Abbreviations: DTI, diffusion tensor imaging, ERQ, Emotion Regulation Questionnaire (calculated as the sum of contributing subscale item scores), SRRS, social readjustment rating scale (calculated from the assessment of life events in the last 2 years). Categorical variables are reported as numbers of cases, continuous variables are reported as mean and standard deviation (SD).

2.2.3 MRI data acquisition

We collected multimodal magnetic resonance imaging (MRI) data with three identical Siemens 3-T scanner systems (Siemens Trio, Erlangen, Germany) located at the three sites. Table 5 provides an overview of participant numbers and characteristics for each data modality.

For fMRI data acquisition, we used gradient-recalled echo-planar imaging (GRE-EPI) sequences with the following parameters: TR 2000ms, TE 30ms, 28 oblique slices per volume, 4mm slice thickness, 1mm slice distance, 80° flip angle, 192mm FOV, and 64 × 64 matrix. For DTI data acquisition, we used spin echo EPI sequences with the following parameters: 1) Mannheim: TR 14000ms, TE 86ms, 2mm slice thickness, 60 non-collinear directions, b-value 1000 s/mm², 1 b0 image, FOV 256 mm; 2) Bonn: TR

12000ms, TE 100ms, 1.7mm slice thickness, 60 non-collinear directions, b-value 1000 s/mm², 11 b0 images, FOV 220mm; 3) Berlin: TR 8200ms, TE 92ms, 2.3mm slice thickness, 64 non-collinear directions, b-value 1200 s/mm², 7 b0 images, FOV 220mm. Since good quality DTI data were only available for a subset of 211 individuals we added 73 DTI data sets from an additional adult cohort of healthy volunteers to obtain comparable sample sizes for the functional and the structural connectivity analyses. The spin echo EPI sequence of the additional Mannheim cohort had the following parameters: TR 1400ms, TE 93ms, 1.7mm slice thickness, 60 non-collinear directions, b-value 1500 s/mm², 3 b0 images, FOV 220mm.

Table 4: Characteristics of individuals included in the neuroimaging analyses

| | DTI | Faces task | Resting state | N-back |
|----------------------------------|-------------------|-------------------|----------------------|------------------|
| Sample size (n) | 284 | 247 | 219 | 254 |
| Site (Mannheim/Berlin/Bonn) | 142 / 41/101 | 63 / 73 / 111 | 57 / 56 / 106 | 66 / 74 / 114 |
| MAOA genotype (H/L) | 200 / 84 | 175 / 72 | 155 / 64 | 179 / 75 |
| Sex (males/females) | 162 / 122 | 159 / 88 | 138 / 81 | 162 / 92 |
| Age (years), mean \pm SD | 31.81 \pm 10.23 | 34.38 \pm 9.83 | 32.53 \pm 9.69 | 34.30 \pm 9.85 |
| Education (years), mean \pm SD | 15.53 \pm 2.49 | 15.42 \pm 2.63 | 15.44 \pm 2.53 | 15.39 \pm 2.63 |

Table 5: Characteristics of individuals included in the sex-matched samples

| | DTI | Faces task | Resting state | N-back |
|----------------------------------|-------------------|-------------------|----------------------|------------------|
| Sample size (n) | 244 | 176 | 162 | 184 |
| Site (Mannheim/Berlin/Bonn) | 122/37/85 | 46/56/74 | 42/42/78 | 49/52/83 |
| MAOA genotype (H/L) | 200/44 | 148/28 | 138/24 | 156/28 |
| Sex (males/females) | 122/122 | 88/88 | 81/81 | 92/92 |
| Age (years), mean \pm SD | 31.62 \pm 10.29 | 34.53 \pm 9.77 | 32.30 \pm 9.71 | 34.17 \pm 9.81 |
| Education (years), mean \pm SD | 15.47 \pm 2.46 | 15.24 \pm 2.52 | 15.33 \pm 2.41 | 15.21 \pm 2.51 |

2.2.4 MRI paradigms

We used three well-established fMRI tasks probing implicit emotion processing (emotional face matching task), resting-state (rs-fMRI) and working memory (n-back task), as previously described in detail (Callicott et al., 2003; Cao, Plichta, Schäfer, et al., 2014; Hariri et al., 2002). All participants were thoroughly trained on the tasks prior to the scan.

The emotional face matching task (Hariri et al., 2002) is described in more detail in paragraph 2.1.3. In brief, is an implicit emotion processing task consisting of an emotional face condition and a control condition. In the emotional face condition, participants were presented with trios of faces showing either angry or fearful expressions and were instructed to match the two facial displays belonging to the same individual. In the control condition, participants were presented with geometric shapes and were instructed to match the identical shapes. The task consisted of eight performance blocks of six trials or 30 s each, with alternating epochs of face- and form-matching conditions (task duration: 4.3 min or 130 whole-brain scans).

Working memory function was studied with an n-back paradigm (Callicott et al., 2004). Briefly, a series of visual stimuli (numbers one to four) was displayed on a screen in a random order at set locations in a diamond-shaped box. Participants responded to each stimulus via a MRI compatible button box with four buttons arranged in the same configuration as the stimuli presented on the screen. In the 2-back working memory condition, participants were asked to encode the currently seen number, simultaneously recall the number seen two presentations previously, and press the button corresponding to the position of the number two presentations earlier. In the control condition (0-back), subjects were asked to press the button corresponding to the position of the current number presentation. The task was presented in eight blocks of 30 seconds each with alternating 0-back and 2-back conditions (task duration: 4.1 min or 124 whole-brain scans). During the resting state scan (Cao, Plichta, Schäfer, et al., 2014), participants were instructed to close their eyes, relax, and refrain from any particular mental activity (task duration: 5.0 min or 150 whole-brain scans). After each scan, investigators confirmed with the participant that they had not fallen asleep in the scanner.

2.2.5 Functional MRI data processing and connectome construction

Functional networks were constructed following previously published procedures (Cao, Plichta, Schäfer, et al., 2014; Zang et al., 2018) using SPM8 and MATLAB and is similar to the approach described in paragraph 2.1.7. In short, data preprocessing included realignment to the mean image of the time series, slice time correction, spatial normalization to the Montreal Neurological Institute (MNI) EPI template, and smoothing with an 8 mm full-width at half-maximum (FWHM) Gaussian kernel. For each participant and fMRI task, we then extracted the mean time series from the 116 brain regions (or nodes) defined by the automated anatomical labeling (AAL) atlas (Tzourio-Mazoyer et al., 2002). From the node time series, we regressed out white matter and cerebrospinal fluid signals, the mean effect of task conditions (active tasks only), and the six head motion parameters from the realignment step. The resulting residual time series were temporally filtered using a 0.008–0.1 Hz bandpass filter for the resting-state data and a highpass filter (cut-off 128 s) for the face matching and n-back data. As functional connectivity data can be severely affected by head micromovements, we used in-house software to estimate frame-wise displacement (FD) for all functional data and scrubbed all data frames with a FD > .5 mm and interpolated the missing frames using a B-spline interpolation. Subjects with more than 10% affected data frames were excluded from the analysis. We then calculated pairwise Pearson correlation coefficients between each pair of nodes resulting in a 116×116 connectivity matrix for each subject and functional data type.

2.2.6 Structural MRI data processing and connectome construction

DTI data preprocessing was performed with standard routines implemented in the software package FSL (Smith et al., 2004) including the following steps: correction of the diffusion images for head motion and eddy currents by affine registration to a reference (b0) image, extraction of nonbrain tissues, and linear diffusion tensor fitting. After estimation of the diffusion tensor, we performed deterministic whole-brain fiber tracking as implemented in DSI Studio using a modified FACT algorithm (Yeh et al., 2013). For the construction of structural connectivity matrices, we initiated 1,000,000 streamlines for each participant. Streamlines with a length of less than 10 mm were removed. The total number of successful streamlines between each pair of nodes defined by the AAL atlas was then used as estimates of structural connectivity, resulting in a 116×116 connectivity matrix for each subject.

2.2.7 Data analysis and statistical inference

We used network-based statistics (NBS) to identify clusters of functional and structural links significantly differing between *MAOA* genotype groups. NBS is a well-established method for controlling cluster-level family-wise error (FWE) rates for link-wise comparisons while providing an increased power compared to mass-univariate tests on individual links (Zalesky et al., 2010). For comparability between data modalities, we used the following identical analysis parameters for all fMRI and DTI data: We identified suprathreshold links and sets of connected link clusters using ANOVA models with genotype as between-subjects factor (*MAOA* high vs. *MAOA* low) and the covariates age, sex, data acquisition site, and sequence protocol (initial threshold: $p \leq .005$, uncorrected). The significance of the link clusters was assessed by performing 5,000 permutations, in which subjects were randomly reassigned to genotype groups, and the maximal extent of the identified cluster was recalculated. The FWE-corrected p -value for the identified clusters was determined by the proportion of cluster sizes in the permutation distribution that was larger than the cluster sizes of the observed group difference. This procedure was applied to all imaging modalities.

2.2.8 Supplemental exploratory analyses

To further quantify the spatial distribution of *MAOA*-affected node connections across the brain and descriptively compare the outcome between different neuroimaging tasks and modalities, we post hoc quantified and illustrated the percentage of significant “isocoupled” versus “anisocoupled” links, that is, connections between neural nodes within the same versus between different major brain subdivisions as defined by the six supraordinate labels of the AAL atlas (i.e., frontal, parietal, occipital, temporal, cingulate, and subcortical regions). Moreover, since *MAOA* is located on the X chromosome, and the gene is of interest for impulsivity and aggression, we further explored the potential impact of sex on the identified *MAOA*-associated cluster links by testing the mean cluster connectivity estimates for potential genotype by sex interaction effects across all imaging modalities. In addition, we tested whether the reported effects of *MAOA* genotype on cluster connectivity remains stable in subsamples with sex-matched genotype groups and in separate analyses of males and females, respectively. Details on the participant numbers of the sex-matched supplemental analyses are provided in table 5.

2.2.9 Relationship to emotion regulation

In addition, since *MAOA* genotype has been linked to dysfunctional responses to negative emotional events (Kim-Cohen et al., 2006), we explored whether the connectivity estimates of the identified *MAOA*-associated sub-networks across tasks and modalities related to the tendency of individuals to employ a maladaptive emotion regulation strategy. For this, we first quantified the mean sub-network connectivity estimates for the *MAOA*-associated networks and the scores for ERQ subscales, representing two emotion regulation strategies, “cognitive reappraisal” (higher values indicate psychiatric resilience) and “expressive suppression” (higher values indicate psychiatric risk) for each individual and subsequently calculated Pearson correlation coefficients, controlling for age, sex, and data acquisition site. We used analogous procedures to test sub-networks across tasks and modalities for potential associations with recent stressful life events (SRRS total scores).

3 RESULTS

3.1 Empirical study 1

3.1.1 Amygdala Activation Analysis

In our sample of 223 healthy subjects, we did not detect significant differences in amygdala activation between the three genotypes, neither in the regression (small-volume PFWE=0.80) nor in the ANCOVA model (small-volume PFWE=0.79).

3.1.2 Network-Based Functional Connectivity Analysis

The NBS analysis identified a functional cluster showing significantly negative correlation between the connectivity estimates of the cluster links and the number of risk alleles (PFWE=0.03, Figure 7a). The cluster consisted of 14 links interconnecting 15 pairs of nodes that primarily mapped to the limbic system (hippocampus, orbitofrontal cortex, anterior cingulate gyrus), visual system (middle occipital gyrus, fusiform gyrus, middle, and inferior temporal gyrus) and subcortex (putamen and thalamus) (see Table 6 for details). The mean connectivity across all links in the cluster was significantly decreased in ls and ss carriers ($P=7e-15$, Figure 7b).

3.1.3 Test–Retest Reliability of the Phenotype

Analysis of the test–retest data revealed relatively high ICC values for the connectivity metrics of the identified subnetwork ($ICC(2,1)=0.69$, $ICC(3,1)=0.68$). This suggests good reliability of the NBS-based subnetwork connectivity estimates.

3.1.4 Relationship to Emotion Regulation

The ANCOVA model revealed a significant difference between the low and high subnetwork connectivity groups with respect to the ERQ suppression scores ($F=6.71$, $P=0.01$, Figure 7e). Here, the group with the lower connectivity showed significantly higher emotion suppression scores than that with the higher connectivity, suggesting that healthy individuals with a lower coupling of the subnetwork are more likely to employ a maladaptive strategy for emotion regulation. No significant group difference was detected for the ERQ reappraisal scores ($F=0.78$, $P=0.38$).

3.1.5 Specificity of the identified genetic association

No significant associations between BDNF rs6265 genotype and network-based functional connectivity were detected by NBS at any of the range of tested thresholds (PFWE > 0.14).

Likewise, no significant associations with connectivity of the 5-HTTLPR- sensitive subnetwork were observed for any of the 10,000 tested randomly selected SNPs after Bonferroni correction (see Figure 6). In contrast, the association between 5-HTTLPR and subnetwork connectivity remained significant even at this very conservative correction threshold ($P = 7e-15$).

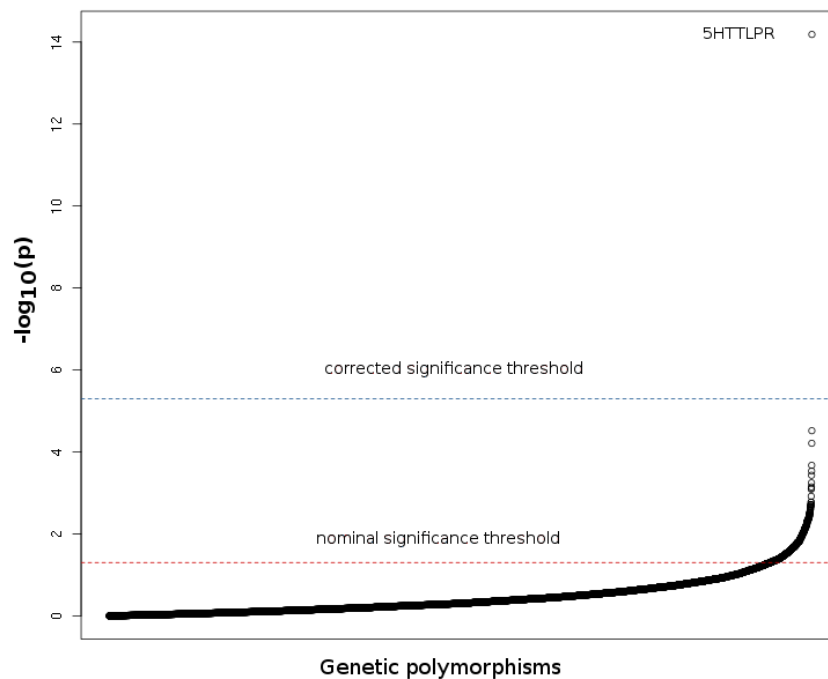


Figure 6: 10,000 randomly selected SNPs were tested for potential associations with mean functional connectivity of the identified subnetwork. Only the association between 5-HTTLPR and subnetwork connectivity remained significant after correcting for multiple comparisons.

3.1.6 Gray Matter Structural Analysis

The VBM analysis revealed no significant differences in mean gray matter volumes of the subnetwork nodes between genotype groups ($F=1.08$, $P=0.34$, Figure 7c) and no significant correlation between mean gray matter volumes and subnetwork connectivity measures ($r=0.05$, $P=0.45$). This suggests that the identified functional network alteration is independent of genotype-related differences in gray matter.

3.1.7 White Matter Structural Analysis

The initial TBSS analysis of 141 individuals revealed no significant differences in FA between genotype groups in visual-limbic fiber bundles ($PFWE>0.6$, Figure 7d). The inclusion of 89 additional subjects further confirmed this negative finding ($PFWE>0.62$). Extending the FA analysis to the whole brain white matter skeleton did not reveal any genotype effect either ($PFWE>0.27$). Similar results emerged in additional analyses focusing on radial and axial diffusivity ($PFWE>0.22$). Together these findings suggest that the identified functional network alteration is independent of genotype-related differences in white matter structure.

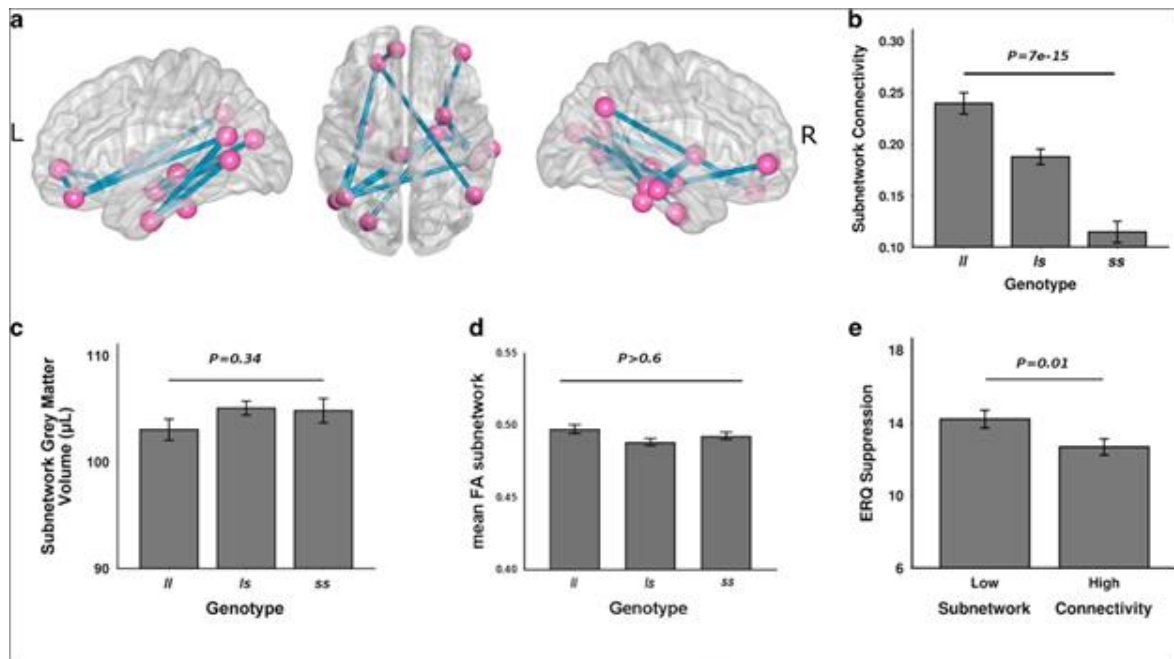


Figure 7: The identified subnetwork associated with 5-HTTLPR polymorphism (a). The functional connectivity of this subnetwork significantly decreased in both ls and ss carriers (cluster-level PFWE=0.03, mean connectivity differences $P=7e-15$) (b). In contrast, the mean grey matter volumes and mean FA values were not significantly different between genotype groups for the identified nodes (c) and inter-connecting visual-limbic white matter tracts (d), respectively. In addition, participants with lower subnetwork connectivity showed higher emotional suppression scores (e). Bars indicate mean values and error bars indicate standard errors.

| | | | |
|----|---|---------------------------------------|------|
| 1 | L. thalamus ^a | R. hippocampus ^a | 4e-6 |
| 2 | L. middle temporal gyrus ^b | L. orbitofrontal cortex ^b | 5e-6 |
| 3 | R. orbitofrontal cortex ^b | R. hippocampus ^a | 6e-6 |
| 4 | L. middle temporal gyrus ^b | R. hippocampus ^a | 1e-5 |
| 5 | L. anterior cingulate cortex ^a | L. orbitofrontal cortex ^b | 2e-5 |
| 6 | R. inferior temporal gyrus ^c | R. putamen ^c | 2e-5 |
| 7 | R. inferior temporal gyrus ^c | R. putamen ^c | 3e-5 |
| 8 | R. angular gyrus ^b | L. orbitofrontal cortex ^b | 4e-5 |
| 9 | L. middle temporal gyrus ^b | R. fusiform gyrus ^b | 5e-5 |
| 10 | L. middle occipital gyrus ^c | R. hippocampus ^a | 6e-5 |
| 11 | L. fusiform gyrus ^b | L. middle temporal gyrus ^b | 7e-5 |
| 12 | R. inferior temporal gyrus ^c | L. middle temporal gyrus ^b | 7e-5 |
| 13 | R. middle temporal gyrus ^b | R. hippocampus ^a | 9e-5 |
| 14 | L. middle temporal gyrus ^b | L. fusiform gyrus ^b | 1e-4 |

Each row represents one pair of connected nodes in the identified subnetwork, ranked by initial p-values. The node regions are annotated for relevance for serotonergic neurotransmission as follows:

| | |
|----|---|
| a) | Regions with 5-HTT expression in postmortem human brain (Kish et al, 2005; Varnas et al, 2004). |
| b) | Implicated by positron emission tomography (Savli et al, 2012) |
| c) | No data on 5-HTT expression available in humans. |

3.2 Empirical study 2

3.2.1 Functional network analyses

In our starting hypothesis to this work, we posited that alterations in the neural functional connectivity in carriers of the risk-associated low expression (L) variant in *MAOA* would involve, but not necessarily be exclusive to, frontal-temporal neural circuits during implicit emotion processing. Consistent with this, our NBS analysis of the emotional face matching task data identified a distributed cluster of node links with a significantly increased functional connectivity in L allele carriers compared to H allele carriers (p FWE = 0.037, Figure 8a). The identified sub-network included, but was not limited to, frontal-temporal areas and consisted of a total of 82 nodes that were connected by 248 links (or edges). To assess the potential specificity of the identified *MAOA*-associated functional network effects for emotion processing, we assessed *MAOA* genotype effects on the functional connectivity of node links also during resting-state and working memory performance. For resting-state fMRI, our NBS analysis detected a comparably distributed cluster of 176 links interconnecting 82 nodes with a significant increase in functional connectivity in *MAOA*-L allele carriers compared to *MAOA*-H allele carriers (p FWE = 0.022, Figure 8b). In contrast, the NBS analysis of the working memory data yielded a null finding (p FWE = 0.540).

3.2.2 Structural network analysis

The NBS analysis of DWI data identified a brain sub-network with a significant increase in structural connectivity in the *MAOA*-L allele carriers compared to H allele carriers (p FWE = 0.044, Figure 8c). The identified cluster consisted of 48 links interconnecting 43 nodes. The cluster was distributed comparably to the *MAOA*-related functional links, although smaller in extent. For all imaging modalities, details on the identified *MAOA*-associated cluster links are provided in Supplemental tables 7-9. For illustration purposes, the tables include the corresponding anatomical location of nodes in AAL standard space and highlight the prominent role of frontal lobe connections (bolded) and “isocoupled” links (italicized) of the respective anatomical labels. Moreover, the top 10% of the most significant *MAOA*-related nodes and interconnecting links for each modality are highlighted in red to facilitate the assessment of important anatomical contributors to the respective *MAOA*-related cluster findings.

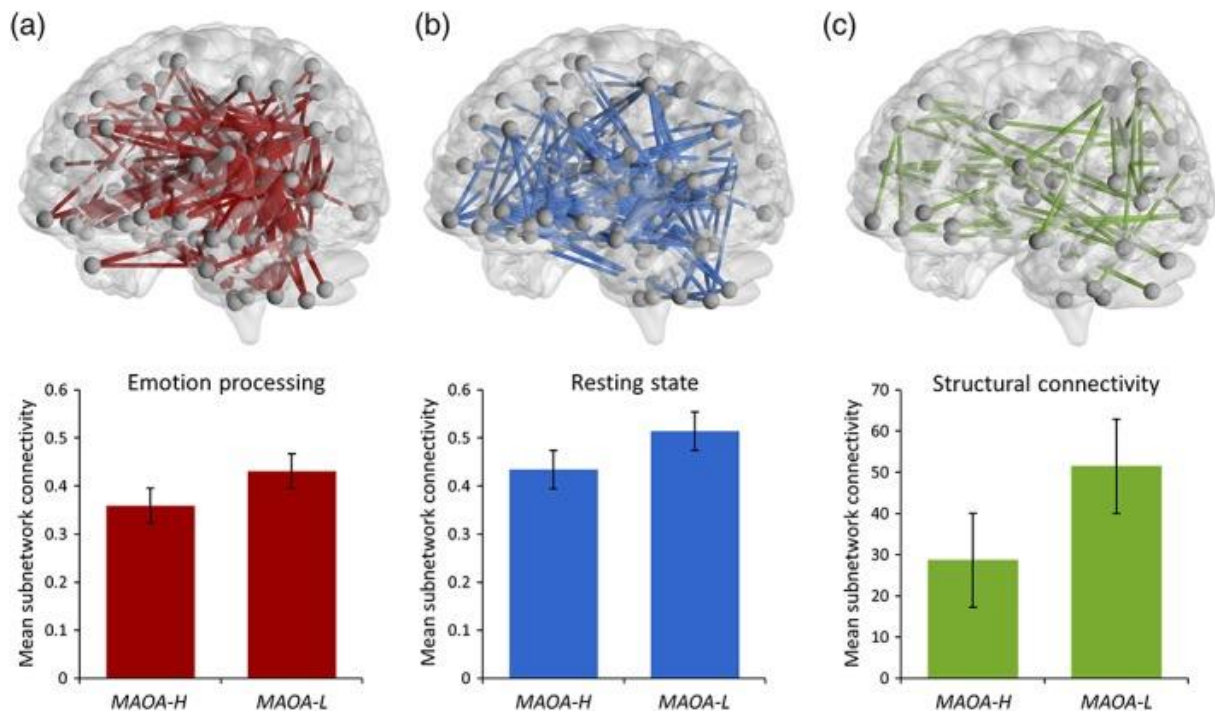


Figure 8: Illustration of the whole-brain spatial distribution (upper panels) and mean connectivity values of the identified *MAOA*-affected brain sub-networks stratified by genotype (lower panels) connectivity in *MAOA*-L allele carriers across (a) emotion processing (p FWE = 0.037, 248 links), (b) resting-state (p FWE = 0.022, 176 links), and (c) diffusion tensor imaging/structural connectivity (p FWE = 0.044, 48 links) data. Bars indicate mean values, error bars indicate standard errors demonstrating significantly increased

3.2.3 Supplemental exploratory analyses

We detected no significant interaction between *MAOA* genotype and sex on mean network connectivity scores in any MRI modality (all p -values >0.88). Post hoc regional quantification of the *MAOA*-significant links suggested a clear commonality across tasks and modalities in the form of a higher ratio of affected connections between neural nodes from different major AAL brain sections (77–88% anisocoupled links, as compared to 12–23% isocoupled links relating different nodes from the same major brain subdivision, Figure 9a). In addition, across all *MAOA*-significant tasks and modalities, a relatively high involvement of links interconnecting the frontal lobe with temporal, occipital, and subcortical regions was apparent. Obvious modality-specific patterns did not arise; the regional distribution of altered connections appeared to be the most unspecific in the structural data and included a higher proportion of *MAOA*-associated links interconnecting subcortical structures (Figure 9b). Notably, the reported effects of *MAOA* genotype on cluster connectivity remained stable in our follow-up analyses in subsamples with sex-matched genotype groups across modalities (all p -values <0.01). Similarly, in the sex-matched subsamples (Table 5), the association of *MAOA* genotype with cluster connectivity estimates remained significant for both genders and across modalities when we analyzed males and females separately (all p -values $<.04$).

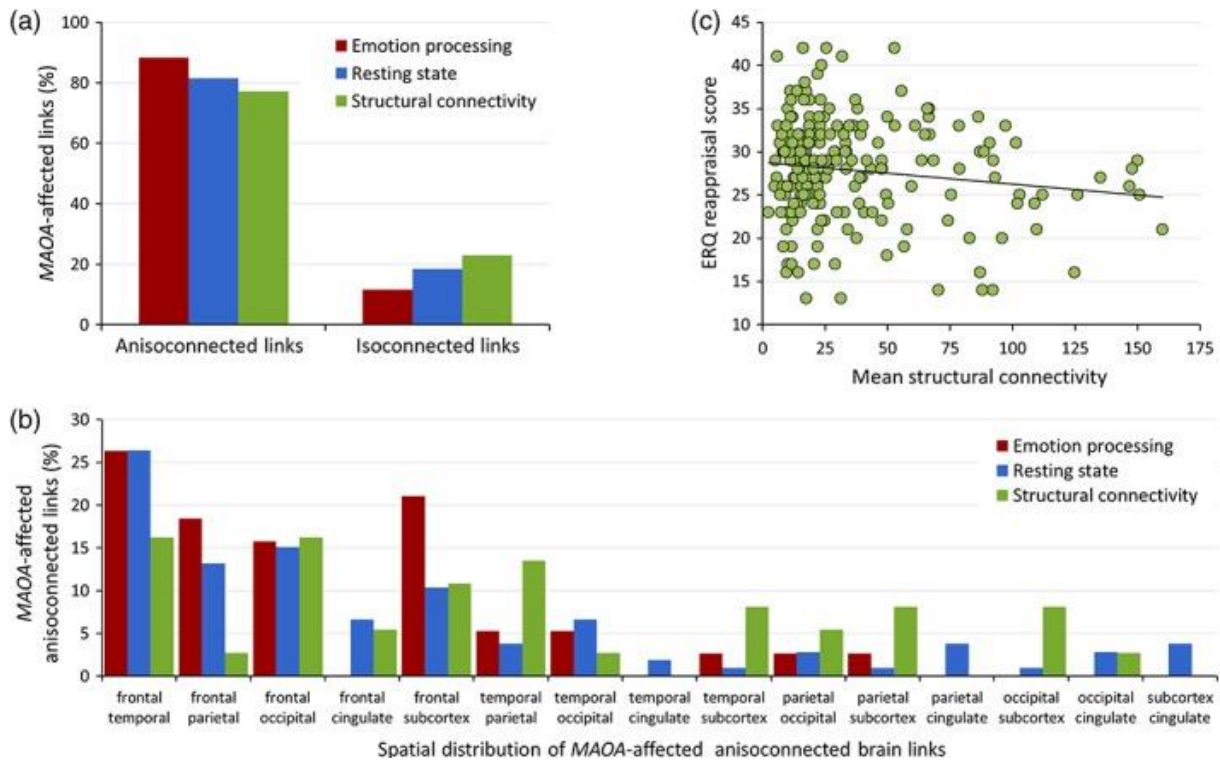


Figure 9: (a) Percentage (y axis) of *MAOA*-affected connections across tasks and modalities stratified by (x axis) the anisocoupled versus isocoupled nature of node links (see text for definition of terms). (b) Percentage (y axis) and spatial distribution (x axis) of *MAOA*-affected anisocoupled brain links across tasks and modalities. (c) Illustration of the association ($p = 0.041$, $r = -0.37$) between Emotion Regulation Questionnaire (ERQ) cognitive reappraisal scores (y axis) and the mean connectivity of the *MAOA*-affected structural network (quantified by the mean of the successful diffusion tensor imaging [DTI] fiber tracking streamlines).

3.2.4 Relationship to emotion regulation

Our exploratory analyses on the relationship between the *MAOA*-associated sub-network parameters and emotion regulation strategy showed a significant negative correlation between the connectivity of the structural network and the ERQ cognitive reappraisal subscale ($p = 0.041$, $r = -0.37$, Figure 9c). No significant correlations of the structural network with the connectivity parameters of the functional sub-networks or the ERQ expressive suppression subscale were seen (all p -values > 0.335). We did not detect any significant associations between *MAOA* genotype and stressful life events as assessed with the Social Readjustment Rating Scale scores (all p -values > 0.18). *MAOA* genotype was not associated with any of the ERQ subscale scores (all p -values > 0.16).

4 DISCUSSION

4.1 5-HTTLPR discussion

The first empirical study used multimodal neuroimaging to identify a potential functional connectivity phenotype associated with the 5-HTTLPR genotype at the brain system level. Our analyses resulted in several interesting findings, which we will discuss in the following. First, in accordance with recent well powered studies (Bastiaansen et al., 2014; Murphy et al., 2013; Viviani et al., 2010), we failed to replicate the association between 5-HTTLPR genotype and amygdala activation reported by prior studies (Hariri et al., 2005; Hariri et al., 2002). The negative finding in our relatively large sample supports the conclusions of recent meta-analyses, which also failed to find a convincing association between amygdala activity and genetic variation in the 5-HTTLPR polymorphism and highlighted a strong publication bias towards a large number of relatively small and probably underpowered neuroimaging studies reporting positive findings (Bastiaansen et al., 2014; Murphy et al., 2013). This outcome fits in well with evidence suggesting that the amygdala strongly habituates to the recurrent presentations of emotional stimuli and yields unreliable, highly variable activation estimates (Johnstone et al., 2005; Plichta et al., 2012). Another plausible contributor to earlier positive findings is the broad range of other genetic (Pezawas et al., 2008; Surguladze et al., 2012) and environmental factors (Rabl et al., 2014; van der Doelen et al., 2014) that have been shown to potentially interact with 5-HTTLPR, making underpowered studies more vulnerable to hidden bias (Bastiaansen et al., 2014). Finally, recent work has identified a strong citation preference for 5-HTTLPR studies reporting positive outcomes and drawing optimistic conclusion about the relevance of amygdala activation for linking the 5-HTTLPR polymorphism with alterations at the neural level. This suggests a systematic bias in the published literature which might have lead to an overestimation of relevance of this polymorphism (de Vries et al., 2016). Together, these findings and our data encourage the critical re-evaluation of amygdala activation as putative neural mechanism linking 5-HTTLPR to emotional behavior and to vulnerability to psychopathology.

Second, we identified a significant association of 5-HTTLPR genotype with the functional connectivity of a visual-limbic subnetwork. Here, the s allele was associated with a dose-dependent decrease in the coupling of several brain regions involved in emotion perception and regulation. The affected brain regions included fusiform gyrus, anterior cingulate gyrus, hippocampus, orbitofrontal cortex, striatum, and thalamus (Etkin et al., 2015; Phillips et al., 2003). There is a wealth of evidence linking brain regions included in the identified subnetwork with emotion processing. For example, the anterior cingulate cortex is a pivotal hub for top-down control of limbic regions (Etkin et al., 2015), the orbitofrontal cortex is associated with emotional decision making (Bechara et al., 2000), and the hippocampus is a key structure for emotion-related memory processing (Etkin et al., 2015; Phillips et al., 2003). The conjoint involvement of this network in emotion processing makes it a plausible target for the study of the role of 5-HTTLPR genetic variation in emotion processing at the neural level.

Notably, a relative enrichment of 5-HTT (Kish et al., 2005; Varnäs et al., 2004) and serotonin receptors (Biegon et al., 1986; Varnäs et al., 2004) has been demonstrated for several subnetwork regions in humans (see Table 6) by several earlier studies. In addition, animal studies point to a sensitivity of these regions to 5-HTTLPR variation.

5-HTT gene knock-out mice are showed enhanced extracellular serotonin level and reduced serotonin receptor gene expression in the hippocampus (Fabre et al., 2000; Mathews et al., 2004), striatum (Mathews et al., 2004; Rioux et al., 1999), and prefrontal cortex (Mathews et al., 2004). In humans, PET studies reported that the s allele of the 5-HTTLPR polymorphism relates to significantly lower 5-HTT binding potentials in the striatum (Praschak-Rieder et al., 2007) and 5-HT_{1A} receptor binding potentials in the hippocampus, anterior cingulate cortex, orbitofrontal cortex, and lateral temporal lobe (David et al., 2005). Moreover, altered functional connectivity of part of the detected 5-HTTLPR sensitive subnetwork has previously been found in s allele carriers, in particular the anterior cingulate cortex (Pezawas et al., 2005), prefrontal cortex (Heinz et al., 2005), and fusiform gyrus (Kruschwitz et al., 2015). Taken together, these prior findings and the results of our analyses support the idea that the neural mechanism behind the involvement 5-HTTLPR in the etiology of psychiatric disorders involves a large-scale network of conjointly interacting visual-limbic brain regions.

Third, several follow-up analyses were performed to probe the robustness of the identified subnetwork, its relationship to emotion regulation, and potential structural basis. In accordance with earlier work of our group (Cao, Plichta, Schäfer, et al., 2014), the reported subnetwork metrics showed good test–retest reliability. These findings are in stark contrast to the poor robustness of amygdala activation measures (Plichta et al., 2012) and encourages the use of network-based approaches in the search for functional neuroimaging phenotypes associated with emotional neural systems.

To assess the potential clinical relevance of the identified subnetwork, we further explored the relationship between this 5-HTTLPR sensitive subnetwork and two complementary emotion regulation strategies, namely cognitive reappraisal and behavioral suppression (Gross & John, 2003). Cognitive reappraisal is an adaptive emotion regulation strategy that relies on cognitive reframing of negative emotions and thereby reduces the negative salience and somatic consequences of emotional experiences. In contrast, the emotion suppression strategy is considered maladaptive and relates to increased health risks. By applying this strategy, the behavioral expression of emotional experiences is inhibited without internally reducing negative emotions and effectively controlling stress-related somatic consequences of negative emotional experiences (Gross, 2002; Gross & John, 2003). In our data, we detected significantly higher suppression scores in the group of individuals showing decreased subnetwork connectivity, suggesting an increased tendency to inhibit outward reactions to emotional experiences. Prior work showed that emotion suppression is associated with increased stress response to negative events (Gross, 2002) and negatively effects on broad range of health-protective variables like well-being, positive emotions, social functioning, social support, and memory (Gross, 2002; Gross & John, 2003). As a consequence, individuals with a stronger tendency to suppress their emotions are at increased risk for stress-related psychiatric conditions including mood and anxiety disorders (Gross, 2002). Our findings complement these data and suggest that the neural mechanism linking 5-HTTLPR to emotional regulation and risk for psychopathology includes connectivity deficits in the visual-limbic system.

We further explored a potential structural basis for the alteration in the identified subnetwork in several follow-up analyses. In our data, the VBM and TBSS analyses detected no evidence for associations between 5-HTTLPR and structural neuroimaging measures. This lack of evidence for structural alterations suggests that the affected network phenotype we identified is primarily functional and unlikely to be accompanied

by associated hidden structural alterations. However, there are several limitations to our study that need to be considered. First, although a relatively large group of individuals was included in empirical study 1, confidence in our findings might benefit from further replication in larger, independent cohorts as failure to replicate prior results has been recognized as an important issue in the field of imaging genetics. Second, we balanced the included 5-HTTLPR genotype groups for a broad range of demographic, psychological, task performance, and data quality-related variables. However, we cannot fully exclude that our results might have been influenced by additional confounds that we were not able to adequately control in our cohort. Third, despite the increasing popularity of NBS-based approaches in the recent literature, the NBS method comes with its own set of challenges. For example, the identified connectivity differences can only be reliably interpreted at the cluster level. Therefore, it is only possible to draw straightforward conclusions about the identified subnetwork as a whole. Any analyses or conclusions about the involvement of specific brain regions are highly speculative. Fourth, empirical study 1 included only healthy participants to avoid confounding our results by the presence of psychiatric disorders. However, to assess the clinical relevance of our findings, future studies exploring the significance of the identified subnetwork in diverse clinical populations, in particular in patients with depression and anxiety disorders might be interesting.

In conclusion, our data provide evidence for coupling deficits in the visual-limbic system as a network-based neuroimaging phenotype underlying the association of genetic variation in the 5-HTTLPR polymorphism with psychiatric risk. The identified connectomic phenotype is test-retest reliable, relates to a maladaptive emotion regulation strategy, and is independent of structural alterations in the identified network nodes and links making up the identified subnetwork. The results of empirical study 1 suggest that further investigating visual-limbic network alterations in larger cohorts including transdiagnostic clinical populations is warranted. Furthermore, our results confirmed that the relationship between amygdala activity and 5-HTTLPR genotype should be critically re-evaluated.

4.2 MAOA discussion

The main goal of empirical study two was to extend the current understanding of the neurogenetic risk architecture of neural networks underlying impulsivity and aggression. Multimodal neuroimaging and whole-brain connectomic methods in healthy participants stratified by MAOA genotype were used to achieve this aim. These analyses detected several structural and functional network alterations in healthy carriers of the risk-associated low expressing variant of the MAOA polymorphism.

First, a functional connectomic phenotype during implicit emotion processing manifesting as a regionally distributed set of hyperconnected brain nodes in individuals with the MAOA-L genotype was identified. Among the affected node links, more than 80% of these MAOA sensitive edges could be classified as affecting functional interactions between distant major anatomical subdivisions of the brain (“anisocoupled links”). These observations suggest that the low expressing MAOA variant preferentially affects long-range connections. These long-range connections might be crucial in the efficient control and integration of information across different brain areas with more specialized neural functions, thereby enabling a rich set of brain dynamics (Alexander-Bloch et al., 2013; Betzel & Bassett, 2018). Nearly half (47%) of the affected long-

range integrative links functionally coupled the frontal cortex to the temporal lobe and subcortical regions. These results are in accordance with the established view that *MAOA-L* mainly exerts its influence on psychiatric risk by impacting prefrontal neural circuits with a top-down regulatory influence on subordinate neural regions generating evolutionarily conserved physiological responses (Dorfman et al., 2014). The directions of the observed *MAOA* genotype effects are in line with earlier reports as well. As in prior connectivity studies on *MAOA-L*, the detected connectomic alterations during the processing of emotionally charged information manifested as a significant increase in functional coupling in empirical study 2 (Buckholtz et al., 2008; Denson et al., 2014). This alteration has been previously interpreted as a neurogenetic disruption of prefrontal regulatory brain networks which predisposes individuals carrying the *MAOA-L* variant to exaggerated and less controlled emotional responses resulting in increased impulsive arousal and negative emotions. With respect to the first research question of empirical study 2, these results suggest that the identified *MAOA*-related alterations in functional connectivity during negative emotion processing are consistent with the hypothesis stating a pronounced, but not exclusive, involvement of prefrontal-limbic circuits. Taken together, the described emotion processing data are well in line with the existing imaging genetics literature and extend our current understanding of *MAOA* by providing novel connectomic insights arising from a whole-brain network approach.

Second, additional resting state and working memory data were analysed to probe the detected network connectivity alterations for specificity to the emotion-processing domain. The study of the human brain at rest provides valuable insights into the basic functional architecture of interacting neural networks since connected brain networks display coordinated low-frequency fluctuations in even the absence of external stimulation. Similar to the emotion-processing domain, the resting-state analysis identified a regionally distributed set of hyperconnected links in *MAOA-L* carriers, which mostly consisted of distributed nodes from distant anatomical subdivisions of the brain. More than two thirds (69%) of the altered links connected the frontal cortex to other cortical and subcortical targets. With respect to the second research question, these findings suggest that the reported neurogenetic modulation of prefrontal regulatory circuits related to *MAOA-L* is likely not limited to the emotion processing domain, but rather indicates a more global alteration of basic functional architecture of the brain. To date, there are only few prior resting state fMRI studies on *MAOA*, making the integration of the presesent findings challenging. However, an earlier exploratory resting-state study using independent component analysis methods reported increased connectivity of several prefrontal and temporal areas in the risk-associated *MAOA-L* carriers (Clemens et al., 2015). This is in accordance with the findings of study 2, despite considerable differences in the employed approach. This assumption of a more global impact of the *MAOA-L* genotype on human brain networkarchitecture is further supported by the structural network findings of study 2. Diffusion-based research is lacking to date in the literature on *MAOA*. The deterministic tracking of white matter projections reported in study 2 revealed first evidence for a distributed pattern of hyperconnected node links in *MAOA-L* carriers. Comparable to the results in the studied functional neuroimaging modalities, a large proportion of the affected connections (40%) mapped to frontal “an-isocoupled” cortical connections. With respect to the third research question, the results of study 2 thus suggest that the assumed predisposition for an alteration in human neural network architecture extends to hard-wired anatomical links. Anatomical long-range connections from prefrontal regulatory networks that likely regulate and integrate bottom-up input from other neural regions seemed most notably affected by *MAOA*-genotype.

No associations between *MAOA*-genotype and neural network connectivity during performance of a working memory task were observed in study 2. This lack of an association appears to contradict the interpretation of global, distributed effects of the variant on network architecture. However, working memory tasks typically require coordinated frontal-parietal functions, and only about 3% of *MAOA*-sensitive structural links identified in study 2 pertained to frontal-parietal connections (see Figure 9). Earlier studies on the relationship of genetic variance in *MAOA* and working memory performance resulted in conflicting evidence. Whereas one study described an association during high-load cognitive conditions (Cerasa, Gioia, Fera, et al., 2008; Cerasa, Gioia, Labate, et al., 2008), several prior studies reported negative findings (Barnett et al., 2011; Dumontheil et al., 2014) (Söderqvist et al., 2014). Importantly, the fMRI n-back task employed in study 2 challenges executive neural networks but is still relatively straightforward, and the load on additional regulatory resources for impulsive and emotional responses is low. Thus, it seems plausible that while *MAOA* genotype impacts distributed regulatory networks involved in top-down prefrontal regulatory control, including alterations in white matter anatomical links, these differences are not focused on frontal-parietal networks. Therefore, the potentially resulting challenges for working memory may remain masked or compensated unless additional task requirements related to high cognitive load including frustration and emotion regulation are added (Cerasa, Gioia, Fera, et al., 2008; Cerasa, Gioia, Labate, et al., 2008). Further research is needed to corroborate this hypothesis.

The results of study 2 support the notion of *MAOA*-related genetic associations with connectivity of cortico-limbic circuits, and structural and functional alterations in these circuits have been linked to maladaptive emotion regulation. *MAOA* genotype itself has been previously related to a number of psychiatric risk-associated behaviors that are related to deficient emotion regulatory capacity including impulsivity (Chester et al., 2015; Meyer-Lindenberg et al., 2006) and aggression (Brunner et al., 1993; Eisenberger et al., 2007; Gallardo-Pujol et al., 2013; Kuepper et al., 2013; McDermott et al., 2009; Raine, 2008) as well as clinical diagnoses of conditions such as major depression (Fan et al., 2010; Liu et al., 2016) and attention deficit hyperactivity disorder (ADHD) (Das et al., 2006; Hwang et al., 2018). Several lines of evidence suggest that these behaviors and disorders are shaped by complex gene–environment interactions (Melas et al., 2013; Palumbo et al., 2018; Shumay et al., 2012). On a molecular level, these gene-environment interactions may relate to epigenetically mediated effects on brain network structure and function. Therefore, the extension of the imaging genetic approach described in study 2 to *MAOA*-related epigenetic network associations and the inclusion of transdiagnostic psychiatric populations in future work appears promising. Next to these suggestions for further research, there are several methodological limitations of study 2 meriting further consideration. Firstly, as in virtually all neuroimaging studies in humans, the analyzed system level metrics are indirect in nature and reflect only to some extent the microscale biological features of neural structure and function. Secondly, since we aimed for a common reference framework, study 2 used the same anatomical atlas for fMRI and DWI to be able to compare the identified *MAOA*-sensitive structural and functional brain networks across data modalities. However, the direct comparison of anatomical and functional connections is limited by the inherently different nature of the respective connectivity metrics. Specifically, while the identified DWI networks represent deterministic reconstructions of putative structural fiber tracts, the investigated functional networks represent the stochastic association between the BOLD-fluctuations of brain regions. Moreover, deterministic structural networks are typically sparse, with only 2–10% of the initiated streamlines reaching their

target (Betzel & Bassett, 2018; Hagmann et al., 2008), while the functional networks are, in principle, fully connected and show a complex structure of interdependent links, based on the correlative methods by which they are constructed. Given these differences between these neuroimaging modalities, study 2 was restricted to a descriptive comparison of modalities. Finally, although the identified association between the connectivity estimates of the identified *MAOA*-sensitive structural network and the relative lack of a protective emotion regulation strategy is plausible in the context of the present literature on that variant, this observation reported by study 2 is derived from an exploratory analysis and requires replication. Nonetheless, reporting this finding might be useful for aiding the formation of specific hypotheses in future studies and encourage replication attempts in independent cohorts. In conclusion, to our knowledge, study 2 is the first whole-brain multimodal connectomic study on the effects of *MAOA*-genotype in healthy human participants. The described data suggest that the low expression variant facilitates global, widely distributed alterations in neural network architecture across imaging modalities and tasks. These *MAOA* sensitive networks preferentially involve longer-range links connecting the prefrontal lobe with temporal, occipital, and subcortical brain regions. The identified multimodal hyperconnectivity profiles of the risk-associated low expression variant include the structural and functional connectome, although functional networks during low to medium working memory load seemed to be unaffected. These findings are well in line with prior studies suggesting *MAOA*-related genetic alterations in cortico-limbic circuits critical for negative emotion regulation. Similar to the associations between 5-HTTLPR and functional connectivity described in study 1, the most likely mechanism behind this association is excessive serotonergic signaling during vulnerable periods of early brain development. The results reported in study 2 extended the existing neuroimaging genetics literature on *MAOA* by novel multimodal whole-brain connectomic insights.

4.3 General discussion

The current work confirmed and extended on earlier research linking serotonergic genetic variants with altered neural connectivity. Applying unbiased, connectomic whole brain approaches confirmed prior findings showing altered fronto-temporal connectivity in carriers of both investigated serotonergic risk variants. The applied novel, connectomic method showed that serotonergic genetic variance affects large, globally distributed brain networks that include but are not limited to frontotemporal regions. The identified global, distributed effect is well in line with research about the serotonergic system and its complex role in neurodevelopment. Whereas serotonin acts as a neurotransmitter in the adult brain and during later stages of neurodevelopment, in early prenatal stages of brain development serotonin is involved in a broad range of processes including neuronal proliferation, migration, axon targeting and circuitry maturation (Riccio et al., 2011; Vicenzi et al., 2021; Vitalis & Parnavelas, 2003; Wang et al., 2011). This fits well with a spatially distributed effect on the neural level. Although certain networks including the frontotemporal networks that have been traditionally associated with serotonergic genetic variance might be more sensitive to alterations in the level of serotonin (Buckholtz & Meyer-Lindenberg, 2008), a highly localized or specific effect seems unlikely. Studies investigating where serotonin is expressed in the brain confirm relatively broad, global expression patterns (Kish et al., 2005). This again corresponds well to our findings of a more generalized pattern that included but was not limited to the frontotemporal regions that were associated with serotonergic risk genes

by earlier studies. Furthermore, the present work confirmed that connectomic, unbiased methods are more sensitive to the often subtle effects of genetic risk polymorphisms. Traditional voxel-based analysis like VBM, ROI analysis and TBSS showed no effects of serotonergic genetic risk variants. In contrast, an unbiased network approach showed effects on extended brain networks for both 5-HTTLPR and *MAOA*. The effect of 5-HTTLPR was only evident during an emotion processing task. In contrast, in addition to an effect on connectivity during emotion processing, variance in *MAOA* genotype had an additional effect on resting state connectivity and anatomic connectivity. One possible explanation for this more general effect of *MAOA* genotype is that in contrast to the 5-HTTLPR polymorphism which selectively affects serotonergic neurotransmission, *MAOA* is not only involved in serotonergic neural signaling but catalyzes the metabolism of other monoaminergic neurotransmitters including noradrenaline and dopamine (Buckholtz & Meyer-Lindenberg, 2008). This more general effect on monoaminergic neurotransmitters might correspond to the observed broader effect on brain connectivity across task domains and imaging modalities. In both studies, connectivity within the network showing sensitivity to the effects of serotonergic genotypes was associated with emotion regulation. This suggests that the networks showing altered connectivity during the faces task (study 1 and study 2), and during the resting state and anatomical connectivity (study 2) are not only linked to genetic variance in the serotonergic system, but are also relevant for emotion processing. In turn, this suggests that the detected serotonin sensitive networks might also be clinically relevant in the etiology of disorders featuring altered emotion processing.

4.4 Limitations

The current study has several limitations. As already mentioned briefly in the discussion of study 2, combining structural and functional MRI in multimodal analyses is not trivial and currently, there is no generally recommended method that can be considered a gold-standard in the field. Voxel-based methods like fMRI activity analysis and more traditional connectivity analyses like PPI (Psychophysiological interaction) or seed-based connectivity analyses for functional connectivity and TBSS or tracking of connections between preselected regions of interest do not produce results that are easy to compare. As NBS only picks up connected clusters of altered connectivity (Zalesky et al., 2010) and structural connectivity matrices are more sparse than functional connectivity matrices (Bassett & Sporns, 2017; Sporns et al., 2005), chances of finding an altered connected network are higher for functional than structural connectivity. Again, this might be a problem for the direct combination of structure and function. Furthermore, network analyses like NBS are highly dependent on atlas choice (Lord et al., 2016). There is no single brain atlas that is optimal for all types of analyses and covers structural and functional subdivisions of the brain equally well. For structural connectivity, differentiating between adjacent regions deep in grey matter is challenging. Because anisotropy is low in grey matter, current fiber tracking algorithms which rely on a dominant fiber direction do not perform well in regions located deep within gray matter. However, for functional connectivity distinguishing accurately between grey matter regions in close proximity but with distinct functions is feasible and informative. Therefore, finding a common parcellation that accurately represent both structure and function is challenging and there might not be an optimal choice.

In the current studies, the main findings were stable at least at a trend level when using an alternative atlas in exploratory analyses. However, the choice of a different atlas for function and structure might have revealed a very different pattern. Testing with a high

number of different brain parcellations requires correction for multiple comparisons which results in reduced power to detect small effects. Therefore, systematically testing different parcellations was not feasible in these studies. Follow-up studies using a multiverse approach to systematically evaluate all analytic choices and their impact on resulting altered networks might be interesting to investigate this aspect more systematically. Even with a parcellation that reflects both structure and function relatively well there are inherent differences between these two modalities which make a direct comparison challenging. Functional and structural connectivity matrices differ in sparsity. Many regions of the brain are not connected directly by white matter bundles and some smaller tracts might not be reliably tracked in the majority of participants resulting in a sparse connectivity matrix. In contrast, functional connectivity between regions when defined as correlation between timeseries extracted from these regions is rarely exactly zero, even when the temporal correlation between regions is low. Additionally, some brain regions that are not directly anatomical connected can show strong temporal correlation resulting in less sparse connectivity matrices for functional connectivity. These differences between functional and structural connectivity matrices make direct comparisons or analyzing brain structure and function together challenging. Another choice that can influence the results of NBS is the statistical threshold (Zalesky et al., 2010). Again, there is no generally recommended value and the results depend heavily on this parameter. Conservative thresholds only allow relatively strong and focused effects to reach statistical significance, whereas more lenient thresholds are needed to detect weaker, global effects (Zalesky et al., 2010). As both localized and global effects can be relevant and often there is no good prior knowledge suggesting the degree of localization of the expected effect, this choice is somewhat arbitrary. The current findings showed at least some stability at different thresholds which suggests that the observed effects are relatively robust. In the current work, we tried to interpret rather distributed, generalized effects by matching brain regions from the atlas of our choice to the four lobes of the brain and the cerebellum in order to search for a pattern that might escape notice using a finer grained parcellation. Although it was possible to identify a pattern suggesting an overrepresentation of fronto-temporal connections among the connections affected by *MAOA* genotype, this analysis was of an exploratory nature. A more systematic approach might be needed to show that this apparent pattern is stronger than what would be expected by chance if the whole brain was equally affected. One of the major strength of this work is the use of multimodal neuroimaging in a thoroughly phenotyped cohort. However, there was only partial overlap of included subjects in the different modalities. Missing data and data that failed quality control are a problem in a subset of subjects. Therefore, combining data at the subject level would have reduced our sample size considerably. However, being able to include a completely overlapping sample which completed all the measurements would have opened up the option to look into the pathway from genetics to neural connectivity and psychological traits, for instance by using mediation analysis. In both studies, there was no evidence for an interaction effect between genotype and stress. This was in conflict with several earlier well-powered studies which showed interactions between genotype and different measure for adversity and stress (Caspi et al., 2003; Kim-Cohen et al., 2006). In the presence of stress, both *MAOA* and 5-HTTLPR risk carriers showed increased negative outcomes, e.g. increased risk for depression and aggression whereas no strong main effect of genotype on any relevant outcome was observed. However, in our data there was no evidence for an interaction between genotype and stress in any modality. A possible explanation is that the measure for stress which we used might not accurately reflect stress in the most sensitive time window for

influencing the monoaminergic system. Whereas several studies which did find an interaction effect did focus on early life adversity (Caspi et al., 2003; Kim-Cohen et al., 2006), in our data only measures of stress within the last two years prior to participation in the study were available. Furthermore, most of our participants reported relatively low exposure to stress resulting in relatively little variance in stress measures. Recruiting participants with a history of high stress exposure, preferably during sensitive periods in development in early childhood, might increase sensitivity for detecting interaction effects.

4.5 Future directions

In the current studies, we did not find any evidence for an effect of serotonergic risk genes on neural connectivity during working memory. However, a similar multimodal approach focusing on genetic variants that have been implicated in working memory performance might be interesting. Focusing on known functional variants involved in working memory might be a promising approach for verifying the idea that functional VNTRs are interesting candidate polymorphisms. In the current study, the effect of serotonergic variants which was clearly present in structural and resting state connectivity but absent when another cognitive system got engaged. A similar pattern could be observed for n-back with genetic variants showing a link to working memory already influencing anatomical connectivity and functional connectivity at rest, but only showing an effect on task connectivity when an already fragile system gets challenged by the demands of a relevant task. For working memory, dopaminergic polymorphisms might be interesting candidates (Bertolino et al., 2006; Diaz-Asper et al., 2008; Fairfield et al., 2022; Meyer-Lindenberg, 2010). As both studies 1 and 2 showed an effect of serotonergic VNTRs on connectivity in an emotion processing network, it seems plausible that there might be a general effect of serotonergic genetic variants on these phenotypes. Further studies could test more stringently if this link to serotonergic neurotransmission is a true biological theme and does not emerge by chance. Several approaches aiming at identifying biologically meaningful themes within sets of genes that are associated with a condition have been successfully applied to neuroimaging genetics (Ramanan et al., 2012; Wang et al., 2018). Additional studies examining an association between a serotonergic pathway and brain connectivity during emotion processing tasks might be an interesting addition.

In adults, methylation of serotonergic risk genes might show stronger effects than genotype. Methylation has been repeatedly shown to be more closely related to serotonergic neurotransmission in the adult brain (Checknita et al., 2020; Shumay et al., 2012). Even treatment outcomes in disorders with emotion processing problems as a symptom has been linked to dynamic changes in methylation. For instance, response to desensitization therapy in panic disorder patients was linked to methylation changes (Ziegler et al., 2016). Therefore, including methylation and methylation changes, possibly even longitudinally following participants might add an interesting dynamic and developmental aspect to our current findings.

In both studies, only healthy controls were included. This approach prevents confounds with presence of disease and thereby is best suited to disentangling biology susceptibility from consequences of living with a neuropsychiatric disorder, e.g. consequences of social isolation or genotype differences in reactions to medication. However, extending the current work to different and diverse transdiagnostic cohorts might be interesting for follow-up studies. As difficulties in regulating emotions are a common symptom

shared by several disorders, differences in emotional processing and associated networks may be present to varying degrees in different disorders (Fernandez et al., 2016; Slee et al., 2008; Visted et al., 2018). By including affected individuals, more variance in relevant traits and brain connectivity as well as exposure to stress might contribute to clarify the clinical relevance of the reported findings. In addition, in cohorts with more varied mental health outcomes, interaction effects between stress and genotype might become more apparent if there is increased variance in exposure to stress compared to our healthy control cohorts. Furthermore, it might be interesting to investigate first degree relatives of different patient populations. An intermediate brain connectivity pattern in-between healthy participants and patients would confirm that the altered networks we observed are indeed linked to biological vulnerability for less efficient emotion processing. Applying more advanced methods for combining structural and functional connectivity might result in a more comprehensive understanding of neural connectivity. For instance, testing for correlations between structural and functional connectivity differences within individuals might shed light on the nature of the connection between altered structural and functional connectivity. Several approaches for combining functional and structural connectivity have been suggested. The current study successfully linked genetic variation in candidate VNTRs with well-known biological functions to alterations in neural connectivity and emotion regulation. However, several well-powered studies failed to replicate genotype effects and genotype by environment interaction effects for traditional candidate genes (Border et al., 2019). This lack of replication led experts in the field to abandon the candidate gene approach completely and focus on GWAS. However, alternative approaches have their own drawbacks. The biological interpretation of GWAS results is often challenging (Gallagher & Chen-Plotkin, 2018). Therefore, focusing on GWAS hits might not always be useful for understanding the biological etiology of neuropsychiatric disorders as GWAS hits are often not easily linked to a specific biological process. Most GWAS hits for complex disorders are located in non-coding regions of the genome (Pickrell, 2014; Welter et al., 2014). Mapping those variants to genes is not straightforward. Even after mapping associated variants successfully to genes, the known function of some genes is not always obviously related to the relevant disorder. Moreover, the resolution of GWAS might not be sufficiently fine grained to identify causal variants within linkage disequilibrium blocks. As genetic variance in linkage disequilibrium blocks is highly correlated, discerning the true source of an association signal is challenging (Boyle et al., 2017). In addition, GWAS for a disorder or trait might produce too many hits (Boyle et al., 2017; Gallagher & Chen-Plotkin, 2018). There is evidence that some complex, multifactorial disorders are influenced by all genes that are expressed in relevant tissues. This might be due to the interconnectedness of gene regulatory networks which causes large numbers of SNPs to contribute to the heritability of genetically complex traits even if only a small set of biologically relevant core genes is informative for explaining the underlying mechanisms (Boyle et al., 2017; Liu et al., 2019). This complicates the selection of GWAS hits to investigate in neuroimaging studies because it is unclear which variants to prioritize and testing a large number of variants causes a heavy burden due to correction for multiple statistical tests. Therefore, with GWAS hits as candidates for subsequent neuroimaging genetics studies it is difficult to derive a good hypothesis about potential effects on the level of the brain and behavior. A different problem for extremely large studies is that thorough, extensive phenotyping is often not feasible in well-powered cohorts. However, most psychiatric phenotypes are complex and a simple binary diagnosis does not map well on biology (Insel et al., 2010). Therefore, minimal phenotyping strategies as used in the majority of GWAS are probably not optimal

for characterizing complex phenomena like depression and anxiety. Even in well powered samples, it was challenging to identify reproducible and significant associations. Effects sizes have mostly been small and replication has been challenging. Larger cohorts did only improve this situation marginally (Howard et al., 2018). For neuroimaging genetics studies, there are similar challenges. Extensive phenotyping, performing advanced neuroimaging analysis techniques and using state-of-the-art techniques for data acquisition are not always feasible in extremely large cohorts. However, these large sample sizes are needed for reproducible and statistically significant results. As innovative technologies and neuroimaging paradigms as well as analysis procedures do need extensive testing before they can be applied, extremely large sample sizes are not always easily obtained when trying to optimize these phenotypes. Although large, unbiased studies of genetic risk for psychiatric disorders are needed to detect stable, replicable associations, giving up on the candidate gene approach altogether might be premature in the view of the limitations affecting data driven approaches. Especially candidate genes with a well understood biological function might be still interesting targets for neuroimaging studies aiming at understanding biological mechanism on the pathway from genes, to the brain and ultimately, psychiatric disorders. As traditional candidate gene approaches and data driven strategies have their respective limitations and merits, the field of neuroimaging genetics might benefit from an integrative approach applying these complimentary strategies to inform each other.

5 SUMMARY

Most neuropsychiatric disorders are at least moderately heritable. Two functional candidate variants affecting monoaminergic neurotransmission are *MAOA* and 5-HTTLPR. Earlier neuroimaging studies connected genetic variance in these polymorphisms with alterations in brain function and structure mainly in corticolimbic circuits. However, these initial findings have been questioned because of failure to replicate in larger cohorts and lack of clear meta-analytic evidence. Therefore, the current work investigated the following hypotheses: 1) Network phenotypes are more sensitive to the subtle effects of typical genetic risk variants than traditional neuroimaging approaches. 2) Applying a whole-brain, connectomic approach will detect widespread effects. 3) Genetic variance in the serotonergic system impacts structural and functional connectivity patterns even without an active task. However, a task that challenges a significant cognitive domain might increase sensitivity. 4) Networks showing altered connectivity patterns in carriers of serotonergic risk variants are also associated with differences in emotion regulation.

Study 1 examined a sample of 223 healthy subjects with an emotional face processing task to re-evaluate the association between 5-HTTLPR and amygdala activation, explore potential network-based functional connectivity phenotypes for associations with 5-HTTLPR, and probe the reliability, behavioral significance and potential structural confounds of the identified network phenotype. The number of risk alleles was significantly correlated with functional connectivity of a visual-limbic subnetwork ($p_{FWE}=0.03$). Notably, individuals with lower subnetwork connectivity had significantly higher emotion suppression scores ($p=0.01$). Study 2 examined healthy individuals and used multimodal neuroimaging (sample size range: 219-284 across modalities) and network-based statistics (NBS) to probe the specificity of *MAOA*-L-related connectomic alterations to cortical-limbic circuits and the emotion processing domain. We assessed the spatial distribution of affected links across several neuroimaging tasks and data modalities to identify potential alterations in network architecture. Our results revealed a distributed network of node links with a significantly increased connectivity in *MAOA*-L carriers compared to the carriers of the high expression (H) variant. The hyperconnectivity phenotype primarily consisted of between-lobe network links and showed a pronounced involvement of frontal-temporal connections. Hyperconnectivity was observed across functional magnetic resonance imaging (fMRI) of implicit emotion processing ($p_{FWE} = 0.037$), resting-state fMRI ($p_{FWE} = 0.022$), and diffusion tensor imaging ($p_{FWE}=0.044$) data. The current work confirmed and extended on earlier research linking serotonergic genetic variants with altered neural connectivity. Applying connectomic whole brain approaches confirmed earlier findings showing altered fronto-temporal connectivity in carriers of serotonergic risk variants. This novel, connectomic method showed that serotonergic genetic variance affects large brain networks that include but are not limited to frontotemporal regions. The present work confirmed that connectomic, unbiased methods are more sensitive to the often subtle effects of genetic risk polymorphisms. Whereas the effect of 5-HTTLPR was only evident during an emotion processing task, *MAOA* genotype had an effect on resting state connectivity and during emotion processing in addition to anatomic connectivity. One possible explanation for this more general effect of *MAOA* genotype is that in contrast to the 5-HTTLPR polymorphism which selectively affects serotonergic neurotransmission, *MAOA* is not only involved in serotonergic neural signaling but catalyzes the metabolism of other monoaminergic neurotransmitters including noradrenaline and dopamine.

6 ZUSAMMENFASSUNG

Die meisten neuropsychiatrischen Störungen sind zumindest teilweise erblich. Zwei funktionelle genetische Polymorphismen, die die monoaminerge Neurotransmission beeinflussen, sind MAOA und 5-HTTLPR. Frühere Hirnbildgebungsstudien haben die genetische Varianz dieser Polymorphismen mit verschiedenen Veränderungen der Hirnfunktion und -struktur in Verbindung gebracht. Diese Ergebnisse wurden jedoch in Frage gestellt, da sie nicht in größeren Stichproben repliziert werden konnten und keine eindeutigen meta-analytischen Beweise vorlagen. Daher wurden in der vorliegenden Arbeit die folgenden Hypothesen untersucht: 1) Netzwerk-Phänotypen sind sensitiver für die subtilen Effekte genetischer Risikovarianten als traditionelle Auswertungsverfahren. 3) Genetische Varianz im serotonergen System beeinflusst strukturelle und funktionelle Konnektivitätsmuster in Abwesenheit einer aktiven Aufgabe. Eine Aufgabe, die eine relevante kognitive Domäne anspricht, kann jedoch die Sensitivität erhöhen. 4) Netzwerke mit veränderten Konnektivitätsmustern bei Trägern serotonerger Risikovarianten sind auch mit einer veränderten Emotionsregulation assoziiert.

In der ersten Studie wurden 223 gesunde Probanden mit einer emotionalen Gesichtsaufgabe im MRT untersucht, um den Zusammenhang zwischen genetischer Varianz in 5-HTTLPR und Amygdalaaktivität zu überprüfen, potentielle netzwerkbasierte funktionelle Konnektivitätsphänotypen zu identifizieren und die Reliabilität, klinische Relevanz und Spezifität potentieller Netzwerkphänotypen zu evaluieren. Unsere Ergebnisse zeigten eine signifikante Korrelation zwischen der Anzahl der Risikoallele und der funktionellen Konnektivität eines visuell-limbischen Subnetzwerkes ($p_{FEW}=0.03$). Dieses Subnetzwerk umfasste Hirnregionen, die für die Emotionsregulation von zentraler Bedeutung sind. Eine geringere Konnektivität innerhalb des identifizierten Subnetzwerkes korrelierte zudem mit einer erhöhten Emotionsunterdrückung ($p_{FWE}=0,01$). In der zweiten Studie untersuchten wir gesunde Probanden mittels multimodaler MRT-Bildgebung des Gehirns. Eine netzwerkbasierte Methode wurde verwendet, um die Spezifität der MAOA-assoziierten Veränderungen für die Emotionsverarbeitungsdomäne und kortikolimbische Hirnregionen zu evaluieren. Wir untersuchten die räumliche Verteilung der veränderten neuronalen Verbindungen in verschiedenen MRI Modalitäten. Unsere Ergebnisse zeigten ein räumlich weit verzweigtes Netzwerk mit erhöhter Konnektivität bei Trägern der aktiveren MAOA-Variante. Dieser Phänotyp der Hyperkonnektivität umfasste vor allem Verbindungen zwischen weiter auseinander liegenden Hirnregionen, wobei insbesondere frontotemporale Verbindungen betroffen waren. Diese Hyperkonnektivität wurde während einer Emotionsverarbeitungsaufgabe ($p_{FWE}=0,037$), im Ruhezustand ($p_{FEW}=0,022$) und in diffusionsgewichteten Daten ($p_{FEW}=0,044$) nachgewiesen. Unsere neue Netzwerkmethod zeigte, dass serotonerge Genvarianten die Konnektivität großer, weit verzweigter neuronaler Netzwerke beeinflussen. Dies bestätigt, dass konnektomische Methoden eine erhöhte Sensitivität für die subtilen Effekte genetischer Risikovarianten auf das menschliche Gehirn aufweisen. Der Effekt des 5-HTTLPR-Polymorphismus wurde ausschließlich während einer Emotionsverarbeitungsaufgabe beobachtet. Im Gegensatz dazu beeinflusste der MAOA-Polymorphismus zusätzlich die Konnektivität im Ruhezustand und die anatomische Konnektivität. Eine mögliche Erklärung für diesen Unterschied ist, dass 5-HTTLPR ausschließlich an der serotonergen Neurotransmission beteiligt ist, während MAOA zusätzlich am Noradrenalin- und Dopaminstoffwechsel beteiligt ist.

7 REFERENCES

- Abler, B., & Kessler, H. (2009). Emotion Regulation Questionnaire—Eine deutschsprachige Fassung des ERQ von Gross und John. [Emotion Regulation Questionnaire—A German version of the ERQ by Gross and John.]. *Diagnostica*, 55, 144-152. <https://doi.org/10.1026/0012-1924.55.3.144>
- Alexander-Bloch, A. F., Vértes, P. E., Stidd, R., Lalonde, F., Clasen, L., Rapoport, J., Giedd, J., Bullmore, E. T., & Gogtay, N. (2013). The anatomical distance of functional connections predicts brain network topology in health and schizophrenia. *Cereb Cortex*, 23(1), 127-138. <https://doi.org/10.1093/cercor/bhr388>
- Barnett, J. H., Xu, K., Heron, J., Goldman, D., & Jones, P. B. (2011). Cognitive effects of genetic variation in monoamine neurotransmitter systems: a population-based study of COMT, MAOA, and 5HTTLPR. *Am J Med Genet B Neuropsychiatr Genet*, 156(2), 158-167. <https://doi.org/10.1002/ajmg.b.31150>
- Bastiaansen, J. A., Servaas, M. N., Marsman, J. B., Ormel, J., Nolte, I. M., Riese, H., & Aleman, A. (2014). Filling the gap: relationship between the serotonin-transporter-linked polymorphic region and amygdala activation. *Psychol Sci*, 25(11), 2058-2066. <https://doi.org/10.1177/0956797614548877>
- Bechara, A., Damasio, H., & Damasio, A. R. (2000). Emotion, decision making and the orbitofrontal cortex. *Cereb Cortex*, 10(3), 295-307. <https://doi.org/10.1093/cercor/10.3.295>
- Benedetti, F., Bollettini, I., Poletti, S., Locatelli, C., Lorenzi, C., Pirovano, A., Smeraldi, E., & Colombo, C. (2015). White matter microstructure in bipolar disorder is influenced by the serotonin transporter gene polymorphism 5-HTTLPR. *Genes Brain Behav*, 14(3), 238-250. <https://doi.org/10.1111/gbb.12206>
- Berletch, J. B., Yang, F., Xu, J., Carrel, L., & Disteche, C. M. (2011). Genes that escape from X inactivation. *Hum Genet*, 130(2), 237-245. <https://doi.org/10.1007/s00439-011-1011-z>
- Betzel, R. F., & Bassett, D. S. (2018). Specificity and robustness of long-distance connections in weighted, interareal connectomes. *Proc Natl Acad Sci U S A*, 115(21), E4880-e4889. <https://doi.org/10.1073/pnas.1720186115>
- Biegon, A., Kargman, S., Snyder, L., & McEwen, B. S. (1986). Characterization and localization of serotonin receptors in human brain postmortem. *Brain Res*, 363(1), 91-98. [https://doi.org/10.1016/0006-8993\(86\)90661-x](https://doi.org/10.1016/0006-8993(86)90661-x)
- Bortolato, M., Godar, S. C., Alzghoul, L., Zhang, J., Darling, R. D., Simpson, K. L., Bini, V., Chen, K., Wellman, C. L., Lin, R. C., & Shih, J. C. (2013). Monoamine oxidase A and A/B knockout mice display autistic-like features. *Int J Neuropsychopharmacol*, 16(4), 869-888. <https://doi.org/10.1017/s1461145712000715>

Brunner, H. G., Nelen, M., Breakefield, X. O., Ropers, H. H., & van Oost, B. A. (1993). Abnormal behavior associated with a point mutation in the structural gene for monoamine oxidase A. *Science (New York, N.Y.)*, 262(5133), 578-580. <https://doi.org/10.1126/science.8211186>

Buckholtz, J. W., Callicott, J. H., Kolachana, B., Hariri, A. R., Goldberg, T. E., Genderson, M., Egan, M. F., Mattay, V. S., Weinberger, D. R., & Meyer-Lindenberg, A. (2008). Genetic variation in MAOA modulates ventromedial prefrontal circuitry mediating individual differences in human personality. *Mol Psychiatry*, 13(3), 313-324. <https://doi.org/10.1038/sj.mp.4002020>

Budisavljevic, S., Kawadler, J. M., Dell'Acqua, F., Rijdsdijk, F. V., Kane, F., Picchioni, M., McGuire, P., Touloupoulou, T., Georgiades, A., Kalidindi, S., Kravariti, E., Murray, R. M., Murphy, D. G., Craig, M. C., & Catani, M. (2016). Heritability of the limbic networks. *Soc Cogn Affect Neurosci*, 11(5), 746-757. <https://doi.org/10.1093/scan/nsv156>
Byrd, A. L., & Manuck, S. B. (2014). MAOA, childhood maltreatment, and antisocial behavior: meta-analysis of a gene-environment interaction. *Biol Psychiatry*, 75(1), 9-17. <https://doi.org/10.1016/j.biopsych.2013.05.004>

Callicott, J., Egan, M. F., Mattay, V., Bertolino, A., Bone, A. D., Verchinski, B. A., & Weinberger, D. R. (2004). Abnormal fMRI response of the dorsolateral prefrontal cortex in cognitively intact siblings of patients with schizophrenia. *American Journal of Psychiatry*, 160(4), 709-719.

Callicott, J. H., Egan, M. F., Mattay, V. S., Bertolino, A., Bone, A. D., Verchinski, B., & Weinberger, D. R. (2003). Abnormal fMRI response of the dorsolateral prefrontal cortex in cognitively intact siblings of patients with schizophrenia. *Am J Psychiatry*, 160(4), 709-719. <https://doi.org/10.1176/appi.ajp.160.4.709>

Canli, T., & Lesch, K. P. (2007). Long story short: the serotonin transporter in emotion regulation and social cognition. *Nat Neurosci*, 10(9), 1103-1109. <https://doi.org/10.1038/nn1964>

Cao, H., Bertolino, A., Walter, H., Schneider, M., Schäfer, A., Taurisano, P., Blasi, G., Haddad, L., Grimm, O., Otto, K., Dixon, L., Erk, S., Mohnke, S., Heinz, A., Romaniczuk-Seiferth, N., Mühleisen, T. W., Mattheisen, M., Witt, S. H., Cichon, S., . . . Meyer-Lindenberg, A. (2016). Altered Functional Subnetwork During Emotional Face Processing: A Potential Intermediate Phenotype for Schizophrenia. *JAMA Psychiatry*, 73(6), 598-605. <https://doi.org/10.1001/jamapsychiatry.2016.0161>

Cao, H., Plichta, M. M., Schafer, A., Haddad, L., Grimm, O., Schneider, M., Esslinger, C., Kirsch, P., Meyer-Lindenberg, A., & Tost, H. (2014). Test-retest reliability of fMRI-based graph theoretical properties during working memory, emotion processing, and resting state. *Neuroimage*, 84, 888-900. <https://doi.org/10.1016/j.neuroimage.2013.09.013>

Cao, H., Plichta, M. M., Schäfer, A., Haddad, L., Grimm, O., Schneider, M., Esslinger, C., Kirsch, P., Meyer-Lindenberg, A., & Tost, H. (2014). Test-retest reliability of fMRI-based graph theoretical properties during working memory, emotion processing, and resting state. *Neuroimage*, 84, 888-900. <https://doi.org/10.1016/j.neuroimage.2013.09.013>

- Cases, O., Seif, I., Grimsby, J., Gaspar, P., Chen, K., Pournin, S., Müller, U., Aguet, M., Babinet, C., Shih, J. C., & et al. (1995). Aggressive behavior and altered amounts of brain serotonin and norepinephrine in mice lacking MAOA. *Science*, 268(5218), 1763-1766. <https://doi.org/10.1126/science.7792602>
- Caspi, A., McClay, J., Moffitt, T. E., Mill, J., Martin, J., Craig, I. W., Taylor, A., & Poulton, R. (2002). Role of genotype in the cycle of violence in maltreated children. *Science*, 297(5582), 851-854. <https://doi.org/10.1126/science.1072290>
- Caspi, A., Sugden, K., Moffitt, T. E., Taylor, A., Craig, I. W., Harrington, H., McClay, J., Mill, J., Martin, J., Braithwaite, A., & Poulton, R. (2003). Influence of life stress on depression: moderation by a polymorphism in the 5-HTT gene. *Science*, 301(5631), 386-389. <https://doi.org/10.1126/science.1083968>
- Cerasa, A., Gioia, M. C., Fera, F., Passamonti, L., Liguori, M., Lanza, P., Muglia, M., Magariello, A., & Quattrone, A. (2008). Ventro-lateral prefrontal activity during working memory is modulated by MAO A genetic variation. *Brain Res*, 1201, 114-121. <https://doi.org/10.1016/j.brainres.2008.01.048>
- Cerasa, A., Gioia, M. C., Labate, A., Lanza, P., Magariello, A., Muglia, M., & Quattrone, A. (2008). MAO A VNTR polymorphism and variation in human morphology: a VBM study. *Neuroreport*, 19(11), 1107-1110. <https://doi.org/10.1097/WNR.0b013e3283060ab6>
- Cheng, A., Scott, A. L., Ladenheim, B., Chen, K., Ouyang, X., Lathia, J. D., Mughal, M., Cadet, J. L., Mattson, M. P., & Shih, J. C. (2010). Monoamine oxidases regulate telencephalic neural progenitors in late embryonic and early postnatal development. *J Neurosci*, 30(32), 10752-10762. <https://doi.org/10.1523/jneurosci.2037-10.2010>
- Chester, D. S., DeWall, C. N., Derefinko, K. J., Estus, S., Peters, J. R., Lynam, D. R., & Jiang, Y. (2015). Monoamine oxidase A (MAOA) genotype predicts greater aggression through impulsive reactivity to negative affect. *Behav Brain Res*, 283, 97-101. <https://doi.org/10.1016/j.bbr.2015.01.034>
- Cicchetti, D. V., & Sparrow, S. A. (1981). Developing criteria for establishing interrater reliability of specific items: applications to assessment of adaptive behavior. *Am J Ment Defic*, 86(2), 127-137.
- Clemens, B., Voß, B., Pawliczek, C., Mingoia, G., Weyer, D., Reppe, J., Eggermann, T., Zerres, K., Reetz, K., & Habel, U. (2015). Effect of MAOA Genotype on Resting-State Networks in Healthy Participants. *Cereb Cortex*, 25(7), 1771-1781. <https://doi.org/10.1093/cercor/bht366>
- Contini, V., Marques, F. Z., Garcia, C. E., Hutz, M. H., & Bau, C. H. (2006). MAOA-uVNTR polymorphism in a Brazilian sample: further support for the association with impulsive behaviors and alcohol dependence. *Am J Med Genet B Neuropsychiatr Genet*, 141b(3), 305-308. <https://doi.org/10.1002/ajmg.b.30290>

- Das, M., Bhowmik, A. D., Sinha, S., Chattopadhyay, A., Chaudhuri, K., Singh, M., & Mukhopadhyay, K. (2006). MAOA promoter polymorphism and attention deficit hyperactivity disorder (ADHD) in Indian children. *Am J Med Genet B Neuropsychiatr Genet*, 141b(6), 637-642. <https://doi.org/10.1002/ajmg.b.30385>
- David, S. P., Murthy, N. V., Rabiner, E. A., Munafó, M. R., Johnstone, E. C., Jacob, R., Walton, R. T., & Grasby, P. M. (2005). A functional genetic variation of the serotonin (5-HT) transporter affects 5-HT_{1A} receptor binding in humans. *J Neurosci*, 25(10), 2586-2590. <https://doi.org/10.1523/jneurosci.3769-04.2005>
- de Vries, Y. A., Roest, A. M., Franzen, M., Munafò, M. R., & Bastiaansen, J. A. (2016). Citation bias and selective focus on positive findings in the literature on the serotonin transporter gene (5-HTTLPR), life stress and depression. *Psychol Med*, 46(14), 2971-2979. <https://doi.org/10.1017/s0033291716000805>
- Denson, T. F., Dobson-Stone, C., Ronay, R., von Hippel, W., & Schira, M. M. (2014). A functional polymorphism of the MAOA gene is associated with neural responses to induced anger control. *J Cogn Neurosci*, 26(7), 1418-1427. https://doi.org/10.1162/jocn_a_00592
- Dima, D., Roberts, R. E., & Frangou, S. (2016). Connectomic markers of disease expression, genetic risk and resilience in bipolar disorder. *Transl Psychiatry*, 6(1), e706. <https://doi.org/10.1038/tp.2015.193>
- Dorfman, H. M., Meyer-Lindenberg, A., & Buckholz, J. W. (2014). Neurobiological mechanisms for impulsive-aggression: the role of MAOA. *Curr Top Behav Neurosci*, 17, 297-313. https://doi.org/10.1007/7854_2013_272
- Dumontheil, I., Jensen, S. K., Wood, N. W., Meyer, M. L., Lieberman, M. D., & Blakemore, S. J. (2014). Preliminary investigation of the influence of dopamine regulating genes on social working memory. *Soc Neurosci*, 9(5), 437-451. <https://doi.org/10.1080/17470919.2014.925503>
- Egan, M. F., Kojima, M., Callicott, J. H., Goldberg, T. E., Kolachana, B. S., Bertolino, A., Zaitsev, E., Gold, B., Goldman, D., Dean, M., Lu, B., & Weinberger, D. R. (2003). The BDNF val66met polymorphism affects activity-dependent secretion of BDNF and human memory and hippocampal function. *Cell*, 112(2), 257-269. [https://doi.org/10.1016/s0092-8674\(03\)00035-7](https://doi.org/10.1016/s0092-8674(03)00035-7)
- Eisenberger, N. I., Way, B. M., Taylor, S. E., Welch, W. T., & Lieberman, M. D. (2007). Understanding genetic risk for aggression: clues from the brain's response to social exclusion. *Biol Psychiatry*, 61(9), 1100-1108. <https://doi.org/10.1016/j.biopsych.2006.08.007>
- Etkin, A., Büchel, C., & Gross, J. J. (2015). The neural bases of emotion regulation. *Nat Rev Neurosci*, 16(11), 693-700. <https://doi.org/10.1038/nrn4044>
- Fabre, V., Beaufour, C., Evrard, A., Rioux, A., Hanoun, N., Lesch, K. P., Murphy, D. L., Lanfumey, L., Hamon, M., & Martres, M. P. (2000). Altered expression and functions

of serotonin 5-HT_{1A} and 5-HT_{1B} receptors in knock-out mice lacking the 5-HT transporter. *Eur J Neurosci*, 12(7), 2299-2310. <https://doi.org/10.1046/j.1460-9568.2000.00126.x>

Fan, M., Liu, B., Jiang, T., Jiang, X., Zhao, H., & Zhang, J. (2010). Meta-analysis of the association between the monoamine oxidase-A gene and mood disorders. *Psychiatr Genet*, 20(1), 1-7. <https://doi.org/10.1097/YPG.0b013e3283351112>

Frodl, T., Koutsouleris, N., Bottlender, R., Born, C., Jäger, M., Mörgenthaler, M., Scheuerecker, J., Zill, P., Baghai, T., Schüle, C., Rupprecht, R., Bondy, B., Reiser, M., Möller, H. J., & Meisenzahl, E. M. (2008). Reduced gray matter brain volumes are associated with variants of the serotonin transporter gene in major depression. *Mol Psychiatry*, 13(12), 1093-1101. <https://doi.org/10.1038/mp.2008.62>

Gallardo-Pujol, D., Andrés-Pueyo, A., & Maydeu-Olivares, A. (2013). MAOA genotype, social exclusion and aggression: an experimental test of a gene-environment interaction. *Genes Brain Behav*, 12(1), 140-145. <https://doi.org/10.1111/j.1601-183X.2012.00868.x>

Gross, J. J. (2002). Emotion regulation: affective, cognitive, and social consequences. *Psychophysiology*, 39(3), 281-291. <https://doi.org/10.1017/s0048577201393198>

Gross, J. J., & John, O. P. (2003). Individual differences in two emotion regulation processes: implications for affect, relationships, and well-being. *J Pers Soc Psychol*, 85(2), 348-362. <https://doi.org/10.1037/0022-3514.85.2.348>

Guo, G., Ou, X. M., Roettger, M., & Shih, J. C. (2008). The VNTR 2 repeat in MAOA and delinquent behavior in adolescence and young adulthood: associations and MAOA promoter activity. *Eur J Hum Genet*, 16(5), 626-634. <https://doi.org/10.1038/sj.ejhg.5201999>

Hagmann, P., Cammoun, L., Gigandet, X., Meuli, R., Honey, C. J., Wedeen, V. J., & Sporns, O. (2008). Mapping the structural core of human cerebral cortex. *PLoS Biol*, 6(7), e159. <https://doi.org/10.1371/journal.pbio.0060159>

Hariri, A. R., Drabant, E. M., Munoz, K. E., Kolachana, B. S., Mattay, V. S., Egan, M. F., & Weinberger, D. R. (2005). A susceptibility gene for affective disorders and the response of the human amygdala. *Arch Gen Psychiatry*, 62(2), 146-152. <https://doi.org/10.1001/archpsyc.62.2.146>

Hariri, A. R., & Holmes, A. (2006). Genetics of emotional regulation: the role of the serotonin transporter in neural function. *Trends Cogn Sci*, 10(4), 182-191. <https://doi.org/10.1016/j.tics.2006.02.011>

Hariri, A. R., Mattay, V. S., Tessitore, A., Kolachana, B., Fera, F., Goldman, D., Egan, M. F., & Weinberger, D. R. (2002). Serotonin transporter genetic variation and the response of the human amygdala. *Science*, 297(5580), 400-403. <https://doi.org/10.1126/science.1071829>

Heinz, A., Braus, D. F., Smolka, M. N., Wrase, J., Puls, I., Hermann, D., Klein, S., Grüsser, S. M., Flor, H., Schumann, G., Mann, K., & Büchel, C. (2005). Amygdala-

prefrontal coupling depends on a genetic variation of the serotonin transporter. *Nat Neurosci*, 8(1), 20-21. <https://doi.org/10.1038/nn1366>

Heinz, A. J., Beck, A., Meyer-Lindenberg, A., Sterzer, P., & Heinz, A. (2011). Cognitive and neurobiological mechanisms of alcohol-related aggression. *Nat Rev Neurosci*, 12(7), 400-413. <https://doi.org/10.1038/nrn3042>

Ho, B. C., Milev, P., O'Leary, D. S., Librant, A., Andreasen, N. C., & Wassink, T. H. (2006). Cognitive and magnetic resonance imaging brain morphometric correlates of brain-derived neurotrophic factor Val66Met gene polymorphism in patients with schizophrenia and healthy volunteers. *Arch Gen Psychiatry*, 63(7), 731-740. <https://doi.org/10.1001/archpsyc.63.7.731>

Holmes, T. H., & Rahe, R. H. (1967). The social readjustment rating scale. *Journal of Psychosomatic Research*, 11(2), 213-218. [https://doi.org/https://doi.org/10.1016/0022-3999\(67\)90010-4](https://doi.org/https://doi.org/10.1016/0022-3999(67)90010-4)

Hu, X., Oroszi, G., Chun, J., Smith, T. L., Goldman, D., & Schuckit, M. A. (2005). An expanded evaluation of the relationship of four alleles to the level of response to alcohol and the alcoholism risk. *Alcohol Clin Exp Res*, 29(1), 8-16. <https://doi.org/10.1097/01.alc.0000150008.68473.62>

Hwang, I. W., Lim, M. H., Kwon, H. J., & Jin, H. J. (2018). Association of Monoamine Oxidase A (MAOA) Gene uVNTR and rs6323 Polymorphisms with Attention Deficit and Hyperactivity Disorder in Korean Children. *Medicina (Kaunas)*, 54(3). <https://doi.org/10.3390/medicina54030032>

Johnstone, T., Somerville, L. H., Alexander, A. L., Oakes, T. R., Davidson, R. J., Kalin, N. H., & Whalen, P. J. (2005). Stability of amygdala BOLD response to fearful faces over multiple scan sessions. *Neuroimage*, 25(4), 1112-1123. <https://doi.org/10.1016/j.neuroimage.2004.12.016>

Kim-Cohen, J., Caspi, A., Taylor, A., Williams, B., Newcombe, R., Craig, I. W., & Moffitt, T. E. (2006). MAOA, maltreatment, and gene-environment interaction predicting children's mental health: new evidence and a meta-analysis. *Mol Psychiatry*, 11(10), 903-913. <https://doi.org/10.1038/sj.mp.4001851>

Kish, S. J., Furukawa, Y., Chang, L. J., Tong, J., Ginovart, N., Wilson, A., Houle, S., & Meyer, J. H. (2005). Regional distribution of serotonin transporter protein in postmortem human brain: is the cerebellum a SERT-free brain region? *Nucl Med Biol*, 32(2), 123-128. <https://doi.org/10.1016/j.nucmedbio.2004.10.001>

Klein, M., van Donkelaar, M., Verhoef, E., & Franke, B. (2017). Imaging genetics in neurodevelopmental psychopathology. *Am J Med Genet B Neuropsychiatr Genet*, 174(5), 485-537. <https://doi.org/10.1002/ajmg.b.32542>

Komorowski, A., James, G. M., Philippe, C., Gryglewski, G., Bauer, A., Hienert, M., Spies, M., Kautzky, A., Vanicek, T., Hahn, A., Traub-Weidinger, T., Winkler, D., Wadsak, W., Mitterhauser, M., Hacker, M., Kasper, S., & Lanzenberger, R. (2017). Association of Protein Distribution and Gene Expression Revealed by PET and Post-

Mortem Quantification in the Serotonergic System of the Human Brain. *Cereb Cortex*, 27(1), 117-130. <https://doi.org/10.1093/cercor/bhw355>

Kruschwitz, J. D., Walter, M., Varikuti, D., Jensen, J., Plichta, M. M., Haddad, L., Grimm, O., Mohnke, S., Pöhlend, L., Schott, B., Wold, A., Mühleisen, T. W., Heinz, A., Erk, S., Romanczuk-Seiferth, N., Witt, S. H., Nöthen, M. M., Rietschel, M., Meyer-Lindenberg, A., & Walter, H. (2015). 5-HTTLPR/rs25531 polymorphism and neuroticism are linked by resting state functional connectivity of amygdala and fusiform gyrus. *Brain Struct Funct*, 220(4), 2373-2385. <https://doi.org/10.1007/s00429-014-0782-0>

Kuepper, Y., Grant, P., Wielpuetz, C., & Hennig, J. (2013). MAOA-uVNTR genotype predicts interindividual differences in experimental aggressiveness as a function of the degree of provocation. *Behav Brain Res*, 247, 73-78. <https://doi.org/10.1016/j.bbr.2013.03.002>

Lee, B. T., & Ham, B. J. (2008). Monoamine oxidase A-uVNTR genotype affects limbic brain activity in response to affective facial stimuli. *Neuroreport*, 19(5), 515-519. <https://doi.org/10.1097/WNR.0b013e3282f94294>

Lesch, K. P., Bengel, D., Heils, A., Sabol, S. Z., Greenberg, B. D., Petri, S., Benjamin, J., Müller, C. R., Hamer, D. H., & Murphy, D. L. (1996). Association of anxiety-related traits with a polymorphism in the serotonin transporter gene regulatory region. *Science (New York, N.Y.)*, 274(5292), 1527-1531. <https://doi.org/10.1126/science.274.5292.1527>

Liu, X., Hairston, J., Schrier, M., & Fan, J. (2011). Common and distinct networks underlying reward valence and processing stages: a meta-analysis of functional neuroimaging studies. *Neurosci Biobehav Rev*, 35(5), 1219-1236. <https://doi.org/10.1016/j.neubiorev.2010.12.012>

Liu, Z., Huang, L., Luo, X. J., Wu, L., & Li, M. (2016). MAOA Variants and Genetic Susceptibility to Major Psychiatric Disorders. *Mol Neurobiol*, 53(7), 4319-4327. <https://doi.org/10.1007/s12035-015-9374-0>

Manor, I., Tyano, S., Mel, E., Eisenberg, J., Bachner-Melman, R., Kotler, M., & Ebstein, R. P. (2002). Family-based and association studies of monoamine oxidase A and attention deficit hyperactivity disorder (ADHD): preferential transmission of the long promoter-region repeat and its association with impaired performance on a continuous performance test (TOVA). *Mol Psychiatry*, 7(6), 626-632. <https://doi.org/10.1038/sj.mp.4001037>

Mathews, T. A., Fedele, D. E., Coppelli, F. M., Avila, A. M., Murphy, D. L., & Andrews, A. M. (2004). Gene dose-dependent alterations in extraneuronal serotonin but not dopamine in mice with reduced serotonin transporter expression. *J Neurosci Methods*, 140(1-2), 169-181. <https://doi.org/10.1016/j.jneumeth.2004.05.017>

McDermott, R., Tingley, D., Cowden, J., Frazzetto, G., & Johnson, D. D. (2009). Monoamine oxidase A gene (MAOA) predicts behavioral aggression following provocation. *Proc Natl Acad Sci U S A*, 106(7), 2118-2123. <https://doi.org/10.1073/pnas.0808376106>

- Melas, P. A., Wei, Y., Wong, C. C., Sjöholm, L. K., Åberg, E., Mill, J., Schalling, M., Forsell, Y., & Lavebratt, C. (2013). Genetic and epigenetic associations of MAOA and NR3C1 with depression and childhood adversities. *Int J Neuropsychopharmacol*, 16(7), 1513-1528. <https://doi.org/10.1017/s1461145713000102>
- Mertins, V., Schote, A. B., Hoffeld, W., Griessmair, M., & Meyer, J. (2011). Genetic susceptibility for individual cooperation preferences: the role of monoamine oxidase A gene (MAOA) in the voluntary provision of public goods. *PLoS One*, 6(6), e20959. <https://doi.org/10.1371/journal.pone.0020959>
- Meyer-Lindenberg, A., Buckholtz, J. W., Kolachana, B., A, R. H., Pezawas, L., Blasi, G., Wabnitz, A., Honea, R., Verchinski, B., Callicott, J. H., Egan, M., Mattay, V., & Weinberger, D. R. (2006). Neural mechanisms of genetic risk for impulsivity and violence in humans. *Proc Natl Acad Sci U S A*, 103(16), 6269-6274. <https://doi.org/10.1073/pnas.0511311103>
- Minichiello, L. (2009). TrkB signalling pathways in LTP and learning. *Nat Rev Neurosci*, 10(12), 850-860. <https://doi.org/10.1038/nrn2738>
- Montag, C., Weber, B., Fliessbach, K., Elger, C., & Reuter, M. (2009). The BDNF Val66Met polymorphism impacts parahippocampal and amygdala volume in healthy humans: incremental support for a genetic risk factor for depression. *Psychol Med*, 39(11), 1831-1839. <https://doi.org/10.1017/s0033291709005509>
- Murphy, S. E., Norbury, R., Godlewska, B. R., Cowen, P. J., Mannie, Z. M., Harmer, C. J., & Munafò, M. R. (2013). The effect of the serotonin transporter polymorphism (5-HTTLPR) on amygdala function: a meta-analysis. *Mol Psychiatry*, 18(4), 512-520. <https://doi.org/10.1038/mp.2012.19>
- Neves-Pereira, M., Cheung, J. K., Pasdar, A., Zhang, F., Breen, G., Yates, P., Sinclair, M., Crombie, C., Walker, N., & St Clair, D. M. (2005). BDNF gene is a risk factor for schizophrenia in a Scottish population. *Mol Psychiatry*, 10(2), 208-212. <https://doi.org/10.1038/sj.mp.4001575>
- Ou, X. M., Chen, K., & Shih, J. C. (2006). Monoamine oxidase A and repressor R1 are involved in apoptotic signaling pathway. *Proc Natl Acad Sci U S A*, 103(29), 10923-10928. <https://doi.org/10.1073/pnas.0601515103>
- Pacheco, J., Beevers, C. G., Benavides, C., McGeary, J., Stice, E., & Schnyer, D. M. (2009). Frontal-limbic white matter pathway associations with the serotonin transporter gene promoter region (5-HTTLPR) polymorphism. *J Neurosci*, 29(19), 6229-6233. <https://doi.org/10.1523/jneurosci.0896-09.2009>
- Palumbo, S., Mariotti, V., Iofrida, C., & Pellegrini, S. (2018). Genes and Aggressive Behavior: Epigenetic Mechanisms Underlying Individual Susceptibility to Aversive Environments. *Front Behav Neurosci*, 12, 117. <https://doi.org/10.3389/fnbeh.2018.00117>
- Passamonti, L., Cerasa, A., Gioia, M. C., Magariello, A., Muglia, M., Quattrone, A., & Fera, F. (2008). Genetically dependent modulation of serotonergic inactivation in the human prefrontal cortex. *Neuroimage*, 40(3), 1264-1273. <https://doi.org/10.1016/j.neuroimage.2007.12.028>

Pezawas, L., Meyer-Lindenberg, A., Drabant, E. M., Verchinski, B. A., Munoz, K. E., Kolachana, B. S., Egan, M. F., Mattay, V. S., Hariri, A. R., & Weinberger, D. R. (2005). 5-HTTLPR polymorphism impacts human cingulate-amygdala interactions: a genetic susceptibility mechanism for depression. *Nat Neurosci*, 8(6), 828-834. <https://doi.org/10.1038/nn1463>

Pezawas, L., Meyer-Lindenberg, A., Goldman, A. L., Verchinski, B. A., Chen, G., Kolachana, B. S., Egan, M. F., Mattay, V. S., Hariri, A. R., & Weinberger, D. R. (2008). Evidence of biologic epistasis between BDNF and SLC6A4 and implications for depression. *Mol Psychiatry*, 13(7), 709-716. <https://doi.org/10.1038/mp.2008.32>

Pezawas, L., Verchinski, B. A., Mattay, V. S., Callicott, J. H., Kolachana, B. S., Straub, R. E., Egan, M. F., Meyer-Lindenberg, A., & Weinberger, D. R. (2004). The brain-derived neurotrophic factor val66met polymorphism and variation in human cortical morphology. *J Neurosci*, 24(45), 10099-10102. <https://doi.org/10.1523/jneurosci.2680-04.2004>

Phillips, M. L., Drevets, W. C., Rauch, S. L., & Lane, R. (2003). Neurobiology of emotion perception I: The neural basis of normal emotion perception. *Biol Psychiatry*, 54(5), 504-514. [https://doi.org/10.1016/s0006-3223\(03\)00168-9](https://doi.org/10.1016/s0006-3223(03)00168-9)

Plichta, M. M., Schwarz, A. J., Grimm, O., Morgen, K., Mier, D., Haddad, L., Gerdes, A. B., Sauer, C., Tost, H., Esslinger, C., Colman, P., Wilson, F., Kirsch, P., & Meyer-Lindenberg, A. (2012). Test-retest reliability of evoked BOLD signals from a cognitive-emotive fMRI test battery. *Neuroimage*, 60(3), 1746-1758. <https://doi.org/10.1016/j.neuroimage.2012.01.129>

Power, J. D., Cohen, A. L., Nelson, S. M., Wig, G. S., Barnes, K. A., Church, J. A., Vogel, A. C., Laumann, T. O., Miezin, F. M., Schlaggar, B. L., & Petersen, S. E. (2011). Functional network organization of the human brain. *Neuron*, 72(4), 665-678. <https://doi.org/10.1016/j.neuron.2011.09.006>

Praschak-Rieder, N., Kennedy, J., Wilson, A. A., Hussey, D., Boovariwala, A., Willeit, M., Ginovart, N., Tharmalingam, S., Masellis, M., Houle, S., & Meyer, J. H. (2007). Novel 5-HTTLPR allele associates with higher serotonin transporter binding in putamen: a [(11)C] DASB positron emission tomography study. *Biol Psychiatry*, 62(4), 327-331. <https://doi.org/10.1016/j.biopsych.2006.09.022>

Rabl, U., Meyer, B. M., Diers, K., Bartova, L., Berger, A., Mandorfer, D., Popovic, A., Scharinger, C., Huemer, J., Kalcher, K., Pail, G., Haslacher, H., Perkmann, T., Windischberger, C., Brocke, B., Sitte, H. H., Pollak, D. D., Dreher, J. C., Kasper, S., . . . Pezawas, L. (2014). Additive gene-environment effects on hippocampal structure in healthy humans. *J Neurosci*, 34(30), 9917-9926. <https://doi.org/10.1523/jneurosci.3113-13.2014>

Raine, A. (2008). From Genes to Brain to Antisocial Behavior. *Current Directions in Psychological Science*, 17(5), 323-328. <https://doi.org/10.1111/j.1467-8721.2008.00599.x>

- Rioux, A., Fabre, V., Lesch, K. P., Moessner, R., Murphy, D. L., Lanfumey, L., Hamon, M., & Martres, M. P. (1999). Adaptive changes of serotonin 5-HT_{2A} receptors in mice lacking the serotonin transporter. *Neurosci Lett*, 262(2), 113-116. [https://doi.org/10.1016/s0304-3940\(99\)00049-x](https://doi.org/10.1016/s0304-3940(99)00049-x)
- Rueckert, D., Sonoda, L. I., Hayes, C., Hill, D. L., Leach, M. O., & Hawkes, D. J. (1999). Nonrigid registration using free-form deformations: application to breast MR images. *IEEE Trans Med Imaging*, 18(8), 712-721. <https://doi.org/10.1109/42.796284>
- Sabatinelli, D., Fortune, E. E., Li, Q., Siddiqui, A., Krafft, C., Oliver, W. T., Beck, S., & Jeffries, J. (2011). Emotional perception: meta-analyses of face and natural scene processing. *Neuroimage*, 54(3), 2524-2533. <https://doi.org/10.1016/j.neuroimage.2010.10.011>
- Sabol, S. Z., Hu, S., & Hamer, D. (1998). A functional polymorphism in the monoamine oxidase A gene promoter. *Hum Genet*, 103(3), 273-279. <https://doi.org/10.1007/s004390050816>
- Shih, J. C., Chen, K., & Ridd, M. J. (1999). Monoamine oxidase: from genes to behavior. *Annu Rev Neurosci*, 22, 197-217. <https://doi.org/10.1146/annurev.neuro.22.1.197>
- Shumay, E., Logan, J., Volkow, N. D., & Fowler, J. S. (2012). Evidence that the methylation state of the monoamine oxidase A (MAOA) gene predicts brain activity of MAOA enzyme in healthy men. *Epigenetics*, 7(10), 1151-1160. <https://doi.org/10.4161/epi.21976>
- Sklar, P., Gabriel, S. B., McInnis, M. G., Bennett, P., Lim, Y., Tsan, G., Schaffner, S., Kirov, G., Jones, I., Owen, M., Craddock, N., DePaulo, J. R., & Lander, E. S. (2002). Family-based association study of 76 candidate genes in bipolar disorder: BDNF is a potential risk locus. Brain-derived neurotrophic factor. *Mol Psychiatry*, 7(6), 579-593. <https://doi.org/10.1038/sj.mp.4001058>
- Smith, S. M. (2002). Fast robust automated brain extraction. *Hum Brain Mapp*, 17(3), 143-155. <https://doi.org/10.1002/hbm.10062>
- Smith, S. M., Jenkinson, M., Johansen-Berg, H., Rueckert, D., Nichols, T. E., Mackay, C. E., Watkins, K. E., Ciccarelli, O., Cader, M. Z., Matthews, P. M., & Behrens, T. E. (2006). Tract-based spatial statistics: voxelwise analysis of multi-subject diffusion data. *Neuroimage*, 31(4), 1487-1505. <https://doi.org/10.1016/j.neuroimage.2006.02.024>
- Smith, S. M., Jenkinson, M., Woolrich, M. W., Beckmann, C. F., Behrens, T. E., Johansen-Berg, H., Bannister, P. R., De Luca, M., Drobnjak, I., Flitney, D. E., Niazy, R. K., Saunders, J., Vickers, J., Zhang, Y., De Stefano, N., Brady, J. M., & Matthews, P. M. (2004). Advances in functional and structural MR image analysis and implementation as FSL. *Neuroimage*, 23 Suppl 1, S208-219. <https://doi.org/10.1016/j.neuroimage.2004.07.051>
- Söderqvist, S., Matsson, H., Peyrard-Janvid, M., Kere, J., & Klingberg, T. (2014). Polymorphisms in the dopamine receptor 2 gene region influence improvements during working memory training in children and adolescents. *J Cogn Neurosci*, 26(1), 54-62. https://doi.org/10.1162/jocn_a_00478

- Spreng, R. N., Mar, R. A., & Kim, A. S. (2009). The common neural basis of autobiographical memory, prospection, navigation, theory of mind, and the default mode: a quantitative meta-analysis. *J Cogn Neurosci*, 21(3), 489-510. <https://doi.org/10.1162/jocn.2008.21029>
- Surguladze, S. A., Radua, J., El-Hage, W., Gohier, B., Sato, J. R., Kronhaus, D. M., Proitsi, P., Powell, J., & Phillips, M. L. (2012). Interaction of catechol O-methyltransferase and serotonin transporter genes modulates effective connectivity in a facial emotion-processing circuitry. *Transl Psychiatry*, 2(1), e70. <https://doi.org/10.1038/tp.2011.69>
- Susumu Mori, S. W., Peter C M van Zijl, L.M. Nagae-Poetscher. (2005). *MRI Atlas of Human White Matter*.
- Tong, J., Meyer, J. H., Furukawa, Y., Boileau, I., Chang, L. J., Wilson, A. A., Houle, S., & Kish, S. J. (2013). Distribution of monoamine oxidase proteins in human brain: implications for brain imaging studies. *J Cereb Blood Flow Metab*, 33(6), 863-871. <https://doi.org/10.1038/jcbfm.2013.19>
- Tost, H., Alam, T., Geramita, M., Rebsch, C., Kolachana, B., Dickinson, D., Verchinski, B. A., Lemaitre, H., Barnett, A. S., Trampush, J. W., Weinberger, D. R., & Marenco, S. (2013). Effects of the BDNF Val66Met polymorphism on white matter microstructure in healthy adults. *Neuropsychopharmacology*, 38(3), 525-532. <https://doi.org/10.1038/npp.2012.214>
- Tzourio-Mazoyer, N., Landeau, B., Papathanassiou, D., Crivello, F., Etard, O., Delcroix, N., Mazoyer, B., & Joliot, M. (2002). Automated anatomical labeling of activations in SPM using a macroscopic anatomical parcellation of the MNI MRI single-subject brain. *Neuroimage*, 15(1), 273-289. <https://doi.org/10.1006/nimg.2001.0978>
- Upton, A. L., Salichon, N., Lebrand, C., Ravary, A., Blakely, R., Seif, I., & Gaspar, P. (1999). Excess of serotonin (5-HT) alters the segregation of ipsilateral and contralateral retinal projections in monoamine oxidase A knock-out mice: possible role of 5-HT uptake in retinal ganglion cells during development. *J Neurosci*, 19(16), 7007-7024. <https://doi.org/10.1523/jneurosci.19-16-07007.1999>
- van der Doelen, R. H., Deschamps, W., D'Annibale, C., Peeters, D., Wevers, R. A., Zelena, D., Homberg, J. R., & Kozicz, T. (2014). Early life adversity and serotonin transporter gene variation interact at the level of the adrenal gland to affect the adult hypothalamo-pituitary-adrenal axis. *Transl Psychiatry*, 4(7), e409. <https://doi.org/10.1038/tp.2014.57>
- Varnäs, K., Halldin, C., & Hall, H. (2004). Autoradiographic distribution of serotonin transporters and receptor subtypes in human brain. *Hum Brain Mapp*, 22(3), 246-260. <https://doi.org/10.1002/hbm.20035>
- Verhagen, M., van der Meij, A., van Deurzen, P. A., Janzing, J. G., Arias-Vasquez, A., Buitelaar, J. K., & Franke, B. (2010). Meta-analysis of the BDNF Val66Met polymorphism in major depressive disorder: effects of gender and ethnicity. *Mol Psychiatry*, 15(3), 260-271. <https://doi.org/10.1038/mp.2008.109>

- Viviani, R., Sim, E. J., Lo, H., Beschoner, P., Osterfeld, N., Maier, C., Seeringer, A., Godoy, A. L., Rosa, A., Comas, D., & Kirchheiner, J. (2010). Baseline brain perfusion and the serotonin transporter promoter polymorphism. *Biol Psychiatry*, 67(4), 317-322. <https://doi.org/10.1016/j.biopsych.2009.08.035>
- Wang, Z. Q., Chen, K., Ying, Q. L., Li, P., & Shih, J. C. (2011). Monoamine oxidase A regulates neural differentiation of murine embryonic stem cells. *J Neural Transm (Vienna)*, 118(7), 997-1001. <https://doi.org/10.1007/s00702-011-0655-0>
- Wechsler, D. (1997) Wechsler Adult Intelligence Scale. 3rd Edition, The Psychological Corporation, San Antonio.
- Wendland, J. R., Martin, B. J., Kruse, M. R., Lesch, K. P., & Murphy, D. L. (2006). Simultaneous genotyping of four functional loci of human SLC6A4, with a reappraisal of 5-HTTLPR and rs25531. *Mol Psychiatry*, 11(3), 224-226. <https://doi.org/10.1038/sj.mp.4001789>
- Williams, L. M., Gatt, J. M., Kuan, S. A., Dobson-Stone, C., Palmer, D. M., Paul, R. H., Song, L., Costa, P. T., Schofield, P. R., & Gordon, E. (2009). A polymorphism of the MAOA gene is associated with emotional brain markers and personality traits on an antisocial index. *Neuropsychopharmacology*, 34(7), 1797-1809. <https://doi.org/10.1038/npp.2009.1>
- Yan, C. G., Cheung, B., Kelly, C., Colcombe, S., Craddock, R. C., Di Martino, A., Li, Q., Zuo, X. N., Castellanos, F. X., & Milham, M. P. (2013). A comprehensive assessment of regional variation in the impact of head micromovements on functional connectomics. *Neuroimage*, 76, 183-201. <https://doi.org/10.1016/j.neuroimage.2013.03.004>
- Yeh, F. C., Verstynen, T. D., Wang, Y., Fernández-Miranda, J. C., & Tseng, W. Y. (2013). Deterministic diffusion fiber tracking improved by quantitative anisotropy. *PLoS One*, 8(11), e80713. <https://doi.org/10.1371/journal.pone.0080713>
- Zalesky, A., Fornito, A., & Bullmore, E. T. (2010). Network-based statistic: identifying differences in brain networks. *Neuroimage*, 53(4), 1197-1207. <https://doi.org/10.1016/j.neuroimage.2010.06.041>
- Zang, Z., Geiger, L. S., Braun, U., Cao, H., Zangl, M., Schäfer, A., Moessnang, C., Ruf, M., Reis, J., Schweiger, J. I., Dixon, L., Moscicki, A., Schwarz, E., Meyer-Lindenberg, A., & Tost, H. (2018). Resting-state brain network features associated with short-term skill learning ability in humans and the influence of N-methyl-d-aspartate receptor antagonism. *Netw Neurosci*, 2(4), 464-480. https://doi.org/10.1162/netn_a_00045

6. SUPPLEMENTAL MATERIAL

Tables 7-9: Nodes and links of the MAOA-associated subnetworks

For clarity of presentation, we projected the coordinates of nodes from significant links to the AAL atlas (Tzourio-Mazoyer et al., 2002) and assigned the respective anatomical mask labels to the nodes. Coordinates are given in MNI space (x, y, z). Please note that the reported t-values of individual links are based on link-wise comparisons that are used to determine the initial network of the NBS analysis. Statistical significance of the NBS model is determined based on the number of connected links. Node labels mapping to the frontal cortex are **bolded**. Node labels corresponding to links connecting different nodes within the same major brain subdivision of the AAL atlas (isocoupled) are *italicized*. The top 10% of the most significant MAOA-associated links for each modality are highlighted in red.

Abbreviations : precentral gyrus (Precentral), superior frontal gyrus (Frontal_Sup), superior frontal gyrus, orbital part (Frontal_Sup_Orb), middle frontal gyrus (Frontal_Mid), middle frontal gyrus, orbital part (Frontal_Mid_Orb), inferior frontal gyrus, pars opercularis (Frontal_Inf_Oper), inferior frontal gyrus, pars triangularis (Frontal_Inf_Tri), inferior frontal gyrus, pars orbitalis (Frontal_Inf_Orb), Rolandic operculum (Rolandic_Oper), supplementary motor area (Supp_Motor_Area), olfactory cortex (Olfactory), medial frontal gyrus (Frontal_Sup_Medial), medial orbitofrontal cortex (Frontal_Med_Orb), gyrus rectus (Rectus), insula (Insula), anterior cingulate gyrus (Cingulum_Ant), midcingulate area (Cingulum_Mid), posterior cingulate gyrus (Cingulum_Post), hippocampus (Hippocampus), parahippocampal gyrus (ParaHippocampal), amygdala (Amygdala), calcarine sulcus (Calcarine), cuneus (Cuneus), lingual gyrus (Lingual), superior occipital gyrus (Occipital_Sup), middle occipital gyrus (Occipital_Mid), inferior occipital gyrus (Occipital_Inf), fusiform gyrus (Fusiform), postcentral gyrus (Postcentral), superior parietal lobule (Parietal_Sup), inferior parietal lobule (Parietal_Inf), supramarginal gyrus (SupraMarginal), angular gyrus (Angular), precuneus (Precuneus), paracentral lobule (Paracentral_Lobule), caudate nucleus (Caudate), putamen (Putamen), globus pallidus (Pallidum), thalamus (Thalamus), transverse temporal gyrus (Heschl), superior temporal gyrus (Temporal_Sup), superior temporal pole (Temporal_Pole_Sup), middle temporal gyrus (Temporal_Mid), middle temporal pole (Temporal_Pole_Mid), inferior temporal gyrus (Temporal_Inf), crus I of cerebellar hemisphere (Cerebellum_Crus1), crus II of cerebellar hemisphere (Cerebellum_Crus2), lobule III of cerebellar hemisphere (Cerebellum_3), lobule IV, V of cerebellar hemisphere (Cerebellum_4_5), lobule VI of cerebellar hemisphere (Cerebellum_6), lobule VIIb of cerebellar hemisphere (Cerebellum_7b), lobule VIII of cerebellar hemisphere (Cerebellum_8), lobule IX of cerebellar hemisphere (Cerebellum_9), lobule X of cerebellar hemisphere (Cerebellum_10), Lobule I, II of vermis (Vermis_1_2), lobule III of vermis (Vermis_3), Lobule IV, V of vermis (Vermis_4_5), Lobule VI of vermis (Vermis_6), Lobule VII of vermis (Vermis_7), Lobule VIII of vermis (Vermis_8), Lobule IX of vermis (Vermis_9), Lobule X of vermis (Vermis_10). The succeeding “R.” and “L.” indicate the right and left hemisphere, respectively.

| Table 7: fMRI emotion processing | | | | | |
|----------------------------------|-----------------------------|-------------------|-------------------|----------|----------|
| Brain node 1* | Brain node 2* | MNI coordinate 1# | MNI coordinate 2# | t-value | p-value |
| Precentral_R | Frontal_Inf_Oper_L | 40 -8 52 | -49 13 19 | 2.789244 | 0.002853 |
| Frontal_Inf_Oper_L | Frontal_Inf_Tri_R | -49 13 19 | 49 30 14 | 2.608844 | 0.004826 |
| Frontal_Inf_Oper_L | Frontal_Inf_Orb_R | -49 13 19 | 40 32 -12 | 2.670695 | 0.004042 |
| Frontal_Sup_L | Rolandic_Oper_L | -19 35 42 | -48 -8 14 | 2.62261 | 0.004641 |
| Frontal_Sup_Orb_L | Rolandic_Oper_L | -18 47 -13 | -48 -8 14 | 2.701509 | 0.003696 |
| Frontal_Mid_L | Rolandic_Oper_L | -34 33 35 | -48 -8 14 | 2.791957 | 0.00283 |
| Frontal_Mid_Orb_L | Rolandic_Oper_L | -32 50 -10 | -48 -8 14 | 3.338318 | 0.000488 |
| Frontal_Mid_Orb_R | Rolandic_Oper_L | 32 53 -11 | -48 -8 14 | 2.624582 | 0.004615 |
| Frontal_Inf_Orb_L | Rolandic_Oper_L | -37 31 -12 | -48 -8 14 | 2.701593 | 0.003695 |
| Frontal_Inf_Orb_R | Rolandic_Oper_L | 40 32 -12 | -48 -8 14 | 2.74621 | 0.003242 |
| Frontal_Inf_Orb_R | Rolandic_Oper_R | 40 32 -12 | 52 -6 15 | 2.664439 | 0.004116 |
| Frontal_Inf_Oper_L | Supp_Motor_Area_L | -49 13 19 | -6 5 61 | 3.065874 | 0.001209 |
| Frontal_Inf_Oper_L | Supp_Motor_Area_R | -49 13 19 | 8 0 62 | 2.931204 | 0.001851 |
| Rolandic_Oper_L | Frontal_Sup_Medial_L | -48 -8 14 | -6 49 31 | 3.007546 | 0.001456 |
| Frontal_Inf_Oper_L | Hippocampus_R | -49 13 19 | 28 -20 -10 | 2.894483 | 0.002073 |
| Frontal_Inf_Tri_L | Hippocampus_R | -47 30 14 | 28 -20 -10 | 2.672375 | 0.004023 |
| Frontal_Inf_Oper_L | ParaHippocampal_L | -49 13 19 | -22 -16 -21 | 2.831707 | 0.002511 |
| Rolandic_Oper_L | ParaHippocampal_L | -48 -8 14 | -22 -16 -21 | 2.784064 | 0.002897 |
| Frontal_Inf_Oper_L | ParaHippocampal_R | -49 13 19 | 24 -15 -20 | 3.443554 | 0.000338 |
| Frontal_Inf_Tri_L | ParaHippocampal_R | -47 30 14 | 24 -15 -20 | 3.072065 | 0.001185 |
| Rolandic_Oper_L | ParaHippocampal_R | -48 -8 14 | 24 -15 -20 | 2.808399 | 0.002693 |
| Rolandic_Oper_R | ParaHippocampal_R | 52 -6 15 | 24 -15 -20 | 2.887219 | 0.00212 |
| Frontal_Inf_Oper_L | Amygdala_L | -49 13 19 | -24 -1 -17 | 3.000939 | 0.001487 |
| Frontal_Inf_Tri_L | Amygdala_L | -47 30 14 | -24 -1 -17 | 2.953339 | 0.001727 |
| Rolandic_Oper_L | Amygdala_L | -48 -8 14 | -24 -1 -17 | 3.057512 | 0.001242 |
| Rolandic_Oper_R | Amygdala_L | 52 -6 15 | -24 -1 -17 | 3.310275 | 0.000537 |
| Frontal_Inf_Oper_L | Amygdala_R | -49 13 19 | 26 1 -18 | 3.012266 | 0.001435 |
| Precentral_R | Calcarine_L | 40 -8 52 | -8 -79 6 | 2.6922 | 0.003798 |
| Frontal_Inf_Oper_L | Calcarine_L | -49 13 19 | -8 -79 6 | 3.102684 | 0.001073 |
| Rolandic_Oper_L | Calcarine_L | -48 -8 14 | -8 -79 6 | 3.70804 | 0.00013 |

| | | | | | |
|----------------------|-----------------|------------|-------------|----------|----------|
| Rolandic_Oper_R | Calcarine_L | 52 -6 15 | -8 -79 6 | 3.605841 | 0.000189 |
| Precentral_R | Calcarine_R | 40 -8 52 | 15 -73 9 | 2.792355 | 0.002826 |
| Rolandic_Oper_L | Calcarine_R | -48 -8 14 | 15 -73 9 | 2.89704 | 0.002057 |
| Rolandic_Oper_R | Calcarine_R | 52 -6 15 | 15 -73 9 | 2.86152 | 0.002293 |
| Precentral_R | Cuneus_L | 40 -8 52 | -7 -80 27 | 2.851949 | 0.002361 |
| Rolandic_Oper_L | Cuneus_L | -48 -8 14 | -7 -80 27 | 2.600447 | 0.004943 |
| Precentral_R | Cuneus_R | 40 -8 52 | 13 -79 28 | 2.66735 | 0.004082 |
| Frontal_Inf_Oper_L | Lingual_L | -49 13 19 | -16 -68 -5 | 3.18562 | 0.000818 |
| Rolandic_Oper_L | Lingual_L | -48 -8 14 | -16 -68 -5 | 3.604013 | 0.00019 |
| Rolandic_Oper_R | Lingual_L | 52 -6 15 | -16 -68 -5 | 3.342133 | 0.000482 |
| Rolandic_Oper_L | Lingual_R | -48 -8 14 | 15 -67 -4 | 3.419842 | 0.000368 |
| Rolandic_Oper_R | Lingual_R | 52 -6 15 | 15 -67 -4 | 2.971499 | 0.001632 |
| Rolandic_Oper_L | Occipital_Inf_L | -48 -8 14 | -37 -78 -8 | 2.639258 | 0.004425 |
| Frontal_Inf_Oper_L | Fusiform_L | -49 13 19 | -32 -40 -20 | 2.74551 | 0.003249 |
| Rolandic_Oper_L | Fusiform_L | -48 -8 14 | -32 -40 -20 | 2.76819 | 0.003037 |
| Frontal_Inf_Oper_L | Postcentral_R | -49 13 19 | 40 -25 53 | 2.665739 | 0.004101 |
| Rolandic_Oper_L | Postcentral_R | -48 -8 14 | 40 -25 53 | 2.701708 | 0.003694 |
| Frontal_Mid_R | Parietal_Inf_R | 37 33 34 | 45 -46 50 | 3.359739 | 0.000453 |
| Frontal_Mid_Orb_R | Parietal_Inf_R | 32 53 -11 | 45 -46 50 | 2.643273 | 0.004375 |
| Frontal_Sup_L | SupraMarginal_L | -19 35 42 | -57 -34 30 | 2.609817 | 0.004813 |
| Frontal_Sup_Orb_L | SupraMarginal_L | -18 47 -13 | -57 -34 30 | 2.993317 | 0.001523 |
| Frontal_Sup_Orb_R | SupraMarginal_L | 17 48 -14 | -57 -34 30 | 3.020688 | 0.001397 |
| Frontal_Mid_L | SupraMarginal_L | -34 33 35 | -57 -34 30 | 2.889888 | 0.002103 |
| Frontal_Mid_R | SupraMarginal_L | 37 33 34 | -57 -34 30 | 2.764285 | 0.003073 |
| Frontal_Mid_Orb_L | SupraMarginal_L | -32 50 -10 | -57 -34 30 | 3.339683 | 0.000486 |
| Frontal_Mid_Orb_R | SupraMarginal_L | 32 53 -11 | -57 -34 30 | 3.512509 | 0.000265 |
| Frontal_Inf_Orb_L | SupraMarginal_L | -37 31 -12 | -57 -34 30 | 2.903568 | 0.002016 |
| Frontal_Inf_Orb_R | SupraMarginal_L | 40 32 -12 | -57 -34 30 | 3.543148 | 0.000237 |
| Frontal_Sup_Medial_L | SupraMarginal_L | -6 49 31 | -57 -34 30 | 3.019961 | 0.0014 |
| Frontal_Sup_Medial_R | SupraMarginal_L | 8 51 30 | -57 -34 30 | 3.078757 | 0.00116 |
| Frontal_Sup_R | SupraMarginal_R | 20 31 44 | 57 -32 34 | 2.724862 | 0.003452 |
| Frontal_Sup_Orb_R | SupraMarginal_R | 17 48 -14 | 57 -32 34 | 2.976884 | 0.001604 |
| Frontal_Mid_L | SupraMarginal_R | -34 33 35 | 57 -32 34 | 2.975767 | 0.00161 |
| Frontal_Mid_R | SupraMarginal_R | 37 33 34 | 57 -32 34 | 3.438229 | 0.000345 |
| Frontal_Mid_Orb_L | SupraMarginal_R | -32 50 -10 | 57 -32 34 | 3.01103 | 0.00144 |
| Frontal_Mid_Orb_R | SupraMarginal_R | 32 53 -11 | 57 -32 34 | 3.328844 | 0.000504 |
| Frontal_Inf_Orb_L | SupraMarginal_R | -37 31 -12 | 57 -32 34 | 2.72396 | 0.003461 |

| | | | | | |
|----------------------|---------------------|------------|------------|----------|----------|
| Frontal_Inf_Orb_R | SupraMarginal_R | 40 32 -12 | 57 -32 34 | 3.519824 | 0.000258 |
| Frontal_Sup_Medial_L | SupraMarginal_R | -6 49 31 | 57 -32 34 | 2.598843 | 0.004965 |
| Frontal_Sup_Medial_R | SupraMarginal_R | 8 51 30 | 57 -32 34 | 2.765881 | 0.003058 |
| Precentral_R | Angular_R | 40 -8 52 | 45 -60 39 | 2.76286 | 0.003086 |
| Frontal_Sup_Medial_R | Angular_R | 8 51 30 | 45 -60 39 | 2.630354 | 0.00454 |
| Frontal_Inf_Oper_L | Putamen_L | -49 13 19 | -25 4 2 | 3.39865 | 0.000396 |
| Rolandic_Oper_L | Putamen_L | -48 -8 14 | -25 4 2 | 2.770999 | 0.003012 |
| Rolandic_Oper_R | Putamen_L | 52 -6 15 | -25 4 2 | 2.997316 | 0.001504 |
| Frontal_Inf_Oper_L | Putamen_R | -49 13 19 | 27 5 2 | 3.294054 | 0.000568 |
| Rolandic_Oper_L | Putamen_R | -48 -8 14 | 27 5 2 | 2.622979 | 0.004636 |
| Rolandic_Oper_R | Putamen_R | 52 -6 15 | 27 5 2 | 3.062953 | 0.00122 |
| Frontal_Inf_Oper_L | Pallidum_L | -49 13 19 | -19 0 0 | 3.496291 | 0.000281 |
| Rolandic_Oper_L | Pallidum_L | -48 -8 14 | -19 0 0 | 2.867384 | 0.002253 |
| Rolandic_Oper_R | Pallidum_L | 52 -6 15 | -19 0 0 | 3.103917 | 0.001069 |
| Frontal_Inf_Oper_L | Pallidum_R | -49 13 19 | 20 0 0 | 3.355868 | 0.00046 |
| Rolandic_Oper_L | Pallidum_R | -48 -8 14 | 20 0 0 | 2.966931 | 0.001655 |
| Rolandic_Oper_R | Pallidum_R | 52 -6 15 | 20 0 0 | 3.251025 | 0.000657 |
| Precentral_R | Heschl_L | 40 -8 52 | -43 -19 10 | 2.834491 | 0.00249 |
| Frontal_Sup_Orb_L | Heschl_L | -18 47 -13 | -43 -19 10 | 2.714338 | 0.00356 |
| Precentral_L | Heschl_R | -40 -6 51 | 45 -17 10 | 2.893906 | 0.002077 |
| Frontal_Inf_Oper_L | Heschl_R | -49 13 19 | 45 -17 10 | 3.165487 | 0.000874 |
| Frontal_Inf_Tri_L | Heschl_R | -47 30 14 | 45 -17 10 | 2.928633 | 0.001865 |
| Frontal_Sup_Medial_L | Heschl_R | -6 49 31 | 45 -17 10 | 2.619154 | 0.004687 |
| Precentral_L | Temporal_Sup_L | -40 -6 51 | -54 -21 7 | 2.762779 | 0.003087 |
| Precentral_R | Temporal_Sup_L | 40 -8 52 | -54 -21 7 | 3.175672 | 0.000845 |
| Frontal_Sup_L | Temporal_Sup_L | -19 35 42 | -54 -21 7 | 3.009291 | 0.001448 |
| Frontal_Sup_Orb_L | Temporal_Sup_L | -18 47 -13 | -54 -21 7 | 3.20227 | 0.000774 |
| Frontal_Mid_L | Temporal_Sup_L | -34 33 35 | -54 -21 7 | 3.175854 | 0.000844 |
| Frontal_Mid_Orb_L | Temporal_Sup_L | -32 50 -10 | -54 -21 7 | 2.650256 | 0.004288 |
| Frontal_Inf_Oper_L | Temporal_Sup_L | -49 13 19 | -54 -21 7 | 2.940814 | 0.001796 |
| Frontal_Inf_Orb_L | Temporal_Sup_L | -37 31 -12 | -54 -21 7 | 2.63616 | 0.004465 |
| Frontal_Sup_Medial_L | Temporal_Sup_L | -6 49 31 | -54 -21 7 | 3.596051 | 0.000196 |
| Frontal_Sup_Medial_R | Temporal_Sup_L | 8 51 30 | -54 -21 7 | 3.201194 | 0.000776 |
| Frontal_Inf_Oper_L | Temporal_Sup_R | -49 13 19 | 57 -22 7 | 3.118342 | 0.00102 |
| Rolandic_Oper_L | Temporal_Pole_Sup_L | -48 -8 14 | -41 15 -20 | 2.627002 | 0.004583 |

| | | | | | |
|-----------------------------|-------------------------|-------------|-------------|----------|----------|
| Frontal_Inf_Oper_L | Temporal_Pole_Su p_R | -49 13 19 | 47 15 -17 | 3.370703 | 0.000437 |
| Frontal_Inf_Tri_L | Temporal_Pole_Su p_R | -47 30 14 | 47 15 -17 | 3.040713 | 0.00131 |
| Rolandic_Oper_L | Temporal_Pole_Su p_R | -48 -8 14 | 47 15 -17 | 2.835791 | 0.00248 |
| Supp_Motor_Area_L | Temporal_Pole_Su p_R | -6 5 61 | 47 15 -17 | 2.718938 | 0.003513 |
| Precentral_R | Temporal_Mid_L | 40 -8 52 | -57 -34 -2 | 2.808383 | 0.002694 |
| Frontal_Inf_Oper_L | Temporal_Mid_L | -49 13 19 | -57 -34 -2 | 3.396092 | 0.0004 |
| Rolandic_Oper_L | Temporal_Mid_L | -48 -8 14 | -57 -34 -2 | 2.877629 | 0.002183 |
| Supp_Motor_Area_R | Temporal_Mid_L | 8 0 62 | -57 -34 -2 | 2.70887 | 0.003618 |
| Frontal_Inf_Oper_L | Temporal_Mid_R | -49 13 19 | 56 -37 -1 | 2.838276 | 0.002461 |
| Rolandic_Oper_L | Temporal_Mid_R | -48 -8 14 | 56 -37 -1 | 2.794799 | 0.002806 |
| Frontal_Inf_Oper_L | Cerebellum_3_L | -49 13 19 | -9 -37 -19 | 3.030009 | 0.001356 |
| Frontal_Inf_Oper_L | Cerebellum_4_5_L | -49 13 19 | -15 -43 -17 | 3.143643 | 0.000939 |
| Rolandic_Oper_L | Cerebellum_4_5_L | -48 -8 14 | -15 -43 -17 | 3.116455 | 0.001026 |
| Frontal_Inf_Oper_L | Cerebellum_6_L | -49 13 19 | -23 -59 -22 | 2.912824 | 0.001959 |
| Rolandic_Oper_L | Cerebellum_6_L | -48 -8 14 | -23 -59 -22 | 3.276311 | 0.000603 |
| Rolandic_Oper_L | Cerebellum_6_R | -48 -8 14 | 25 -58 -24 | 2.729007 | 0.00341 |
| Rolandic_Oper_R | Cerebellum_6_R | 52 -6 15 | 25 -58 -24 | 2.626579 | 0.004589 |
| Rolandic_Oper_L | Cerebellum_7b_L | -48 -8 14 | -33 -60 -43 | 2.975994 | 0.001609 |
| Frontal_Inf_Oper_L | Cerebellum_8_L | -49 13 19 | -26 -55 -48 | 2.655705 | 0.004221 |
| Rolandic_Oper_L | Cerebellum_8_L | -48 -8 14 | -26 -55 -48 | 3.150936 | 0.000917 |
| Frontal_Sup_L | Cerebellum_9_L | -19 35 42 | -11 -49 -46 | 2.765881 | 0.003058 |
| Frontal_Sup_R | Cerebellum_9_L | 20 31 44 | -11 -49 -46 | 2.808698 | 0.002691 |
| Rolandic_Oper_L | Cerebellum_9_L | -48 -8 14 | -11 -49 -46 | 2.813476 | 0.002653 |
| Frontal_Sup_Medial_R | Cerebellum_9_L | 8 51 30 | -11 -49 -46 | 2.864813 | 0.00227 |
| Frontal_Inf_Oper_L | Vermis_1_2 | -49 13 19 | 1 -39 -20 | 2.779338 | 0.002938 |
| Rolandic_Oper_L | Vermis_7 | -48 -8 14 | 1 -72 -25 | 2.811836 | 0.002666 |
| Frontal_Inf_Oper_L | Vermis_10 | -49 13 19 | 0 -46 -32 | 2.782079 | 0.002914 |
| Insula_L | Amygdala_L | -36 7 3 | -24 -1 -17 | 2.888621 | 0.002111 |
| Insula_R | Amygdala_L | 38 6 2 | -24 -1 -17 | 3.218185 | 0.000734 |
| Insula_L | Postcentral_R | -36 7 3 | 40 -25 53 | 2.738212 | 0.003319 |
| ParaHippocampal_L | Heschl_L | -22 -16 -21 | -43 -19 10 | 2.816006 | 0.002632 |
| Amygdala_L | Heschl_L | -24 -1 -17 | -43 -19 10 | 2.868592 | 0.002244 |
| Fusiform_L | Heschl_L | -32 -40 -20 | -43 -19 10 | 2.834629 | 0.002489 |
| Insula_L | Heschl_R | -36 7 3 | 45 -17 10 | 2.623471 | 0.00463 |
| Amygdala_L | Heschl_R | -24 -1 -17 | 45 -17 10 | 3.171374 | 0.000857 |
| Insula_L | Temporal_Sup_R | -36 7 3 | 57 -22 7 | 2.709538 | 0.003611 |
| Temporal_Sup_L | Temporal_Sup_R | -54 -21 7 | 57 -22 7 | 2.856756 | 0.002327 |
| Heschl_R | Temporal_Pole_Su p_L | 45 -17 10 | -41 15 -20 | 2.717225 | 0.00353 |
| Temporal_Sup_L | Temporal_Mid_L | -54 -21 7 | -57 -34 -2 | 2.786839 | 0.002873 |
| Temporal_Sup_L | Temporal_Mid_R | -54 -21 7 | 56 -37 -1 | 2.597953 | 0.004978 |

| | | | | | |
|----------------------------|----------------------------|-------------|-------------|----------|----------|
| <i>Fusiform_L</i> | <i>Temporal_Pole_Mid_L</i> | -32 -40 -20 | -37 15 -34 | 2.804776 | 0.002723 |
| <i>Fusiform_R</i> | <i>Temporal_Pole_Mid_L</i> | 33 -39 -20 | -37 15 -34 | 2.740031 | 0.003301 |
| <i>ParaHippocampal_R</i> | <i>Temporal_Pole_Mid_R</i> | 24 -15 -20 | 43 15 -32 | 2.968823 | 0.001646 |
| <i>Fusiform_R</i> | <i>Temporal_Pole_Mid_R</i> | 33 -39 -20 | 43 15 -32 | 2.63286 | 0.004507 |
| <i>Heschl_L</i> | <i>Temporal_Inf_L</i> | -43 -19 10 | -51 -28 -23 | 2.683405 | 0.003896 |
| <i>Amygdala_R</i> | <i>Cerebellum_4_5_L</i> | 26 1 -18 | -15 -43 -17 | 2.799043 | 0.00277 |
| <i>Heschl_L</i> | <i>Cerebellum_4_5_L</i> | -43 -19 10 | -15 -43 -17 | 2.682549 | 0.003906 |
| <i>Heschl_L</i> | <i>Cerebellum_6_L</i> | -43 -19 10 | -23 -59 -22 | 3.194575 | 0.000794 |
| <i>Temporal_Sup_L</i> | <i>Cerebellum_6_L</i> | -54 -21 7 | -23 -59 -22 | 3.083956 | 0.00114 |
| <i>Heschl_L</i> | <i>Cerebellum_6_R</i> | -43 -19 10 | 25 -58 -24 | 2.625821 | 0.004599 |
| <i>Heschl_L</i> | <i>Cerebellum_7b_L</i> | -43 -19 10 | -33 -60 -43 | 3.011118 | 0.00144 |
| <i>ParaHippocampal_R</i> | <i>Cerebellum_7b_R</i> | 24 -15 -20 | 35 -64 -47 | 2.609186 | 0.004822 |
| <i>Heschl_L</i> | <i>Cerebellum_8_L</i> | -43 -19 10 | -26 -55 -48 | 3.123467 | 0.001003 |
| <i>Heschl_L</i> | <i>Cerebellum_8_R</i> | -43 -19 10 | 25 -56 -49 | 2.647387 | 0.004323 |
| <i>ParaHippocampal_L</i> | <i>Cerebellum_9_L</i> | -22 -16 -21 | -11 -49 -46 | 2.822023 | 0.002585 |
| <i>ParaHippocampal_R</i> | <i>Cerebellum_9_L</i> | 24 -15 -20 | -11 -49 -46 | 2.77425 | 0.002983 |
| <i>Fusiform_L</i> | <i>Cerebellum_9_L</i> | -32 -40 -20 | -11 -49 -46 | 2.680481 | 0.00393 |
| <i>Fusiform_R</i> | <i>Cerebellum_9_L</i> | 33 -39 -20 | -11 -49 -46 | 3.032645 | 0.001345 |
| <i>Heschl_L</i> | <i>Cerebellum_9_L</i> | -43 -19 10 | -11 -49 -46 | 2.741878 | 0.003284 |
| <i>Temporal_Inf_R</i> | <i>Cerebellum_9_L</i> | 53 -31 -22 | -11 -49 -46 | 2.842775 | 0.002428 |
| <i>ParaHippocampal_R</i> | <i>Cerebellum_9_R</i> | 24 -15 -20 | 9 -49 -46 | 2.622846 | 0.004638 |
| <i>Fusiform_L</i> | <i>Cerebellum_9_R</i> | -32 -40 -20 | 9 -49 -46 | 2.82647 | 0.002551 |
| <i>Fusiform_R</i> | <i>Cerebellum_9_R</i> | 33 -39 -20 | 9 -49 -46 | 3.05025 | 0.001271 |
| <i>Heschl_L</i> | <i>Cerebellum_9_R</i> | -43 -19 10 | 9 -49 -46 | 2.64633 | 0.004336 |
| <i>Temporal_Inf_R</i> | <i>Cerebellum_9_R</i> | 53 -31 -22 | 9 -49 -46 | 2.846208 | 0.002403 |
| <i>Heschl_L</i> | <i>Vermis_8</i> | -43 -19 10 | 1 -64 -34 | 2.648404 | 0.004311 |
| <i>Fusiform_R</i> | <i>Vermis_10</i> | 33 -39 -20 | 0 -46 -32 | 2.727145 | 0.003429 |
| <i>Temporal_Pole_Mid_R</i> | <i>Vermis_10</i> | 43 15 -32 | 0 -46 -32 | 2.80612 | 0.002712 |
| <i>Parietal_Inf_L</i> | <i>SupraMarginal_R</i> | -44 -46 47 | 57 -32 34 | 2.653946 | 0.004243 |
| <i>Parietal_Inf_R</i> | <i>SupraMarginal_R</i> | 45 -46 50 | 57 -32 34 | 3.596016 | 0.000196 |
| <i>Postcentral_R</i> | <i>Angular_R</i> | 40 -25 53 | 45 -60 39 | 2.767595 | 0.003043 |
| <i>Parietal_Inf_L</i> | <i>Putamen_L</i> | -44 -46 47 | -25 4 2 | 2.667323 | 0.004082 |
| <i>SupraMarginal_L</i> | <i>Putamen_L</i> | -57 -34 30 | -25 4 2 | 2.808417 | 0.002693 |
| <i>SupraMarginal_L</i> | <i>Putamen_R</i> | -57 -34 30 | 27 5 2 | 2.725411 | 0.003447 |
| <i>SupraMarginal_R</i> | <i>Putamen_R</i> | 57 -32 34 | 27 5 2 | 2.639713 | 0.00442 |
| <i>Postcentral_L</i> | <i>Pallidum_L</i> | -43 -23 49 | -19 0 0 | 2.646974 | 0.004328 |
| <i>Parietal_Sup_L</i> | <i>Pallidum_L</i> | -24 -60 59 | -19 0 0 | 2.818748 | 0.002611 |
| <i>Parietal_Inf_L</i> | <i>Pallidum_L</i> | -44 -46 47 | -19 0 0 | 2.915913 | 0.00194 |
| <i>Parietal_Inf_R</i> | <i>Pallidum_L</i> | 45 -46 50 | -19 0 0 | 2.698369 | 0.00373 |
| <i>SupraMarginal_L</i> | <i>Pallidum_L</i> | -57 -34 30 | -19 0 0 | 3.064196 | 0.001215 |
| <i>SupraMarginal_R</i> | <i>Pallidum_L</i> | 57 -32 34 | -19 0 0 | 3.001252 | 0.001486 |
| <i>Parietal_Inf_L</i> | <i>Pallidum_R</i> | -44 -46 47 | 20 0 0 | 2.610988 | 0.004797 |
| <i>SupraMarginal_L</i> | <i>Pallidum_R</i> | -57 -34 30 | 20 0 0 | 2.678445 | 0.003953 |
| <i>SupraMarginal_R</i> | <i>Pallidum_R</i> | 57 -32 34 | 20 0 0 | 2.80597 | 0.002713 |
| <i>Postcentral_R</i> | <i>Heschl_L</i> | 40 -25 53 | -43 -19 10 | 3.232439 | 0.000699 |
| <i>Postcentral_R</i> | <i>Heschl_R</i> | 40 -25 53 | 45 -17 10 | 2.87488 | 0.002202 |

| | | | | | |
|------------------|------------------|-------------|-------------|----------|----------|
| Postcentral_R | Temporal_Sup_L | 40 -25 53 | -54 -21 7 | 3.511396 | 0.000266 |
| Parietal_Sup_L | Temporal_Sup_L | -24 -60 59 | -54 -21 7 | 2.600494 | 0.004942 |
| Parietal_Inf_R | Temporal_Sup_L | 45 -46 50 | -54 -21 7 | 2.850556 | 0.002371 |
| Postcentral_R | Temporal_Sup_R | 40 -25 53 | 57 -22 7 | 2.892967 | 0.002083 |
| SupraMarginal_L | Temporal_Sup_R | -57 -34 30 | 57 -22 7 | 2.623751 | 0.004626 |
| SupraMarginal_L | Temporal_Mid_L | -57 -34 30 | -57 -34 -2 | 2.689875 | 0.003824 |
| SupraMarginal_R | Temporal_Mid_L | 57 -32 34 | -57 -34 -2 | 2.656672 | 0.004209 |
| SupraMarginal_R | Temporal_Mid_R | 57 -32 34 | 56 -37 -1 | 2.672157 | 0.004025 |
| Postcentral_R | Cerebellum_4_5_L | 40 -25 53 | -15 -43 -17 | 2.63115 | 0.004529 |
| Parietal_Inf_R | Cerebellum_6_L | 45 -46 50 | -23 -59 -22 | 3.190445 | 0.000805 |
| SupraMarginal_L | Cerebellum_6_L | -57 -34 30 | -23 -59 -22 | 2.624361 | 0.004618 |
| SupraMarginal_R | Cerebellum_6_L | 57 -32 34 | -23 -59 -22 | 2.723474 | 0.003466 |
| Angular_R | Cerebellum_6_L | 45 -60 39 | -23 -59 -22 | 3.02152 | 0.001393 |
| SupraMarginal_L | Cerebellum_9_L | -57 -34 30 | -11 -49 -46 | 2.675232 | 0.00399 |
| Angular_R | Cerebellum_9_L | 45 -60 39 | -11 -49 -46 | 2.724065 | 0.00346 |
| Angular_R | Cerebellum_9_R | 45 -60 39 | 9 -49 -46 | 2.696723 | 0.003748 |
| Lingual_L | Postcentral_L | -16 -68 -5 | -43 -23 49 | 2.608688 | 0.004829 |
| Calcarine_L | Postcentral_R | -8 -79 6 | 40 -25 53 | 2.685396 | 0.003874 |
| Calcarine_R | Postcentral_R | 15 -73 9 | 40 -25 53 | 2.958247 | 0.001701 |
| Cuneus_L | Postcentral_R | -7 -80 27 | 40 -25 53 | 2.95643 | 0.001711 |
| Lingual_L | Postcentral_R | -16 -68 -5 | 40 -25 53 | 2.655342 | 0.004226 |
| Calcarine_L | SupraMarginal_L | -8 -79 6 | -57 -34 30 | 2.869188 | 0.00224 |
| Cuneus_L | SupraMarginal_L | -7 -80 27 | -57 -34 30 | 2.607824 | 0.00484 |
| Calcarine_L | SupraMarginal_R | -8 -79 6 | 57 -32 34 | 3.251247 | 0.000657 |
| Calcarine_R | SupraMarginal_R | 15 -73 9 | 57 -32 34 | 2.715451 | 0.003549 |
| Lingual_L | SupraMarginal_R | -16 -68 -5 | 57 -32 34 | 2.750953 | 0.003197 |
| Occipital_Sup_L | SupraMarginal_R | -18 -84 28 | 57 -32 34 | 2.662391 | 0.004141 |
| Calcarine_L | Heschl_L | -8 -79 6 | -43 -19 10 | 2.964357 | 0.001669 |
| Lingual_L | Heschl_L | -16 -68 -5 | -43 -19 10 | 2.718108 | 0.003521 |
| Calcarine_L | Heschl_R | -8 -79 6 | 45 -17 10 | 3.034207 | 0.001338 |
| Lingual_L | Heschl_R | -16 -68 -5 | 45 -17 10 | 3.158041 | 0.000896 |
| Lingual_R | Heschl_R | 15 -67 -4 | 45 -17 10 | 2.725905 | 0.003442 |
| Calcarine_L | Temporal_Sup_L | -8 -79 6 | -54 -21 7 | 3.137581 | 0.000958 |
| Lingual_L | Temporal_Sup_L | -16 -68 -5 | -54 -21 7 | 2.944979 | 0.001773 |
| Calcarine_L | Temporal_Sup_R | -8 -79 6 | 57 -22 7 | 2.689129 | 0.003832 |
| Cuneus_R | Temporal_Mid_L | 13 -79 28 | -57 -34 -2 | 2.604252 | 0.00489 |
| Occipital_Sup_L | Temporal_Mid_L | -18 -84 28 | -57 -34 -2 | 2.643959 | 0.004366 |
| Cingulum_Post_L | Amygdala_R | -6 -43 25 | 26 1 -18 | 2.650216 | 0.004288 |
| Cingulum_Post_R | Amygdala_R | 6 -42 22 | 26 1 -18 | 2.843841 | 0.00242 |
| Cingulum_Mid_L | Calcarine_L | -6 -15 42 | -8 -79 6 | 2.699047 | 0.003723 |
| Cingulum_Mid_R | Calcarine_L | 7 -9 40 | -8 -79 6 | 2.843981 | 0.002419 |
| Cingulum_Mid_L | Calcarine_R | -6 -15 42 | 15 -73 9 | 2.678941 | 0.003947 |
| Cingulum_Mid_L | Cuneus_L | -6 -15 42 | -7 -80 27 | 2.604551 | 0.004886 |
| Pallidum_L | Heschl_L | -19 0 0 | -43 -19 10 | 2.65299 | 0.004254 |
| Putamen_L | Cerebellum_9_L | -25 4 2 | -11 -49 -46 | 2.871398 | 0.002225 |
| Cerebellum_4_5_L | Cerebellum_9_L | -15 -43 -17 | -11 -49 -46 | 2.708632 | 0.00362 |
| Cerebellum_6_R | Cerebellum_9_L | 25 -58 -24 | -11 -49 -46 | 2.609321 | 0.00482 |
| Putamen_L | Cerebellum_9_R | -25 4 2 | 9 -49 -46 | 2.617878 | 0.004704 |
| Cerebellum_4_5_L | Cerebellum_9_R | -15 -43 -17 | 9 -49 -46 | 3.465129 | 0.000314 |
| Cerebellum_4_5_R | Cerebellum_9_R | 17 -43 -18 | 9 -49 -46 | 2.898954 | 0.002045 |
| Cerebellum_6_R | Cerebellum_9_R | 25 -58 -24 | 9 -49 -46 | 2.705926 | 0.003649 |

| | | | | | |
|-------------------------|------------------|-------------|-----------|----------|----------|
| <i>Cerebellum_9_L</i> | <i>Vermis_7</i> | -11 -49 -46 | 1 -72 -25 | 3.040696 | 0.001311 |
| <i>Cerebellum_9_R</i> | <i>Vermis_7</i> | 9 -49 -46 | 1 -72 -25 | 2.773311 | 0.002991 |
| <i>Cerebellum_9_L</i> | <i>Vermis_8</i> | -11 -49 -46 | 1 -64 -34 | 3.233686 | 0.000696 |
| <i>Cerebellum_9_R</i> | <i>Vermis_8</i> | 9 -49 -46 | 1 -64 -34 | 2.921687 | 0.001906 |
| <i>Vermis_7</i> | <i>Vermis_9</i> | 1 -72 -25 | 1 -55 -35 | 2.704707 | 0.003662 |
| <i>Vermis_8</i> | <i>Vermis_9</i> | 1 -64 -34 | 1 -55 -35 | 3.296187 | 0.000564 |
| <i>Cerebellum_3_L</i> | <i>Vermis_10</i> | -9 -37 -19 | 0 -46 -32 | 3.103545 | 0.00107 |
| <i>Cerebellum_4_5_L</i> | <i>Vermis_10</i> | -15 -43 -17 | 0 -46 -32 | 3.108277 | 0.001054 |
| <i>Vermis_1_2</i> | <i>Vermis_10</i> | 1 -39 -20 | 0 -46 -32 | 2.737448 | 0.003327 |

Table 8: fMRI resting state:

| Brain node 1* | Brain node 2* | MNI coordinate 1# | MNI coordinate 2# | t-value | p-value |
|----------------------------------|------------------------------------|-------------------|-------------------|----------|----------|
| <i>Precentral_L</i> | <i>Precentral_R</i> | -40 -6 51 | 40 -8 52 | 3.310026 | 0.000548 |
| <i>Frontal_Sup_L</i> | <i>Frontal_Sup_Orb_L</i> | -19 35 42 | -18 47 -13 | 2.957296 | 0.001727 |
| <i>Frontal_Sup_L</i> | <i>Frontal_Sup_Orb_R</i> | -19 35 42 | 17 48 -14 | 3.42589 | 0.000368 |
| <i>Frontal_Sup_Orb_R</i> | <i>Frontal_Mid_L</i> | 17 48 -14 | -34 33 35 | 3.102135 | 0.001091 |
| <i>Frontal_Mid_Orb_R</i> | <i>Frontal_Inf_Oper_R</i> | 32 53 -11 | 49 15 21 | 2.661537 | 0.004186 |
| <i>Precentral_L</i> | <i>Rolandic_Oper_L</i> | -40 -6 51 | -48 -8 14 | 2.770618 | 0.003045 |
| <i>Precentral_L</i> | <i>Rolandic_Oper_R</i> | -40 -6 51 | 52 -6 15 | 3.065516 | 0.001227 |
| <i>Rolandic_Oper_L</i> | <i>Rolandic_Oper_R</i> | -48 -8 14 | 52 -6 15 | 2.715473 | 0.003581 |
| <i>Frontal_Sup_L</i> | <i>Olfactory_L</i> | -19 35 42 | -9 15 -12 | 3.24721 | 0.000677 |
| <i>Frontal_Sup_Orb_L</i> | <i>Frontal_Sup_Medial_L</i> | -18 47 -13 | -6 49 31 | 2.764868 | 0.003097 |
| <i>Frontal_Sup_Orb_R</i> | <i>Frontal_Sup_Medial_L</i> | 17 48 -14 | -6 49 31 | 3.392131 | 0.000413 |
| <i>Olfactory_L</i> | <i>Frontal_Sup_Medial_L</i> | -9 15 -12 | -6 49 31 | 2.678632 | 0.003985 |
| <i>Olfactory_R</i> | <i>Frontal_Sup_Medial_L</i> | 8 16 -11 | -6 49 31 | 2.700088 | 0.003745 |
| <i>Olfactory_L</i> | <i>Rectus_L</i> | -9 15 -12 | -6 37 -18 | 2.647651 | 0.004356 |
| <i>Olfactory_R</i> | <i>Rectus_L</i> | 8 16 -11 | -6 37 -18 | 2.805089 | 0.002748 |
| <i>Rectus_L</i> | <i>Rectus_R</i> | -6 37 -18 | 7 36 -18 | 3.076873 | 0.001183 |
| <i>Frontal_Mid_Orb_L</i> | <i>Insula_L</i> | -32 50 -10 | -36 7 3 | 2.648647 | 0.004343 |
| <i>Frontal_Inf_Oper_L</i> | <i>Insula_L</i> | -49 13 19 | -36 7 3 | 2.747888 | 0.003256 |
| <i>Frontal_Mid_Orb_L</i> | <i>Insula_R</i> | -32 50 -10 | 38 6 2 | 2.810025 | 0.002708 |
| <i>Frontal_Inf_Orb_L</i> | <i>Insula_R</i> | -37 31 -12 | 38 6 2 | 2.669163 | 0.004095 |
| <i>Frontal_Med_Orb_L</i> | <i>ParaHippocampal_L</i> | -6 54 -7 | -22 -16 -21 | 3.052396 | 0.00128 |
| <i>Rectus_L</i> | <i>ParaHippocampal_L</i> | -6 37 -18 | -22 -16 -21 | 2.707983 | 0.00366 |
| <i>Precentral_R</i> | <i>Amygdala_L</i> | 40 -8 52 | -24 -1 -17 | 2.691636 | 0.003838 |
| <i>Rolandic_Oper_L</i> | <i>Amygdala_L</i> | -48 -8 14 | -24 -1 -17 | 3.030543 | 0.001372 |

| | | | | | |
|--------------------|---------------------|------------|-------------|----------|----------|
| Rolandic_Oper_R | Amygdala_L | 52 -6 15 | -24 -1 -17 | 3.192868 | 0.000811 |
| Frontal_Med_Orb_L | Amygdala_L | -6 54 -7 | -24 -1 -17 | 3.118694 | 0.001034 |
| Rectus_L | Amygdala_L | -6 37 -18 | -24 -1 -17 | 2.677342 | 0.003999 |
| Frontal_Med_Orb_L | Fusiform_L | -6 54 -7 | -32 -40 -20 | 2.918419 | 0.001948 |
| Precentral_L | Heschl_L | -40 -6 51 | -43 -19 10 | 2.623463 | 0.004667 |
| Frontal_Inf_Oper_L | Heschl_L | -49 13 19 | -43 -19 10 | 2.880777 | 0.002186 |
| Frontal_Inf_Tri_L | Heschl_L | -47 30 14 | -43 -19 10 | 2.606768 | 0.004893 |
| Rolandic_Oper_L | Heschl_L | -48 -8 14 | -43 -19 10 | 3.252335 | 0.000665 |
| Frontal_Med_Orb_L | Heschl_L | -6 54 -7 | -43 -19 10 | 2.603532 | 0.004938 |
| Precentral_L | Heschl_R | -40 -6 51 | 45 -17 10 | 3.283419 | 0.000599 |
| Precentral_R | Heschl_R | 40 -8 52 | 45 -17 10 | 3.004683 | 0.001489 |
| Frontal_Inf_Oper_L | Heschl_R | -49 13 19 | 45 -17 10 | 2.831648 | 0.002537 |
| Rolandic_Oper_L | Heschl_R | -48 -8 14 | 45 -17 10 | 2.845439 | 0.002434 |
| Frontal_Med_Orb_L | Heschl_R | -6 54 -7 | 45 -17 10 | 2.679178 | 0.003978 |
| Frontal_Inf_Oper_L | Temporal_Sup_R | -49 13 19 | 57 -22 7 | 2.767341 | 0.003074 |
| Frontal_Mid_Orb_R | Temporal_Pole_Sup_R | 32 53 -11 | 47 15 -17 | 2.887549 | 0.002141 |
| Frontal_Sup_R | Temporal_Mid_L | 20 31 44 | -57 -34 -2 | 2.837863 | 0.00249 |
| Frontal_Sup_Orb_R | Temporal_Mid_L | 17 48 -14 | -57 -34 -2 | 3.139313 | 0.000967 |
| Frontal_Mid_R | Temporal_Mid_L | 37 33 34 | -57 -34 -2 | 3.404252 | 0.000396 |
| Frontal_Inf_Tri_R | Temporal_Mid_L | 49 30 14 | -57 -34 -2 | 2.737197 | 0.00336 |
| Frontal_Sup_Orb_R | Temporal_Inf_L | 17 48 -14 | -51 -28 -23 | 2.908232 | 0.00201 |
| Supp_Motor_Area_L | Temporal_Inf_L | -6 5 61 | -51 -28 -23 | 2.803213 | 0.002763 |
| Supp_Motor_Area_R | Temporal_Inf_L | 8 0 62 | -51 -28 -23 | 2.873163 | 0.002238 |
| Precentral_L | Postcentral_L | -40 -6 51 | -43 -23 49 | 2.910698 | 0.001995 |
| Precentral_L | Postcentral_R | -40 -6 51 | 40 -25 53 | 2.776823 | 0.002989 |
| Frontal_Mid_Orb_L | SupraMarginal_L | -32 50 -10 | -57 -34 30 | 3.124828 | 0.001013 |
| Frontal_Mid_Orb_R | SupraMarginal_L | 32 53 -11 | -57 -34 30 | 2.604744 | 0.004921 |
| Frontal_Inf_Oper_L | SupraMarginal_L | -49 13 19 | -57 -34 30 | 3.806711 | 0.000092 |
| Frontal_Inf_Tri_L | SupraMarginal_L | -47 30 14 | -57 -34 30 | 3.333842 | 0.000505 |
| Frontal_Mid_Orb_L | SupraMarginal_R | -32 50 -10 | 57 -32 34 | 2.669335 | 0.004093 |
| Frontal_Mid_Orb_R | SupraMarginal_R | 32 53 -11 | 57 -32 34 | 2.843103 | 0.002451 |
| Frontal_Inf_Tri_L | SupraMarginal_R | -47 30 14 | 57 -32 34 | 2.878164 | 0.002204 |
| Frontal_Sup_Orb_R | Angular_L | 17 48 -14 | -45 -61 36 | 2.635808 | 0.004506 |
| Frontal_Inf_Tri_R | Angular_L | 49 30 14 | -45 -61 36 | 2.603538 | 0.004938 |
| Supp_Motor_Area_R | Angular_L | 8 0 62 | -45 -61 36 | 2.64333 | 0.00441 |
| Frontal_Med_Orb_R | Angular_R | 7 52 -7 | 45 -60 39 | 2.664605 | 0.004149 |

| | | | | | |
|--------------------|-----------------|------------|-------------|----------|----------|
| Frontal_Sup_Orb_R | Calcarine_L | 17 48 -14 | -8 -79 6 | 3.02667 | 0.001389 |
| Frontal_Med_Orb_L | Calcarine_L | -6 54 -7 | -8 -79 6 | 2.840392 | 0.002471 |
| Rectus_L | Calcarine_L | -6 37 -18 | -8 -79 6 | 3.112357 | 0.001055 |
| Rectus_R | Calcarine_L | 7 36 -18 | -8 -79 6 | 3.021908 | 0.00141 |
| Frontal_Med_Orb_L | Calcarine_R | -6 54 -7 | 15 -73 9 | 3.084391 | 0.001155 |
| Rectus_L | Calcarine_R | -6 37 -18 | 15 -73 9 | 2.942496 | 0.001808 |
| Rectus_R | Calcarine_R | 7 36 -18 | 15 -73 9 | 2.780431 | 0.002957 |
| Frontal_Med_Orb_L | Lingual_L | -6 54 -7 | -16 -68 -5 | 2.760344 | 0.003139 |
| Frontal_Med_Orb_L | Lingual_R | -6 54 -7 | 15 -67 -4 | 2.670781 | 0.004076 |
| Rectus_L | Occipital_Sup_L | -6 37 -18 | -18 -84 28 | 2.651426 | 0.004309 |
| Frontal_Med_Orb_L | Occipital_Sup_R | -6 54 -7 | 23 -81 31 | 2.703143 | 0.003712 |
| Frontal_Inf_Oper_L | Occipital_Mid_L | -49 13 19 | -33 -81 16 | 2.809851 | 0.002709 |
| Frontal_Med_Orb_L | Occipital_Mid_L | -6 54 -7 | -33 -81 16 | 2.658799 | 0.004219 |
| Frontal_Mid_L | Occipital_Mid_R | -34 33 35 | 36 -80 19 | 2.727978 | 0.003452 |
| Frontal_Inf_Oper_L | Occipital_Mid_R | -49 13 19 | 36 -80 19 | 2.623193 | 0.00467 |
| Frontal_Med_Orb_L | Occipital_Mid_R | -6 54 -7 | 36 -80 19 | 2.934207 | 0.001855 |
| Frontal_Inf_Oper_L | Occipital_Inf_L | -49 13 19 | -37 -78 -8 | 3.082428 | 0.001162 |
| Frontal_Med_Orb_L | Occipital_Inf_R | -6 54 -7 | 37 -82 -8 | 2.662238 | 0.004177 |
| Rectus_L | Occipital_Inf_R | -6 37 -18 | 37 -82 -8 | 2.631176 | 0.004565 |
| Frontal_Sup_Orb_L | Putamen_L | -18 47 -13 | -25 4 2 | 3.169034 | 0.000877 |
| Frontal_Sup_Orb_R | Putamen_L | 17 48 -14 | -25 4 2 | 3.408039 | 0.000391 |
| Frontal_Mid_L | Putamen_L | -34 33 35 | -25 4 2 | 2.69068 | 0.003848 |
| Frontal_Mid_R | Putamen_L | 37 33 34 | -25 4 2 | 2.730799 | 0.003424 |
| Frontal_Mid_Orb_L | Putamen_L | -32 50 -10 | -25 4 2 | 2.937998 | 0.001834 |
| Frontal_Mid_Orb_R | Putamen_L | 32 53 -11 | -25 4 2 | 2.78863 | 0.002886 |
| Frontal_Mid_R | Putamen_R | 37 33 34 | 27 5 2 | 2.69543 | 0.003796 |
| Frontal_Mid_Orb_L | Putamen_R | -32 50 -10 | 27 5 2 | 3.154627 | 0.00092 |
| Frontal_Inf_Oper_L | Putamen_R | -49 13 19 | 27 5 2 | 2.769493 | 0.003055 |
| Frontal_Sup_Orb_L | Pallidum_L | -18 47 -13 | -19 0 0 | 2.924488 | 0.001912 |
| Frontal_Sup_Orb_R | Pallidum_L | 17 48 -14 | -19 0 0 | 3.543006 | 0.000243 |
| Frontal_Sup_Orb_R | Pallidum_R | 17 48 -14 | 20 0 0 | 3.034144 | 0.001356 |
| Precentral_L | Cerebellum_6_L | -40 -6 51 | -23 -59 -22 | 2.779254 | 0.002968 |
| Rolandic_Oper_R | Cerebellum_6_R | 52 -6 15 | 25 -58 -24 | 2.85338 | 0.002376 |
| Frontal_Sup_L | Cerebellum_7b_L | -19 35 42 | -33 -60 -43 | 2.810573 | 0.002703 |
| Frontal_Mid_L | Cerebellum_7b_L | -34 33 35 | -33 -60 -43 | 3.015258 | 0.00144 |
| Frontal_Sup_L | Cerebellum_8_L | -19 35 42 | -26 -55 -48 | 2.677109 | 0.004002 |

| | | | | | |
|--------------------------|----------------------------|-------------|-------------|----------|----------|
| Frontal_Sup_Orb_R | Cerebellum_9_L | 17 48 -14 | -11 -49 -46 | 2.733556 | 0.003396 |
| Frontal_Med_Orb_L | Cerebellum_9_L | -6 54 -7 | -11 -49 -46 | 2.701698 | 0.003727 |
| Frontal_Med_Orb_R | Cerebellum_9_L | 7 52 -7 | -11 -49 -46 | 2.667925 | 0.00411 |
| Precentral_L | Vermis_4_5 | -40 -6 51 | 1 -52 -6 | 2.73655 | 0.003366 |
| <i>Hippocampus_R</i> | <i>ParaHippocampal_L</i> | 28 -20 -10 | -22 -16 -21 | 2.607378 | 0.004885 |
| <i>Hippocampus_L</i> | <i>ParaHippocampal_R</i> | -26 -21 -10 | 24 -15 -20 | 2.713228 | 0.003604 |
| <i>ParaHippocampal_L</i> | <i>Fusiform_R</i> | -22 -16 -21 | 33 -39 -20 | 2.640001 | 0.004452 |
| <i>ParaHippocampal_L</i> | <i>Heschl_L</i> | -22 -16 -21 | -43 -19 10 | 2.67281 | 0.004052 |
| <i>Amygdala_L</i> | <i>Heschl_L</i> | -24 -1 -17 | -43 -19 10 | 3.442398 | 0.000347 |
| <i>Hippocampus_L</i> | <i>Heschl_R</i> | -26 -21 -10 | 45 -17 10 | 2.923192 | 0.001919 |
| <i>Hippocampus_R</i> | <i>Heschl_R</i> | 28 -20 -10 | 45 -17 10 | 3.051368 | 0.001284 |
| <i>ParaHippocampal_L</i> | <i>Heschl_R</i> | -22 -16 -21 | 45 -17 10 | 3.143233 | 0.000954 |
| <i>ParaHippocampal_R</i> | <i>Heschl_R</i> | 24 -15 -20 | 45 -17 10 | 2.680964 | 0.003958 |
| <i>Amygdala_L</i> | <i>Heschl_R</i> | -24 -1 -17 | 45 -17 10 | 3.617983 | 0.000185 |
| <i>Fusiform_L</i> | <i>Heschl_R</i> | -32 -40 -20 | 45 -17 10 | 2.752058 | 0.003216 |
| <i>Fusiform_R</i> | <i>Heschl_R</i> | 33 -39 -20 | 45 -17 10 | 3.188558 | 0.000823 |
| <i>Heschl_L</i> | <i>Heschl_R</i> | -43 -19 10 | 45 -17 10 | 2.782393 | 0.00294 |
| <i>Amygdala_L</i> | <i>Temporal_Sup_L</i> | -24 -1 -17 | -54 -21 7 | 2.966345 | 0.001679 |
| <i>Heschl_R</i> | <i>Temporal_Sup_L</i> | 45 -17 10 | -54 -21 7 | 2.869956 | 0.00226 |
| <i>Amygdala_L</i> | <i>Temporal_Sup_R</i> | -24 -1 -17 | 57 -22 7 | 3.132532 | 0.000988 |
| <i>Heschl_R</i> | <i>Temporal_Sup_R</i> | 45 -17 10 | 57 -22 7 | 2.999887 | 0.001511 |
| <i>Insula_R</i> | <i>Temporal_Pole_Sup_L</i> | 38 6 2 | -41 15 -20 | 2.824411 | 0.002593 |
| <i>Heschl_R</i> | <i>Temporal_Mid_L</i> | 45 -17 10 | -57 -34 -2 | 3.299017 | 0.000569 |
| <i>Temporal_Sup_R</i> | <i>Temporal_Mid_L</i> | 57 -22 7 | -57 -34 -2 | 2.949734 | 0.001768 |
| <i>Heschl_R</i> | <i>Temporal_Mid_R</i> | 45 -17 10 | 56 -37 -1 | 2.770025 | 0.00305 |
| <i>Temporal_Mid_L</i> | <i>Temporal_Mid_R</i> | -57 -34 -2 | 56 -37 -1 | 3.522856 | 0.000261 |
| <i>Heschl_R</i> | <i>Temporal_Inf_R</i> | 45 -17 10 | 53 -31 -22 | 2.931432 | 0.001871 |
| <i>ParaHippocampal_L</i> | <i>Calcarine_L</i> | -22 -16 -21 | -8 -79 6 | 2.712044 | 0.003617 |
| <i>ParaHippocampal_L</i> | <i>Calcarine_R</i> | -22 -16 -21 | 15 -73 9 | 2.749748 | 0.003238 |
| <i>Amygdala_L</i> | <i>Occipital_Mid_L</i> | -24 -1 -17 | -33 -81 16 | 2.601968 | 0.00496 |
| <i>ParaHippocampal_L</i> | <i>Occipital_Mid_R</i> | -22 -16 -21 | 36 -80 19 | 2.704032 | 0.003702 |
| <i>Amygdala_L</i> | <i>Occipital_Mid_R</i> | -24 -1 -17 | 36 -80 19 | 2.778286 | 0.002976 |
| <i>ParaHippocampal_L</i> | <i>Cerebellum_4_5_L</i> | -22 -16 -21 | -15 -43 -17 | 3.19629 | 0.000802 |
| <i>Amygdala_L</i> | <i>Cerebellum_4_5_L</i> | -24 -1 -17 | -15 -43 -17 | 2.691229 | 0.003842 |
| <i>Amygdala_L</i> | <i>Cerebellum_6_L</i> | -24 -1 -17 | -23 -59 -22 | 2.891583 | 0.002115 |
| <i>Heschl_R</i> | <i>Cerebellum_6_L</i> | 45 -17 10 | -23 -59 -22 | 2.816005 | 0.00266 |
| <i>Temporal_Mid_L</i> | <i>Cerebellum_6_L</i> | -57 -34 -2 | -23 -59 -22 | 2.706167 | 0.003679 |
| <i>Insula_R</i> | <i>Cerebellum_6_R</i> | 38 6 2 | 25 -58 -24 | 2.750852 | 0.003228 |
| <i>Amygdala_L</i> | <i>Cerebellum_6_R</i> | -24 -1 -17 | 25 -58 -24 | 2.610102 | 0.004847 |
| <i>Heschl_R</i> | <i>Cerebellum_6_R</i> | 45 -17 10 | 25 -58 -24 | 3.529704 | 0.000255 |
| <i>Temporal_Sup_L</i> | <i>Cerebellum_6_R</i> | -54 -21 7 | 25 -58 -24 | 2.643649 | 0.004406 |
| <i>Temporal_Sup_R</i> | <i>Cerebellum_6_R</i> | 57 -22 7 | 25 -58 -24 | 2.84481 | 0.002439 |
| <i>Heschl_R</i> | <i>Vermis_7</i> | 45 -17 10 | 1 -72 -25 | 2.763879 | 0.003106 |

| | | | | | |
|--------------------|--------------------|-------------|-------------|----------|----------|
| Parietal_Sup_R | Temporal_Inf_L | 25 -59 62 | -51 -28 -23 | 2.71179 | 0.003619 |
| SupraMarginal_L | Angular_L | -57 -34 30 | -45 -61 36 | 2.650908 | 0.004315 |
| Angular_R | Pallidum_R | 45 -60 39 | 20 0 0 | 2.600855 | 0.004975 |
| Angular_L | Cerebellum_8_L | -45 -61 36 | -26 -55 -48 | 2.776903 | 0.002989 |
| Angular_L | Cerebellum_9_L | -45 -61 36 | -11 -49 -46 | 3.167401 | 0.000882 |
| Angular_R | Cerebellum_9_L | 45 -60 39 | -11 -49 -46 | 2.787784 | 0.002893 |
| Angular_R | Cerebellum_9_R | 45 -60 39 | 9 -49 -46 | 2.685082 | 0.003911 |
| Precuneus_R | Cerebellum_9_R | 9 -56 44 | 9 -49 -46 | 2.76376 | 0.003107 |
| Lingual_L | Heschl_R | -16 -68 -5 | 45 -17 10 | 2.877591 | 0.002208 |
| Lingual_R | Heschl_R | 15 -67 -4 | 45 -17 10 | 2.946722 | 0.001785 |
| Cingulum_Mid_L | Putamen_L | -6 -15 42 | -25 4 2 | 2.854903 | 0.002365 |
| Cingulum_Mid_R | Putamen_L | 7 -9 40 | -25 4 2 | 2.921205 | 0.001931 |
| Cingulum_Mid_L | Putamen_R | -6 -15 42 | 27 5 2 | 2.677698 | 0.003995 |
| Cingulum_Mid_R | Putamen_R | 7 -9 40 | 27 5 2 | 2.675438 | 0.004022 |
| Putamen_L | Heschl_L | -25 4 2 | -43 -19 10 | 2.64912 | 0.004337 |
| Putamen_L | Heschl_R | -25 4 2 | 45 -17 10 | 3.036365 | 0.001347 |
| Pallidum_L | Heschl_R | -19 0 0 | 45 -17 10 | 2.631471 | 0.004562 |
| Putamen_L | Temporal_Sup_L | -25 4 2 | -54 -21 7 | 2.650953 | 0.004315 |
| Putamen_L | Temporal_Sup_R | -25 4 2 | 57 -22 7 | 2.60751 | 0.004883 |
| Putamen_R | Temporal_Inf_L | 27 5 2 | -51 -28 -23 | 2.976984 | 0.001624 |
| Putamen_R | Cerebellum_Crus1_R | 27 5 2 | 37 -67 -30 | 2.606937 | 0.004891 |
| Pallidum_L | Cerebellum_6_L | -19 0 0 | -23 -59 -22 | 2.838414 | 0.002486 |
| Cerebellum_6_L | Cerebellum_6_R | -23 -59 -22 | 25 -58 -24 | 2.848944 | 0.002408 |
| Putamen_L | Cerebellum_7b_L | -25 4 2 | -33 -60 -43 | 2.642881 | 0.004416 |
| Pallidum_L | Cerebellum_7b_L | -19 0 0 | -33 -60 -43 | 2.848798 | 0.002409 |
| Cerebellum_Crus1_R | Cerebellum_9_L | 37 -67 -30 | -11 -49 -46 | 2.959981 | 0.001712 |
| Cerebellum_Crus2_R | Cerebellum_9_L | 32 -69 -40 | -11 -49 -46 | 3.330639 | 0.000511 |
| Cerebellum_7b_L | Cerebellum_9_L | -33 -60 -43 | -11 -49 -46 | 2.691941 | 0.003834 |
| Cerebellum_7b_R | Cerebellum_9_L | 35 -64 -47 | -11 -49 -46 | 2.721479 | 0.003518 |
| Cerebellum_8_L | Cerebellum_9_L | -26 -55 -48 | -11 -49 -46 | 2.61161 | 0.004826 |
| Putamen_L | Vermis_3 | -25 4 2 | 1 -40 -11 | 2.679493 | 0.003975 |
| Putamen_R | Vermis_3 | 27 5 2 | 1 -40 -11 | 2.674559 | 0.004032 |
| Pallidum_L | Vermis_3 | -19 0 0 | 1 -40 -11 | 2.646315 | 0.004372 |
| Pallidum_R | Vermis_3 | 20 0 0 | 1 -40 -11 | 2.623737 | 0.004663 |
| Cerebellum_8_L | Vermis_7 | -26 -55 -48 | 1 -72 -25 | 2.602372 | 0.004954 |
| Cerebellum_9_L | Vermis_7 | -11 -49 -46 | 1 -72 -25 | 2.857837 | 0.002344 |
| Cerebellum_9_R | Vermis_7 | 9 -49 -46 | 1 -72 -25 | 2.615067 | 0.004779 |

Table 9: Diffusion tensor imaging

| Brain node 1* | Brain node 2* | MNI coordinate 1# | MNI coordinate 2# | t-value | p-value |
|--------------------------|--------------------------|-------------------|-------------------|----------|----------|
| Frontal_Sup_Orb_R | Frontal_Mid_R | 17 48 -14 | 37 33 34 | 2.948183 | 0.001734 |
| Frontal_Mid_R | Frontal_Mid_Orb_R | 37 33 34 | 32 53 -11 | 2.965526 | 0.001642 |
| Frontal_Sup_Orb_R | Hippocampus_R | 17 48 -14 | 28 -20 -10 | 3.043932 | 0.00128 |
| Frontal_Sup_R | Heschl_R | 20 31 44 | 45 -17 10 | 2.815486 | 0.00261 |

| | | | | | |
|--------------------------|---------------------|-------------|-------------|----------|----------|
| Frontal_Sup_R | Temporal_Mid_L | 20 31 44 | -57 -34 -2 | 2.772786 | 0.002967 |
| Frontal_Mid_R | Temporal_Mid_L | 37 33 34 | -57 -34 -2 | 2.912428 | 0.001939 |
| Frontal_Sup_R | Temporal_Inf_L | 20 31 44 | -51 -28 -23 | 3.001188 | 0.001467 |
| Frontal_Inf_Tri_R | Temporal_Inf_L | 49 30 14 | -51 -28 -23 | 3.090496 | 0.001101 |
| Frontal_Inf_Tri_L | Precuneus_L | -47 30 14 | -8 -56 48 | 2.726434 | 0.003405 |
| Frontal_Mid_L | Cuneus_R | -34 33 35 | 13 -79 28 | 3.061236 | 0.00121 |
| Frontal_Med_Orb_L | Cuneus_R | -6 54 -7 | 13 -79 28 | 2.616205 | 0.00469 |
| Frontal_Inf_Tri_R | Occipital_Sup_L | 49 30 14 | -18 -84 28 | 2.632934 | 0.00447 |
| Frontal_Inf_Tri_R | Occipital_Mid_L | 49 30 14 | -33 -81 16 | 2.655832 | 0.004185 |
| Frontal_Sup_Orb_L | Occipital_Inf_L | -18 47 -13 | -37 -78 -8 | 2.68464 | 0.003849 |
| Rectus_L | Occipital_Inf_L | -6 37 -18 | -37 -78 -8 | 2.606679 | 0.004819 |
| Frontal_Sup_R | Cingulum_Mid_R | 20 31 44 | 7 -9 40 | 2.756724 | 0.003113 |
| Frontal_Mid_R | Cingulum_Mid_R | 37 33 34 | 7 -9 40 | 2.753009 | 0.003148 |
| Frontal_Inf_Tri_R | Thalamus_L | 49 30 14 | -12 -18 8 | 2.605123 | 0.00484 |
| Frontal_Sup_Orb_R | Cerebellum_3_R | 17 48 -14 | 12 -34 -19 | 2.907542 | 0.001969 |
| Frontal_Inf_Tri_R | Cerebellum_7b_L | 49 30 14 | -33 -60 -43 | 2.864093 | 0.002251 |
| Frontal_Inf_Tri_R | Vermis_7 | 49 30 14 | 1 -72 -25 | 2.692651 | 0.00376 |
| Hippocampus_L | Pallidum_R | -26 -21 -10 | 20 0 0 | 3.457133 | 0.000316 |
| Hippocampus_L | Thalamus_R | -26 -21 -10 | 12 -18 8 | 2.87939 | 0.002148 |
| Hippocampus_R | Vermis_7 | 28 -20 -10 | 1 -72 -25 | 3.164489 | 0.000863 |
| Precuneus_L | Temporal_Sup_L | -8 -56 48 | -54 -21 7 | 3.314631 | 0.00052 |
| Precuneus_L | Temporal_Pole_Sup_L | -8 -56 48 | -41 15 -20 | 3.140185 | 0.000936 |
| Parietal_Sup_L | Temporal_Mid_L | -24 -60 59 | -57 -34 -2 | 2.994856 | 0.001497 |
| Precuneus_L | Temporal_Mid_L | -8 -56 48 | -57 -34 -2 | 3.015499 | 0.001402 |
| Parietal_Sup_L | Temporal_Inf_L | -24 -60 59 | -51 -28 -23 | 2.681395 | 0.003886 |
| Precuneus_L | Pallidum_R | -8 -56 48 | 20 0 0 | 3.430424 | 0.000347 |
| SupraMarginal_R | Cerebellum_Crus1_L | 57 -32 34 | -36 -67 -29 | 2.737971 | 0.003291 |
| Precuneus_L | Cerebellum_3_R | -8 -56 48 | 12 -34 -19 | 2.832031 | 0.002482 |
| Calcarine_L | Temporal_Sup_R | -8 -79 6 | 57 -22 7 | 3.047353 | 0.001266 |
| Cuneus_R | Parietal_Inf_L | 13 -79 28 | -44 -46 47 | 2.654728 | 0.004198 |
| Occipital_Mid_L | Parietal_Inf_L | -33 -81 16 | -44 -46 47 | 2.630423 | 0.004503 |
| Calcarine_L | Occipital_Mid_L | -8 -79 6 | -33 -81 16 | 2.911814 | 0.001943 |
| Calcarine_L | Occipital_Inf_L | -8 -79 6 | -37 -78 -8 | 2.765985 | 0.003028 |
| Cuneus_L | Thalamus_L | -7 -80 27 | -12 -18 8 | 3.044983 | 0.001275 |
| Occipital_Mid_L | Cerebellum_10_L | -33 -81 16 | -23 -34 -42 | 2.664906 | 0.004076 |
| Calcarine_L | Vermis_7 | -8 -79 6 | 1 -72 -25 | 3.445874 | 0.000329 |
| Cingulum_Post_R | Calcarine_L | 6 -42 22 | -8 -79 6 | 2.774792 | 0.00295 |
| Pallidum_L | Thalamus_L | -19 0 0 | -12 -18 8 | 3.133992 | 0.000955 |
| Thalamus_R | Cerebellum_Crus1_L | 12 -18 8 | -36 -67 -29 | 2.981882 | 0.00156 |
| Pallidum_R | Cerebellum_Crus1_R | 20 0 0 | 37 -67 -30 | 2.719439 | 0.003476 |
| Cerebellum_6_R | Cerebellum_7b_L | 25 -58 -24 | -33 -60 -43 | 3.289062 | 0.000568 |
| Cerebellum_6_R | Cerebellum_9_L | 25 -58 -24 | -11 -49 -46 | 2.692418 | 0.003763 |
| Cerebellum_Crus1_R | Cerebellum_10_L | 37 -67 -30 | -23 -34 -42 | 2.785143 | 0.00286 |
| Cerebellum_7b_R | Vermis_7 | 35 -64 -47 | 1 -72 -25 | 2.768849 | 0.003003 |

8 CURRICULUM VITAE

PERSONAL INFORMATION

Name: Anais Buhl, geb. Harneit
Date of birth: 19.09.1985
Place of birth: Hagen

SECONDARY EDUCATION

2002 – 2006 Mallinkrodt-Gymnasium Dortmund
26/06/2006 Abitur

ACADEMIC EDUCATION

2008-2011 Psychology
University of Twente
31/08/2011 Bachelor of Science
2012-2014 Cognitive Neuroscience
Radboud University Nijmegen
2013-2014 Masterthesis
24/12/2014 Master of Science, GPA: 8.5

PROFESSIONAL EXPERIENCE

2014-present Researcher and doctoral candidate at the Central Institute of Mental Health in Mannheim

PUBLICATIONS

Sutcliffe JS, **Harneit A**, Tost H, Meyer-Lindenberg A. Neuroimaging Intermediate Phenotypes of Executive Control Dysfunction in Schizophrenia. *Biol Psychiatry Cogn Neurosci Neuroimaging*. 2016 1(3):218-229.

Cao H*, **Harneit A***, Walter H, Erk S, Braun U, Moessnang C, Geiger LS, Zang Z, Mohnke S, Heinz A, Romanczuk-Seiferth N, Mühleisen T, Mattheisen M, Witt SH, Cichon S, Nöthen MM, Rietschel M, Meyer-Lindenberg A, Tost H. The 5-HTTLPR Pol-

ymorphism Affects Network-Based Functional Connectivity in the Visual-Limbic System in Healthy Adults. *Neuropsychopharmacology*. 2018 43(2):406-414. Epub 2017 Jun 7. *Shared first authors.

Harneit A, Braun U, Geiger-Primo L, Zang Z, Hakobjan M, van Donkelaar MM, Schweiger J, Schwarz K, Gan G, Erk S, Heinz A, Romanczuk-Seiferth N, Witt S, Rietschel M, Walter H, Franke B, Meyer-Lindenberg A, Tost H. MAOA-VNTR genotype affects structural and functional connectivity in distributed brain networks. *Hum Brain Mapp*. 2019 40(18):5202-5212. Epub 2019 Aug 23.

Schweiger J, Bilek E, Schäfer A, Braun U, Moessnang C, **Harneit A**, Post P, Schwarz K, Romanczuk-Seiferth N, Erk S, Wackerhagen C, Mattheisen M, Mühleisen TW, Cichon S, Nöthen MM, Frank J, Witt S, Rietschel M, Heinz A, Walter H, Meyer-Lindenberg A, Tost H. Effects of BDNF ValMet genotype and schizophrenia familial risk on a neural functional network for cognitive control in humans. *Neuropsychopharmacology*. 2019 44(3):590-597. Epub 2018 Oct 25.

Chen J, Zang Z, Braun U, Schwarz K, **Harneit A**, Kremer T, Ma R, Schweiger J, Mössnang C, Geiger-Primo L, Cao H, Degenhardt F, Nöthen MM, Tost H, Meyer-Lindenberg A, Schwarz, Ph.D E. Association of a Reproducible Epigenetic Risk Profile for Schizophrenia With Brain Methylation and Function. *JAMA Psychiatry*. 2020 77(6):628-636. Epub 2020 Feb 12.

Fehlner P, Bilek E, **Harneit A**, Böhringer A, Moessnang C, Meyer-Lindenberg A, Tost H. Neural responses to social evaluative threat in the absence of negative investigator feedback and provoked performance failures. *Hum Brain Mapp*. 2020 41(8):2092-2103. Epub 2020 Jan 20.

Wasserthal J, Maier-Hein KH, Neher PF, Northoff G, Kubera KM, Fritze S, **Harneit A**, Geiger-Primo L, Tost H, Wolf RC, Hirjak D. Multiparametric mapping of white matter microstructure in catatonia. *Neuropsychopharmacology*. 2020 45(10):1750-1757. Epub 2020 May 5.

Braun U, **Harneit A**, Pergola G, Menara T, Schäfer A, Betzel RF, Zang Z, Schweiger J, Zhang X, Schwarz K, Chen J, Blasi G, Bertolino A, Durstewitz D, Pasqualetti F, Schwarz E, Meyer-Lindenberg A, Bassett DS, Tost H. Brain network dynamics during working memory are modulated by dopamine and diminished in schizophrenia. *Nat Commun*. 2021 12(1):3478.

Fritze S, **Harneit A**, Waddington JL, Kubera KM, Schmitgen MM, Otte ML, Geiger LS, Tost H, Meyer-Lindenberg A, Wolf RC, Hirjak D. Structural alterations in brainstem, basal ganglia and thalamus associated with parkinsonism in schizophrenia spectrum disorders. *Eur Arch Psychiatry Clin Neurosci*. 2021 271(8):1455-1464. Epub 2021 May 5.

Wasserthal J, Maier-Hein KH, Neher PF, Wolf RC, Northoff G, Waddington JL, Kubera KM, Fritze S, **Harneit A**, Geiger-Primo L, Tost H, Hirjak D. White matter microstructure alterations in cortico-striatal networks are associated with parkinsonism in schizophrenia spectrum disorders. *Eur Neuropsychopharmacol*. 2021 50:64-74. Epub 2021 May 10.

Zhang X, Braun U, **Harneit A**, Zang Z, Geiger-Primo L, Betzel RF, Chen J, Schweiger J, Schwarz K, Reinwald J, Fritze S, Witt S, Rietschel M, Nöthen MM, Degenhardt F, Schwarz, Ph.D E, Hirjak D, Meyer-Lindenberg A, Bassett DS, Tost H. Generative network models of altered structural brain connectivity in schizophrenia. *Neuroimage*. 2021 225:117510. Epub 2020 Nov 4.

O'Leary A, Fernández-Castillo N, Gan G, Yang Y, Yotova AY, Kranz TM, Grünewald L, Freudenberg F, Antón-Galindo E, Cabana-Domínguez J, **Harneit A**, Schweiger J, Schwarz K, Ma R, Chen J, Schwarz E, Rietschel M, Tost H, Meyer-Lindenberg A, Pané-Farré CA, Kircher T, Hamm AO, Burguera D, Mota NR, Franke B, Schweiger S, Winter J, Heinz A, Erk S, Romanczuk-Seiferth N, Walter H, Ströhle A, Fehm L, Fydrich T, Lueken U, Weber H, Lang T, Gerlach AL, Nöthen MM, Alpers GW, Arolt V, Witt S, Richter J, Straube B, Cormand B, Slattery DA, Reif A. Behavioural and functional evidence revealing the role of RBFOX1 variation in multiple psychiatric disorders and traits. *Mol Psychiatry*. 2022 27(11):4464-4473. Epub 2022 Aug 10.

Schwarz K, Mößnang C, Schweiger JI, **Harneit A**, Schneider M, Chen J, Cao H, Schwarz E, Witt S, Rietschel M, Nöthen M, Degenhardt F, Wackerhagen C, Erk S, Romanczuk-Seiferth N, Walter H, Tost H, Meyer-Lindenberg A. Ventral Striatal-Hippocampus Coupling During Reward Processing as a Stratification Biomarker for Psychotic Disorders. *Biol Psychiatry*. 2022 91(2):216-225. Epub 2021 Jul 24.

9 ACKNOWLEDGEMENTS

I thank Prof. Dr. Dr. Heike Tost for giving me the opportunity to work on such an exciting topic and being part of an excellent research group. I especially appreciate her help and support through all stages of my dissertation project, her encouragement during times of slower progress in my project and her advice and help in publication processes.

Further, I would like to thank Dr. Urs Braun for his advice, help and for sharing his extensive experience with me.

I would like to thank Dr. Jamila Andoh for the help and advice with the writing process, reading several versions of my dissertations and her valuable feedback and encouragement during the writing process.

Last but not least I thank my husband Dr. Patrick Buhl for his support, encouragement and understanding during all the stages of my PhD journey.